Doctoral theses at NTNU, 2021:239

Assís Arañó Barenys

Experimental study of reinforced concrete slabs subjected to fire exposure and blast loading

Doctoral thesis

NTNU
Norwegian University of Science and Technology
Thesis for the Degree of
Philosophiae Doctor
Faculty of Engineering
Department of Structural Engineering

NTNU
Norwegian University of
Science and Technology

Assís Arañó Barenys

Experimental study of reinforced concrete slabs subjected to fire exposure and blast loading

Thesis for the Degree of Philosophiae Doctor

Trondheim, June 2021

Norwegian University of Science and Technology
Faculty of Engineering
Department of Structural Engineering

NTNU
Norwegian University of
Science and Technology

NTNU
Norwegian University of Science and Technology

Thesis for the Degree of Philosophiae Doctor

Faculty of Engineering
Department of Structural Engineering

ISBN 978-82-326-5289-1 (printed ver.)
ISBN 978-82-326-5876-3 (electronic ver.)
ISSN 1503-8181 (printed ver.)
ISSN 2703-8084 (online ver.)

Doctoral theses at NTNU, 2021:239

Printed by NTNU Grafisk senter

Abstract

Safety considerations are essential in the design of reinforced concrete (RC) structures in order to withstand exceptional load conditions throughout its entire service life. Particularly for tunnels, increased attention is paid to the combined action of fire and explosive loads due to the increase of traffic carrying hazardous goods and recent terrorist attacks, being an accidental scenario which needs to be investigated. This specific scenario is a crucial safety design condition also for submerged floating tube bridges (SFTBs), which represent a feasible alternative solution for crossing wide and deep fjords along the Norwegian west coast, and are therefore considered for the *Coastal Highway Route E39* project.

The main objective of this thesis is the investigation of the combined effect of fire exposure and subsequent blast loading on RC slabs. For this purpose, the following experimental programme consisting of three phases was defined to investigate: *i)* the mechanical characterization of concrete at high temperatures, *ii)* the impact of the combination of fire and static loading on RC circular slabs, and *iii)* the impact of the combination of fire and dynamic loading on RC circular slabs. A hydrocarbon fire curve, typically considered for the design of tunnels, was applied in the fire tests by means of a gas burner, while a shock tube device was used to perform the dynamic tests. The obtained experimental results were either compared with the literature and standards, or discussed by means of analytical and numerical approaches.

A complete material characterization of concrete at high temperatures is necessary in order to evaluate the effect of fire exposure on concrete structures, allowing the assessment of the remaining capacity to withstand additional loads, e.g. explosion. However, previous experimental studies of concrete material at high temperatures in the literature show inconsistency on the results for the basic mechanical properties (e.g. compressive strength and modulus of elasticity), and lack of research for additional relevant properties (e.g. fracture energy and evolution of internal damage). For this reason, this study first provides a complete material characterization of concrete at elevated temperatures, investigating the compressive and tensile constitutive behaviour in residual conditions. Results confirm the adverse effect of temperature on the basic mechanical properties reported in the literature. Furthermore, exposure to high temperatures results in flattened stress-strain relationships, leading to a decrease of specific fracture energy in compression at elevated temperatures, while it increases in tension.

The comprehensive knowledge of the mechanical response of the material at elevated temperatures is a necessary requirement to evaluate the effect of fire exposure, but often not sufficient. Structural effects from a rapid and non-uniform increase of temperatures may lead to a further lowering of the structural resistance of the

member. On the contrary, confinement effects from surrounding elements may lead to an increase of the loading resistance due to redistribution of stresses, leading to a more robust structure. Experimental static tests performed on small-scale RC slabs show similar failure mechanisms after exposure to fire, compared to non-exposed specimens, resulting in an enhanced bending capacity due to an arching effect and an enhanced ultimate load due to the tensile membrane action (TMA). While the arching mechanism is greatly affected by the fire exposure, due to the adverse effect on the compressive behaviour of concrete, the strong recovery of steel in residual conditions leads to similar results for the ultimate load. Simplified predictions using the yield-line approach provide satisfactory interpretations of the observed thermally damaged bending capacity of the RC slab.

The acquired knowledge from the abovementioned studies allows to investigate the dynamic behaviour of the RC slab subjected to the combination of fire exposure and blast loading. Both the effect of fire, using a low-pressure (LP) shock wave inducing an elastic response to the specimen, and the combined action of fire and blast, using a high-pressure (HP) shock wave, were investigated. Results indicate a considerable reduction of the fundamental frequency of the slab, which is mainly caused by the decrease of stiffness after the high temperatures. In addition, thermal damage and microcracking due to fire exposure and blast loading increase the energy dissipation, thus leading to a higher damping ratio on the RC slab. The results of single degree of freedom (SDOF) and finite element (FE) models support the experimental findings.

The lack of experimental research on this topic highlights the challenge of the work here presented, as well as its contribution. The findings of this study are intended to be a reliable benchmark for developing a calibrated numerical model which, upon upscaling, can assess the design of SFTBs in the *Coastal Highway Route E39* project.

Keywords— experimental study, material characterization, residual conditions, fire exposure, blast loading, shock tube, RC slabs

Acknowledgements

There are many people who contributed to this work and made it possible. First of all, I would like to thank my main supervisor Jan A. Øverli, for giving me this opportunity and for supporting me in all the circumstances, both professional and personal. I wish to thank also my co-supervisor Max A. N. Hendriks, for giving precious feedback and always being available for valuable discussions. Special thanks also go to Terje Kanstad for finding easy solutions to all problems and always being available for a talk.

A large part of this project was performed in Italy, and I would like to thank all the research group in Lecco that made this possible. Special thanks go to Matteo Colombo, for always suggesting new ideas and aiming at improving what we had, both in terms of results and writing, including the present thesis. I would also like to thank Paolo Martinelli, for helping with the experiments and for giving detailed revisions, thus raising the bar of the work performed. Many thanks also go to Giulio Zani for helping with nice discussions. I would also like to thank Marco di Prisco, for the precious discussions and also for initiating this collaboration together with Terje Kanstad.

This work would not have been accomplished without the people that I met along the journey. Special thanks go to the concrete group at NTNU, for the warm and cozy atmosphere at work, despite the long winters in Norway. I would also like to thank the colleagues from the department, including those who came for an exchange, for adding some fun to my working days, even the challenging ones. In addition, I would like to thank the colleagues in Lecco, for making me feel part of the group from the beginning and for the nice time spent together. I would also like to thank all the other friends in Trondheim, this small family which makes living abroad a little bit easier.

Finally, I would like to give my most sincere thanks to these people. To my close friends, with whom I have shared some of the most special moments in my life; and they have always been there for me. To my family, the reference point in my life which I know I can always rely on. To my parents, the best teachers that I ever had, and the main reason for what I have achieved and become. To my three brothers, to whom despite the distance I feel emotionally very close, for this I will always be grateful. To Cristiana, the most wonderful person I have ever met, for her unconditional support and love, and with whom I will always be grateful to share every single day of my life.

Preface

This doctoral thesis is submitted in partial fulfilment of the requirements for the degree of *Philosophiae Doctor* (Ph.D.) at the Norwegian University of Science and Technology (NTNU). The research was carried out at the Department of Structural Engineering, Faculty of Engineering at NTNU in Trondheim, Norway, and at the Department of Civil and Environmental Engineering at *Politecnico di Milano* in Lecco, Italy. The main supervisor was Professor Jan A. Øverli from NTNU, and the co-supervisor was Professor Max A. N. Hendriks from NTNU and Delft University of Technology in the Netherlands.

The Ph.D. project is a part of the ongoing research project *Coastal Highway Route E39* carried out under the auspices of the Norwegian Public Roads Administration. NTNU and the *Coastal Highway Route E39* project funded this Ph.D. work. The project started in February 2017 and the thesis was submitted in April 2021.

The thesis is written as a collection of papers and consists of two parts. The first part describes the context of the work, summarizes the main contributions and draws the main conclusions. The second part consists of three appended papers, of which two have been published and one is under review, all in international scientific peer-reviewed journals.

The author, Assís Arañó Barenys, declares that the work presented herein is his own and that it contains no material that has previously been submitted for a degree at this university or any other institution.

Trondheim, April 2021

Assís Arañó Barenys

Table of Contents

II APPENDED PAPERS

Paper I – *Material characterization approach for modelling high-strength concrete after cooling from elevated temperatures*

Paper II – *Failure characteristics of reinforced concrete circular slabs subjected to fire exposure and static load: an experimental study*

Paper III – *Experimental investigation on the structural response of RC slabs subjected to combined fire and blast*

List of publications

Appended journal publications

Arano, A., Colombo, M., Martinelli, P., Øverli, J. A., Hendriks, M. A. N., Kanstad, T. and di Prisco, M. "Material characterization approach for modelling high-strength concrete after cooling from elevated temperatures". *ASCE Journal of Materials in Civil Engineering*, 2021, 33(5): 04021086. doi: `https://doi.org/10.1061/(ASCE)MT.1943-5533.0003694`

Arano, A., Colombo, M., Martinelli, P., Øverli, J. A., Hendriks, M. A. N., Kanstad, T. and di Prisco, M. "Failure characteristics of reinforced concrete circular slabs subjected to fire exposure and static load: an experimental study". *Under review in "Engineering Structures"*, 2021.

Colombo, M., Martinelli, P., Arano, A., Øverli, J. A., Hendriks, M. A. N., Kanstad, T. and di Prisco, M. "Experimental investigation on the structural response of RC slabs subjected to combined fire and blast". *Structures*, 2021, 31: 1017-1030. doi: `https://doi.org/10.1016/j.istruc.2021.02.029`

Conference publications

Colombo, M., Martinelli, P., Arano, A., Shu, J., Kanstad, T. and di Prisco, M. "RC slabs subjected to fire and blast". PROTECT 2019: 7^{th} International Colloquium on *'Performance, Protections & Strengthening of Structures Under Extreme Loading Events'*, Whistler (BC, Canada), September 16^{th}-17^{th}, 2019.

Arano, A., Colombo, M., Martinelli, P., Øverli, J. A., Hendriks, M. A. N., Kanstad, T. and di Prisco, M. "Heated reinforced concrete slabs subjected to blast load: Experimental and numerical results". Proceedings of the 17^{th} *fib* Symposium on *'Concrete Structures for Resilient Society'*, Online, Shanghai (China), November 22^{nd}-24^{th}, 2020.

Technical lectures

Arano, A., Shu, J., Øverli, J. A., Hendriks, M. A. N. and Kanstad, T. "Heated reinforced concrete slabs subjected to blast load: Configuring experiments by numerical analyses". In 12^{th} International DIANA Users Meeting, University of Porto, Porto (Portugal), October 12^{th}, 2018.

Arano, A., Shu, J., Øverli, J. A., Hendriks, M. A. N., Kanstad, T. and Colombo, M. "Heated reinforced concrete slabs subjected to static load: Experimental results and numerical simulations". In 13^{th} International DIANA Users Meeting, Norwegian University of Science and Technology, Trondheim (Norway), May 23^{rd}, 2019.

Declaration of authorship

Assís Arañó Barenys has planned and conducted all the experimental work in the abovementioned publications, in collaboration with co-authors Matteo Colombo and Paolo Martinelli. The author has also evaluated the results and written Papers I and II, and contributed in processing and discussing the results, and reviewing the manuscript in Paper III. In addition, the author has written this thesis. The co-authors have contributed in discussing the results and reviewing the manuscripts.

Part I

EXTENDED SUMMARY

Chapter 1

Introduction

1.1 Background and motivation

Reinforced concrete (RC) structures represent the major part of today's infrastructure, for example in bridges and tunnels. In addition to the normal design loadings, RC structures may be exposed to extreme hazards throughout their service life, comprising accidental actions (fire exposure), natural disasters (earthquakes) or even terrorist attacks [85, 104]. This can cause a huge deterioration of the structure, affecting both the serviceability and the structural resistance.

In the case of tunnels, the consequences of extreme events can be even worse due to the closed environment of the structure, especially concerning the effects related to fire exposure which is often regarded as the main physical threat in their design. Recent disastrous fire events in tunnels in Europe, e.g. Mont Blanc Tunnel (1999), Gotthard Tunnel (2001), Tauern Tunnel (2002), Frejus Tunnel (2005), and Viamala Tunnel (2006), have increased the attention paid to safety issues in this type of structures, underlining the importance of investigating these infrastructures from human and economical points of view. However, nowadays fire can no longer be considered alone when evaluating extreme actions, due to tragic accidents caused by an increase of traffic carrying hazardous goods and recent terrorist attacks. An internal explosion after a fire exposure may lead to potentially disastrous consequences, easily aggravating the damage or even causing the complete collapse of the structure [25, 105]. The recent tragic collision in *Casalecchio*, Italy (2018), can be regarded as an example of this kind of scenario. Two trucks loaded with flammable materials triggered a chain of explosions that gutted an overpass infrastructure.

The investigation of the combined action of fire and explosion loads in tunnels is of great interest also for the Norwegian Public Roads Administration's (NPRA) *Coastal Highway Route E39* project [73]. This project is aimed at establishing an improved, and potentially ferry-free, highway route between Kristiansand and Trondheim along the Norwegian west coast, reducing the current travel time by half. To do so, this pioneering project needs to evaluate many fjord crossings, including seven ferry connections. Conventional structures, e.g. suspension bridges and rock undersea tunnels, can be used as fixed connections for many of the crossings. However, the uncommon dimensions of some fjords like *Sulafjorden*, which is 5 km wide and more than 1 km deep, make these conventional structures not feasible for those crossings. Alternative solutions therefore need to be considered, as for example floating bridges

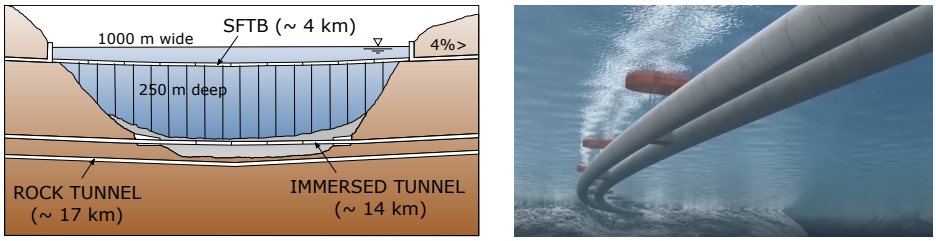

(a) (b)

Figure 1.1: (a) Different crossing alternatives (modified from [69]); and, (b) image of the SFTB [73].

or submerged floating tube bridges (SFTBs) [69]. Figure 1.1a shows a comparison of different fjord crossing alternatives.

The SFTB is a type of floating bridge, submerged at a defined position under the sea level, as shown in Figure 1.1b. In the case of deep fjords, the depth of the SFTB allows to optimize the length of the crossing, compared to conventional undersea tunnels [37], see Figure 1.1a. The research studies promoted by the NPRA, in conjunction with the advanced offshore technology available in Norway, have demonstrated the feasibility of the SFTB [69]. Nevertheless, ongoing research projects are still oriented towards investigating safety considerations to ensure robustness and redundancy for the whole structure. The specific scenario of the combined action of fire and subsequent internal explosion, illustrated in Figure 1.2, represents a crucial safety design condition for this structure. However, the lack of research available on the combined effect of such two extreme loads makes the study of this accidental scenario a great engineering challenge [69].

Large-scale experimental tests on RC structures are seldom carried out due to the high cost and testing difficulties. In fact, there are no experimental studies

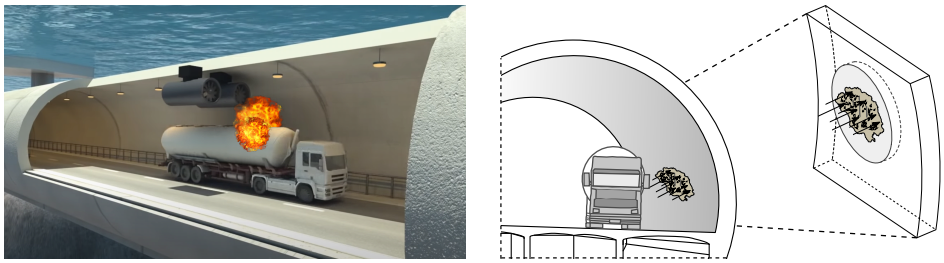

(a) (b)

Figure 1.2: (a) Accidental scenario of fire and blast loads (modified from [73]); and, (b) sketch of the SFTB cross-section.

in the literature investigating tunnels subjected to internal blast loads at present. Alternatively, small-scale tests in RC concrete members, such as slabs, beams, or tunnel linings, are carried out. The accidental loads are reproduced in such elements and their structural behaviour is then investigated with the objective of assessing the scenario in the large structure.

In a general tunnel serviceability condition, a compressive membrane state of stress is the most important action. Nevertheless, when an accidental action hits the tunnel, non-symmetric load condition can be applied to the structure, thus leading to bending action that could drive the global failure of the structure. For this reason, RC slabs can be considered as reference elements to be investigated.

The assessment of a complex structure under extreme load conditions typically requires the use of advanced numerical models. The predictions of such models are often compared to experimental results in order to be calibrated and thus be considered reliable design tools. The experimental findings of this study are therefore valuable to define a reliable benchmark for numerical models which, with numerical upscaling, will be instrumental for the design of the SFTB under exceptional load conditions, such as the combined action of fire and subsequent blast loading.

1.2 Scope and limitations

This study experimentally investigates the combined effect of fire exposure and blast loading on RC slabs. Figure 1.3 shows the research strategy for the investigated case scenario, illustrating the scope of this study within the background project and the future research. As seen, the study comprises material tests on concrete cylinders, and fire tests in combination with static and dynamic tests on RC circular slabs. The findings of this study are of interest to assess the safety considerations of the future SFTB structure.

The investigation of RC slabs subjected to fire and blast comprises a broad field, and some of the topics that fall out of the present research study are here mentioned. For the material testing, the effects of elevated temperatures are investigated on the

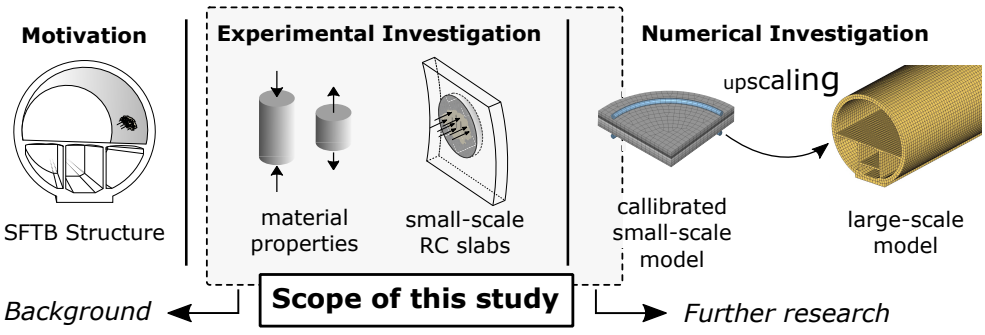

Figure 1.3: Scope of the present research study seen in context.

specific concrete mix intended to be used in future SFTB structures. The behaviour of the material is evaluated at a macrostructural level, and changes at a smaller meso or microstructural level are not addressed. In addition, the material behaviour of this type of concrete at high strain rates is not investigated. For the experiments on RC circular slabs, one geometry configuration is studied, dictated by the dimensions of the shock tube device. Effects of different reinforcement ratios, thicknesses or concrete covers are therefore not addressed. The fire exposure applied on the slabs represents a hydrocarbon fire, using two different fire exposure times. Two different pressure levels are considered in the dynamic tests.

The findings from this research study can be used as input in a non-linear finite element analysis (NLFEA). Preliminary numerical analysis were performed and results can be found in [5]. The experimental data on the mechanical properties at high temperatures can be implemented in a detailed material model in order to develop advanced numerical models. The experiments performed on RC slabs can represent a reliable benchmark to calibrate such models. At a final stage, a large-scale model of the complete structure can be developed, considering the upscaling effects, to investigate different accidental scenarios and thus assess the safety considerations in the design of SFTBs in the *Coastal Highway Route E39* project.

1.3 Objectives

The ultimate goal of this study was to *investigate the combined effect of fire exposure and blast loading on the structural response of RC slabs*, providing a reliable benchmark for further numerical investigation. For this purpose, three research studies were defined, presented as the appended journal publications (Papers I-III), where the following research objectives were addressed:

i Obtain a complete material characterization of concrete at elevated temperatures.

(a) What is the effect of temperature on the uniaxial constitutive (compressive and tensile) behaviour for this type of concrete?

(b) Is there agreement between the obtained results of fundamental material properties and the reported values in the literature and standards?

(c) How is the evolution of the specific fracture energy and internal damage at high temperatures?

ii Evaluate the effect of fire exposure on the residual static structural response of RC slabs.

(a) Is there a change in failure mechanism and structural response after the fire exposure?

(b) Is the ultimate capacity of the RC slab reduced after the fire?

(c) Can the fire-damaged bending capacity be estimated using a simplified approach?

iii Investigate the dynamic structural response of RC slabs under blast loading after a fire exposure.

(a) What is the effect of fire exposure on the dynamic response of the RC slab?

(b) Is there an increase of damage on the fundamental dynamic properties due the blast loading?

(c) Can the dynamic behaviour of RC slabs be assessed using simplified numerical analyses?

1.4 Outline of the thesis

This thesis is divided into two parts. Part I is an extended summary of the work carried out and consists of four chapters. Chapter 1 presents the aim and background of the study, delimiting the scope and research goals. A general background of the research topic at different levels (material, structural and numerical) is given in Chapter 2. Chapter 3 presents the contributions and main conclusions of the different journal publications, together with a discussion of the obtained results and the limitations of the research conducted. In Chapter 4, the concluding remarks of this study are given, also introducing topics for future research. In Part II, the scientific publications are appended, corresponding to the three journal publications (Papers I-III).

Chapter 2

Effect of fire exposure and blast loading on tunnels: material properties, structural evaluation, and numerical modelling

2.1 Introduction

The accidental scenario of the combined action of fire exposure and blast loading in a tunnel structure is a complex problem which presents many difficulties at different levels. On the one hand, concrete material changes its mechanical response when exposed to elevated temperatures or tested at high strain rates. On the other hand, the material characterization is a required, but not sufficient, condition. Despite the decrease on the material performance, the response of the structure may be aggravated or relieved due to rapid temperature increase or stress redistribution from the surrounding elements. In order to study these complex actions on RC structures, numerical models are typically used, which often need to be validated with results from small-scale experimental tests. Advanced numerical models make use of detailed material parameters which are not always available in the literature. In addition, the lack of experimental research studies hinders the calibration of such models, especially in the specific case of combined fire and blast action.

This chapter gives a overview of the effect of fire exposure and blast loading, corresponding to the general context where this study falls under. First, a brief description of the material mechanical behaviour subjected to elevated temperatures and high strain rates is presented. Then, the two loads acting in the structure are described separately, fire exposure and blast loading, also presenting the research available investigating the combined action. Finally, a short introduction into the numerical assessment of this accidental scenario in RC structures is provided.

2.2 Effect of temperature and strain rate on the mechanical behaviour of concrete

2.2.1 Concrete exposed to high temperatures

Concrete is perhaps the most complex building material nowadays used [54]. This complexity increases even more when the material is heated due to the extensive damage caused by elevated temperatures [81], and can be aggravated after cooling [30, 32]. Structural safety requires a good understanding of the behaviour of heated concrete, which can be achieved through an adequate characterization of the mechanical properties at high temperatures. In this section, the behaviour of the overall mechanical properties of concrete at elevated temperatures is presented.

A variation on the mechanical properties is mainly caused by changes in the meso and microstructural level of concrete. As concrete is exposed to high temperature, the evaporation of water from the porous and chemical dehydration of cement causes a build-up of pressure, causing microcracking and internal damage [54]. Other changes occur due to the different thermal expansion between aggregates and cement paste at elevated temperatures, further damaging the material and decreasing its mechanical performance. The temperature values at which these changes take place strongly depend on the mix of the concrete used. The investigation of the changes at a meso and microstructural level is not the aim of this study. There are many research studies available in the literature where such changes are extensively described [57, 58, 65, 67, 83].

The performance of the material is typically evaluated at a larger scale in terms of mechanical properties, such as stiffness and strength in compression and in tension. It is well known that elevated temperatures adversely affect the mechanical behaviour of concrete. Furthermore, such negative effect is often irreversible, i.e. the material does not recover the properties after cooling from elevated temperatures, unlike other material such as steel [31, 38]. To quantify the severity of the thermal damage, comprehensive research has been carried out in the last decades testing normal-strength concrete (NSC) subjected to elevated temperatures [1, 4, 29, 42, 49, 53, 56, 71, 87, 89], some of these studies being also referred to in the codes [18, 19]. In addition to the NSC, many different concrete types are nowadays used, for which the response to high temperatures differs due to the different material composition. Less extensive research has been conducted for example for high-strength concrete (HSC) [6, 9, 29, 81], fibre reinforced concrete (FRC) [61, 74, 75, 84, 100], or self-compacting concrete (SCC) [10, 27, 94]. The effect of temperature on the different mechanical properties of HSC is here described.

High-strength concretes, often characterized with a compressive strength between 60 and 130 MPa, are increasingly popular. The dense microstructure that characterizes HSC has a beneficial effect on the compressive strength, compared to NSC, at room temperature [81]. However, such compact microstructure is highly impermeable and does not allow moisture to escape. This becomes detrimental at high temperatures, resulting in a rapid development of microcracking and a faster deterioration of strength. In addition, favouring steam pressure to build-up may lead to explosive

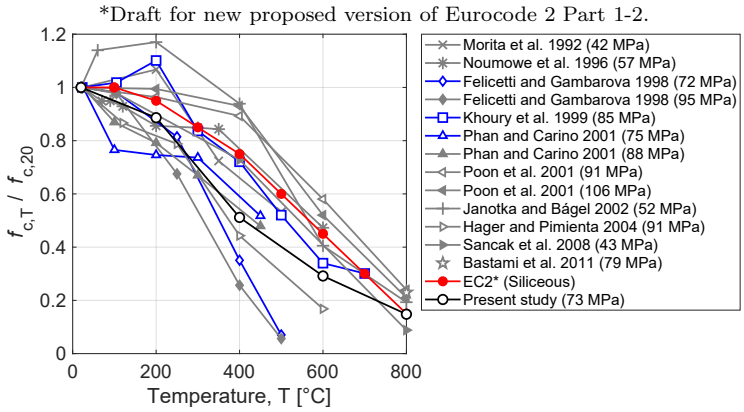

Figure 2.1: Evolution of compressive strength at elevated temperatures [6].

spalling, making HSCs even more sensitive to high temperatures [29]. A commonly adopted solution to prevent the effect of explosive spalling is to add polypropylene (PP) microfibers in the concrete mix, which releases the internal pressure in the material [41, 52].

The most important mechanical properties determining the response of RC members in the case of fire are compressive and tensile strengths, modulus of elasticity, and the stress-strain relationship [57, 91, 93]. Many research studies have investigated the compressive strength and modulus of elasticity at elevated temperatures; data on the other mechanical properties is less available. However, the reported findings from research studies in the literature present discrepancies, even when similar concretes are compared. This is because results from the mechanical tests are greatly influenced by several factors, such as the concrete mix (cement and aggregate type), conditions of the specimen (moisture content, sealing conditions), specimen size, testing conditions (hot or residual), heating/cooling thermal rates, load-level during heating, or stabilization phase duration [11]. The lack of standardization on experimental set-ups and procedures makes it difficult to extract a generalized outcome for the material properties when different studies are compared [57, 67].

Figure 2.1 shows the evolution of compressive strength at high temperature from various research studies. The general behaviour shows a slightly variation of strength between 20 and 300 °C, where in some cases it even increases. Afterwards, a consistent pronounced decrease of the strength is observed up to 800 °C, where only 10-20% of the initial strength is left. As seen, despite the common decreasing trend observed, the strength degradation in HSC is not consistent and significant variation in strength loss is reported in the literature [57]. The relationship proposed in the new version of the Eurocode 2 Part 1–2 [20] is also shown in Figure 2.1 for a concrete with a compressive strength of 73 MPa. As seen, it follows the average decreasing behaviour, and mostly overestimates the residual strength when compared to studies with a similar initial concrete strength.

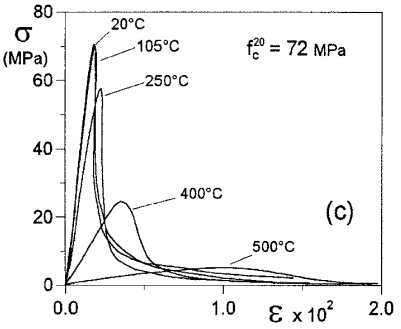

Figure 2.2: Compressive stress-strain curves at different temperatures [29].

The modulus of elasticity typically experiences a more pronounced decrease than the compressive strength at high temperature [81]. Such decrease of stiffness can be attributed to the excessive thermal stresses and changes in the microstructure [57]. An even larger scatter can be encountered when comparing the results from different research studies. In addition, the dynamic modulus is commonly measured, in tests performed in residual conditions, due to the simplicity using ultrasonic pulse velocity (UPV) measurements, where higher velocities indicate better material quality [48]. The dynamic modulus is typically higher than the static modulus because it is measured without load, therefore excluding immediate creep in the specimen.

The knowledge of strength and modulus of elasticity is typically sufficient for structures subjected to small strain conditions using elastic analysis. However, when large strains are involved, e.g. when a structure is subjected to elevated temperature, elastic-plastic analyses are required, involving the use of stress-strain relations at different temperature levels [71]. Such relationships contain information about the complete constitutive behaviour comprising the peak-strength, modulus of elasticity, strain at maximum stress and the ultimate (crushing) strain. It can be also used to calculate the specific fracture energy, i.e. the energy per unit area of crack needed to propagate a crack [30].

Figure 2.2 illustrates typical compressive stress-strain relationships obtained from concrete cylinders at different temperatures. At room temperature the relationship has a nearly elastic ascending branch, with a nonlinear range close to the peak. The curvature of the elastic range can be attributed to the presence of interfaces between the cement paste and the aggregate, including bond microcracks at these interfaces [22]. After the peak, HSCs experience a very steep descending branch due to the brittle behaviour of the material. An increase of temperature causes a reduction of the slope of the elastic range (reduced modulus of elasticity), the maximum stress (reduced compressive strength), and the slope of the descending branch (less brittle material), flattening off the overall stress-strain curve, as seen in Figure 2.2. This results in an increase of the strain at maximum stress and the ultimate strain with temperature.

When concrete is heated in presence of load, concrete exhibits thermal-creep

strains, which is a stress induced component resulting from physical and chemical transformations of the material's microstructure [83]. An important component of the thermal-creep strains is due to transient creep which occurs during the first heating of concrete under load. Such strain, also referred to as load-induced thermal strain (LITS), is much larger than the elastic strain and may contribute to considerably relax and redistribute thermal stresses in heated concrete structures under loading [55]. Thus, structural analyses that do not take the LITS into account may yield inaccurate results, especially for structural elements in compression, e.g. columns and walls. Another beneficial effect of heating under load is that the compacted concrete material inhibits the development of cracks [54]. As a result, a smaller reduction of compressive strength and elastic modulus with increase of temperature is observed, leading to less pronounced effects on the stress-strain relationships between different temperatures [56].

The tensile behaviour is often neglected in concrete since the tensile strength is much lower than the compressive strength. However, the tensile strength is an important property in fire resistance, as cracking is typically due to exceeding tensile stresses and structural damage in tension is often generated by propagation of microcracking. At high temperatures, HSCs experience a rapid loss of tensile strength due to the inner pore pressure in the dense microstructure [57]. Measuring the complete stress-strain relationship in direct tension is complex since it requires special equipment, which makes that experimental results are rarely available in the literature. As temperature increases, the slope of the stress-strain curve in tension decreases, together with the peak stress. Both the strains at peak stress and at failure increase with the temperature, resulting in an increase of the specific fracture energy [12].

2.2.2 Concrete at high strain rates

The behaviour of RC structures subjected to dynamic loads, e.g. blast load, can largely differ from the response under static loading. This is because the material behaviour can considerably change depending on the strain rate to which it is subjected. As a comparison, a static compressive load can be defined at a strain rate of about $3 \times 10^{-5}\,\mathrm{s}^{-1}$ [34], whereas concrete subjected to blast loading can experience strain rates around $1\,\mathrm{s}^{-1}$ [26]. Many studies have shown that the strain rate greatly influences concrete resistance, failure mode, crack pattern, and crack velocity [13,16,77–79]. The effect of strain rate on concrete is typically evaluated using the dynamic increase factor (DIF), which is the ratio between the dynamic and the static strength for a given strain rate value [68], expressed in a log-normal or log-log scale.

Figure 2.3 shows a comparison of several research studies investigating the dynamic behaviour of concrete at high strain rates, both in compression and in tension. The analytical relationships presented in the Model Code (2010 [36] and 1990 [34]) are also shown. As seen, concrete exhibits an increase in compressive strength when loaded at higher strain rates than the static loading case. A similar behaviour is observed for the tensile behaviour, exhibiting an even larger DIF. The large variation between the compared studies is mainly caused by the diverse loading techniques, and different methods to analyse and interpret the results [16]. Despite the scatter in the

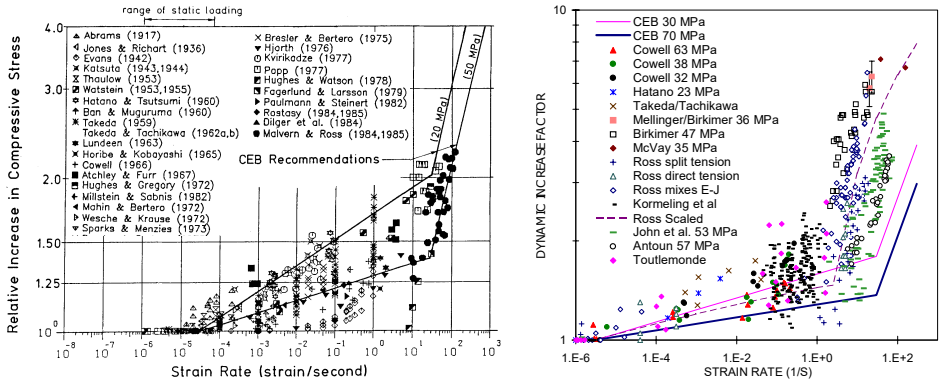

(a) (b)

Figure 2.3: Strain rate effects on the (a) compressive strength [16], and (b) tensile strength [68].

experimental values, two defined logarithmic increase intervals can be distinguished in both cases, with different strain rate dependencies. A first interval, with a lower increase rate, is observed up to the so-called *transition zone* [50], at strain rates about $30-50\,\mathrm{s}^{-1}$. After, another interval with a considerably higher increase rate is observed.

The dynamic behaviour of concrete and its rate-dependent response can be explained through different effects: i) through the rate dependency of the growing microcracks (influence of inertia at the microlevel); ii) through the viscous behaviour of the bulk material between the cracks (viscosity due to the water content), and iii) through the influence of structural inertia forces [76, 78, 79]. For quasi-brittle materials like concrete, the first two effects are important for relatively low and medium strain rates. At higher strain rates, the effect of structural inertia forces becomes dominant and significantly increases the DIF, although the other two effects cannot be neglected [76].

The modulus of elasticity also increases during dynamic loading. However, the enhancement is less pronounced that that observed for tensile strength. The enhancement of modulus of elasticity at dynamic loading can be ascribed to the decrease of internal microcracking at a given stress level with increasing strain rate [16]. Relationships of DIF for the modulus of elasticity are also proposed in the Model Code 2010 [36].

2.2.3 Combined effect: heated concrete at high strain rates

The previous subsections separately describe the effect of high temperatures and strain rate on the concrete behaviour. In an accidental scenario with a fire and a subsequent blast load, the two effects may be present together in the material. There is scarce research investigating the combined effect of strain rate effects on thermally damaged concrete. Here the main findings are briefly presented.

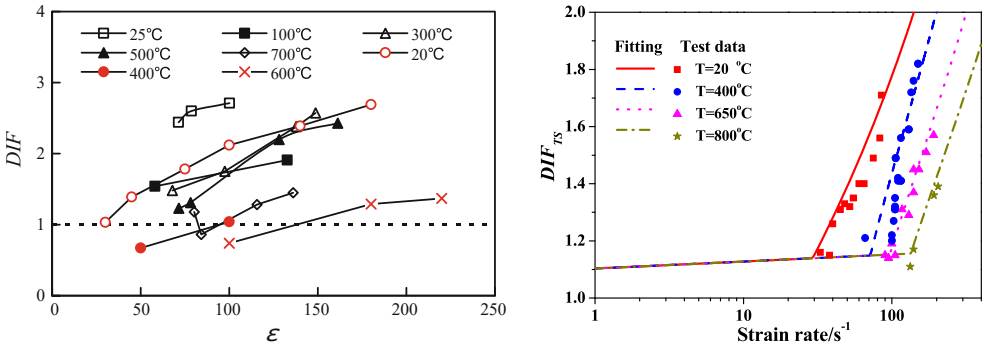

Figure 2.4: Effect of high temperatures on the (a) DIF [45], and (b) transition zone [21].

The effect of elevated temperatures on the dynamic behaviour of concrete has been mostly investigated for plain NSC and HSC with compressive strengths between 30 and 85 MPa [21, 44, 45, 64, 99, 101, 103], and 135 MPa [62]. Some results are also available on FRC [17, 21] but the results are not presented here. Most of the studies investigate the effect of temperature on the DIF for the compressive strength [21, 44, 45, 62, 64, 99, 101, 103], with only a few evaluating the effect on the DIF for the tensile strength [17, 99]. Temperatures up to 1000 °C have been investigated, together with a wide range of strain rates up to $300\,\mathrm{s}^{-1}$. In addition, the dynamic behaviour has been also investigated comparing the effects of temperature in hot conditions and in residual [21, 99].

Figure 2.4 shows some of the reported results on the variation of DIF at different temperatures. As seen, concrete still exhibits a great strain rate effect after exposure to high temperatures despite the considerable degradation of the material. A recent comparison of the previous studies concluded that the strain rate effect plays a dominant role for temperatures below 400 °C, without significantly affecting the residual compressive strength [64]. For temperatures in the range 400-600 °C, the thermal softening of the material is in balance with the strain rate increase for the concrete strength. For higher temperatures, the considerable decrease of strength of concrete with temperature shows less sensitivity to moderate strain rate. Some studies [21, 62, 99] reported that an increase in the maximum exposure temperature causes a shift of the transition zone towards higher strain rates, as clearly shown in Figure 2.4b.

Most of these studies concluded that further investigation is needed in this research topic, as the few and sometimes not consistent experimental data is not sufficient to accurately define strain rate relationships which are also temperature dependent. As mentioned in the previous subsections, high temperature effects and strain rate effects may be greatly influenced by the testing equipment used. It is therefore expected that the combination of the two phenomena yields even larger variations in the results. Alternatively, considering the effects from the two phenomena separately might be

a better approach, firstly using quasi-static temperature-dependent relationships to consider the thermal damage in the mechanical properties as concrete is heated, and afterwards consider the DIF of the material at high strain rates using the strain rate constitutive laws at room temperature.

2.3 Structural effect of fire exposure and blast loading on tunnels

2.3.1 Fire exposure

Fire has been regarded as one of the main physical threat for concrete and has always been a challenge for the design of RC structures [3, 8, 33, 39, 43, 54, 97]. Many different concrete structures may be subjected to a fire throughout their service life, e.g. bridges, buildings and offshore structures. However, such extreme load is particularly dangerous for tunnels, and even if accidents are generally less likely to occur in tunnels than in open air, the consequences can be far more serious [14]. Disastrous events that occurred in tunnels in Europe, such as those of the Mont Blanc (1999), the Gotthard (2001), the Tauern (2002), the Frejus (2005), and the Viamala (2006), increased the attention paid to safety issues, underlining the risks and consequences of high thermal loads on reinforced concrete structures from human and economical points of views. In addition, this problem will potentially get worse in the future, since more and longer tunnels are conducted as traffic densities continue to increase [14].

The effect of a fire event on the load-bearing capacity of a tunnel structure is usually considered through the heat exposure to which it is subjected. Due to the confined conditions, fires in tunnels can be more severe than equivalent fires in open air, in terms of growth rate and maximum temperatures, leading to a considerably higher heat exposure on the structure [14, 46]. The actual fire exposure depends on different factors, such as the geometry of the tunnel, the ventilation system, or the type of fire. For this reason, standardized time-temperature curves are typically used to calculate temperature rises in a structure. Figure 2.5 shows a hydrocarbon fire curve, typically used in the case of tunnels [47], characterized by a fast growth rate exceeding 1000 °C within the first 15 min.

The behaviour of the structure exposed to fire essentially depends on the temperature levels reached along the cross-section. The rapid heating of the fire initially leads to a large thermal gradient inside the concrete member, where mostly the region closer to the surface is exposed to high temperatures, and thus seriously damaged. Nevertheless, fire events in tunnels can last several days [46], which also makes the concrete in the inner zones likely to be exposed to very high temperatures. The pronounced decrease of concrete mechanical performance at high temperatures is often in detriment of the structural capacity. In general, RC structures lose great part of their load-bearing capacity when also the reinforcement is exposed to high temperatures. Failure in the structure could occur due to loss of bending or tensile strength, loss of bond, loss of shear strength, loss of compressive strength and spalling of concrete [54]. The effect of fire on the structural capacity may then depend on

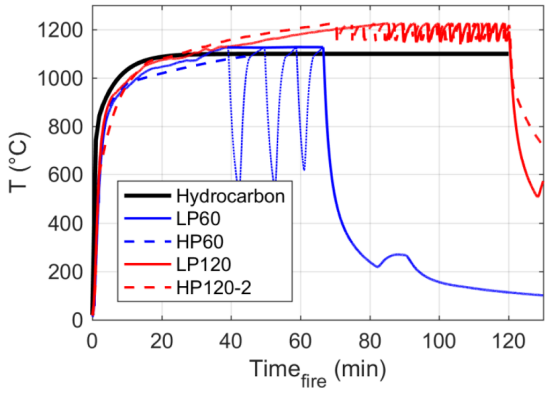

Figure 2.5: Theoretical and experimental hydrocarbon fire curve [25].

many factors, such as the surface temperature (related to the type of fire), the cover thickness (insulation for reinforcement), the fire duration (progressively damaging the inner regions), and the mechanical properties of concrete (temperature dependent and adversely affected).

Fire and accidents involving high temperatures should be properly investigated in a RC structure both during the preliminary design stage and in the assessment of the residual capacity after a fire event. The performance assessment of RC structures such tunnels is typically carried out through experimental investigation using temperature-time curves on individual structural members, such as beams, slabs or, in this case, tunnel linings. A wide range of research activities comprising experimental tests and modelling methods have been devoted to the investigation of this problem [2, 28, 63, 82, 86, 88, 95, 96, 98, 102]. Such studies contribute to the development of design criteria and guidelines [14, 18, 19, 47, 59] to the evaluation of the fire resistance, often regarded as the ability of a concrete element to fulfil its required functions for a specified fire exposure and exposure time.

A significant challenge arises, however, when applying detailed small-scale behaviour of concrete at high temperatures to the performance of a structural member in realistic fires. In this case, the unevenly distributed thermal damage, the change in failure mode or the appearance of explosive spalling may play an important role in the fire resistance of a tunnel structure. The behaviour of such structural elements within the context of a complete structure can vary widely from independent responses [38]. Structural members subjected to high temperatures can exhibit enlarged thermal stresses due to the restraining forces induced by the rest of the structure, leading to an early collapse. On the contrary, a tunnel structure could benefit from an improved robustness, where, despite failed individual members, the overall structure remains intact due to load and stress redistribution [38]. The use of numerical simulations on calibrated models can be of great interest, allowing to predict structural interactions and recreate alternative fire scenarios.

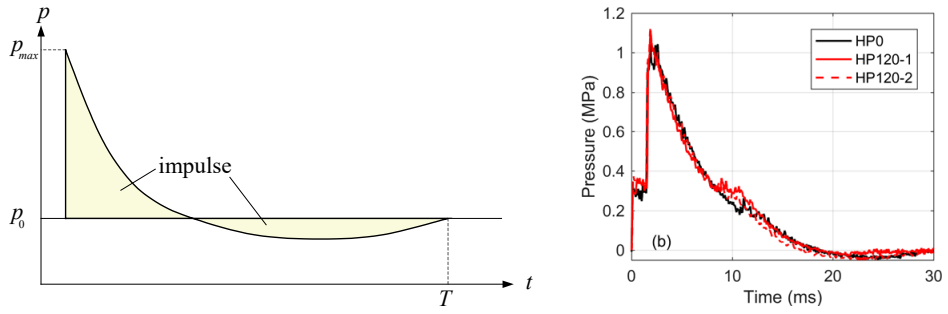

Figure 2.6: (a) Schematic view of an ideal shock wave; and, (b) experimental measurements of the shock wave applied by a shock tube device [25].

2.3.2 Blast loading

Dynamic loads involve a wide range of time intervals, e.g. vehicle crash, earthquake, drop hammer and blast, yielding different responses both for the material and the overall structure [40]. In the accidental scenario of an internal explosion inside a tunnel, a blast load is generated which impinges the structure as a shock wave.

A blast load or shock wave is usually defined in terms of peak load (pressure or force) and impulse; this latter being defined as the area enclosed by the load-time curve [60]. The experimental investigation of structural members subjected to a blast load can be performed by means of a shock tube device [23]. Figure 2.6 shows the idealized shape of the shock wave, together with the experimental values from the shock tube [25]. Unlike explosive charges, a shock tube device has the advantage of generating a planar wave front (uniformly distributed pressure pulse) acting on the structural element, in addition to increasing repeatability (Figure 2.6b) and being less hazardous compared to explosive charges. A uniform load condition is important for both precise experimental measurements and modelling purposes [24], unlike the complex pressure evolution with a spherical wave front generated by explosive charges.

Figure 2.6a shows the idealized form of a shock wave, where the pressure raises from the ambient pressure to the peak pressure almost in an immediate period of time. The pressure then decreases to ambient pressure, forming a partial vacuum in the process. Such behaviour is well distinguished in the experimental measurements shown in Figure 2.6b.

Often for structural dynamic analyses, a designer is mainly concerned with final states (i.e. maximum displacements and stresses) rather than a detailed knowledge of the response histories of the structure. In this context, the structural response evaluation of RC members can be carried out through the generation of a pressure–impulse (P–I) diagram, a commonly used design tool that allows to evaluate the damage level of structural components induced by blast loads [7]. For a certain response parameter (maximum displacement, ductility, etc.), the diagram provides the

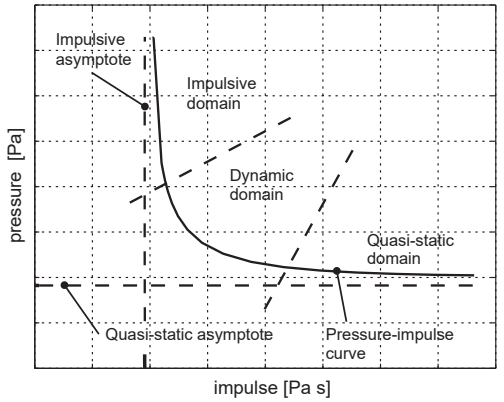

Figure 2.7: Scheme of a typical pressure-impulse (P–I) diagram [24].

combination of pressure and impulse values that produce the same limit state level in the structural member [24].

Figure 2.7 shows an example of a P–I diagram for a simply supported RC plate subjected to blast load. As seen, the P–I curve itself defines two regions: above and to the right of the curve where the selected limit state is exceeded, and below and to the left where the selected response parameter does not exceed the limit state. The P–I diagrams may contain several curves defining different degrees of damage, limit state or failure criteria (e.g. bending or shear) [92].

The dynamic structural response of an element is governed by a strong relationship between the natural frequency of a structural element (ω) and the duration of the acting load (t_d) [15, 60]. Such relationship can categorize the structural behaviour into three regimes: impulse, quasi-static and dynamic [7], which are clearly identified in the P–I diagram (Figure 2.7). Adopting this classification, the maximum response may depend only on the applied impulse (impulsive region), only on the pressure value (quasi-static region), or on both the impulse and pressure values (dynamic region) [60]. Horizontal and vertical asymptotes define limiting values for each parameter. The impulsive asymptote represents the minimum impulse required to reach a certain limit state level, which is approached asymptotically by the P–I curve at high pressures, while the quasi-static asymptote defines the minimum peak pressure required to reach the specified limit state [24].

The material response with respect to the strain rate was described in Subsection 2.2.2, showing the DIF that concrete experiences when it is subjected to high strain rates. Such strain rate does not only depend on the acting load (pressure and impulse values), but also the stiffness of the structural element plays an important role. For an undamped, perfectly elastic system subjected to an exponentially decaying load, the three loading domains may be quantified as the following [7]:

- Impulsive: $\omega \cdot t_d < 0.4$
- Dynamic: $0.4 < \omega \cdot t_d < 40$

- Quasi-static: $\omega \cdot t_d > 40$

A similar blast load then may be within the impulsive domain when acting to a certain structure, while being in the dynamic domain for a stiffer element.

2.3.3 Research studies on RC structures under fire exposure and blast loading

Limited research is available in the literature on the combined effects of fire and blast loads on RC structures, and is mostly confined to numerical studies. Kakogiannis et al. [51] and Pascualena et al. [80] reported the analysis of the blast bearing capacity of RC hollow core slabs when they are subjected first to fire and then to a blast load. The blast response of the hollow core slab was assessed numerically in [80] and both numerically and experimentally in [51]. The blast tests were conducted in hot conditions by using explosives, although reaching temperatures below 500 °C. A numerical investigation into dynamic responses of RC columns subjected to fire and blast was proposed by Ruan et al. [85]. Zhai et al. [104] reported an experimental and numerical investigation of RC beams subjected to a blast after exposure to fire, in residual conditions, reaching temperatures up to 750 °C. Moving the attention to tunnels, the response behaviour of a tunnel lining under the action of vehicle impact and fire load has been numerically analysed [105]. A numerical simplified procedure was proposed by Colombo et al. [26] for the response behaviour of underground tunnels subjected to combined fire and internal explosion.

The scarce available research on the combined effect of fire and subsequent blast loading clearly highlights the need for further investigation. The two loads separately present a great challenge at a material level due to the testing conditions and the effect of elevated temperatures and strain rate on the response of concrete. Such complex behaviour may differ when the combined effect is evaluated in a large-scale structure, such as a tunnel. Numerical simulations could then be the most feasible tool to study and assess this accidental scenario. However, reliable numerical tools are calibrated comparing their predictions with small-scale experimental results. In this context, further experimental investigation on concrete members, such as RC slabs or RC beams, are still needed.

2.4 Numerical modelling strategy

Nowadays, it is possible to perform numerical studies using advanced numerical tools which can realistically simulate complex structural problems, such as fire exposure or blast loading. Numerical models can be very useful to carry out safety checks and assessments, and develop design rules to ensure structural integrity under extreme events. The accidental scenario of fire exposure and blast loading can be numerically tackled by performing two different analyses: i) a thermo-mechanical (staggered) analysis to evaluate the effects of the fire exposure, and ii) a dynamic analysis to include the blast loading.

A thermo-mechanical analysis is a widely used method for the assessment of fire resistance of concrete structures, being incorporated in the majority of the available FE software, e.g. Diana or Abaqus. This method consists of two separate thermal and mechanical analyses, also known as a staggered analysis, where the output temperature field of the former is used as input to the latter to obtain the resulting strains and stresses. This analysis typically incorporates temperature-dependent relationships in the material models to account for thermal expansion and decrease of mechanical properties at elevated temperatures. The main disadvantage of the thermo-mechanical models is that the two analyses are not fully coupled, thus ignoring variations in the inner pore structure. This may provide less accurate results when moisture and evaporation play a significant role in the material behaviour, especially at temperatures between 100 and 200 °C. Nevertheless, validation of the results from such methods has shown to be reasonably accurate for the prediction of deformation of individual members exposed to fire, such as beams or slabs, as well as columns when the effect of transient creep (or LITS) is incorporated into the model [35]. For this reason, these models offer reasonably accurate and cost-effective solutions for predicting fire resistance in terms of total deformations, after one or two hours of fire exposure [90].

A more advanced fully coupled thermo-hydro-mechanical model incorporates chemical and physical changes in the microstructure of the material, allowing to predict explosive spalling in the structure [90]. However, such models can be highly computationally demanding due to the level of detail in the material evaluation and therefore may not be feasible for relatively large structures.

The blast load can be simulated by performing a dynamic analysis, using a FE software capable of performing explicit time integration analyses, e.g. LS-DYNA or Abaqus, due to the high strain rates of the load. As models commonly evaluate the material at a macro or mesoscale level, the strain rate effects due to inertia at microstructure and due to water content are not modelled, and should be incorporated using a DIF relationship in the material model (Subsection 2.2.2). The effects due to structural inertia forces, however, which cause the sharp enhancement of the DIF, should be automatically accounted for in the numerical analysis [78].

A numerical study by Magallanes et al. [66] investigated the strain rate effects of concrete in compression and in tension, comparing the numerical predictions with experimental data. The study showed that in compression, the FE model captured the effects of structural inertia for high strain rates, and therefore only using the first branch of the DIF relationship showed satisfactory predictions. However, a different behaviour was observed in tension, where the two branches of the DIF relationship were needed to properly simulate the effects due to structural inertia forces [66].

The relatively simple thermo-mechanical models combined with a dynamic analysis can be extremely useful predicting tools if properly applied. In an engineering design context, it is essential that predictions from a numerical model lead to acceptable design decisions. The location and severity of an accident in a RC structure are usually unknown, being numerical models often used by designers to examine various scenarios [14]. The use of advanced structural analyses therefore provides a better understanding of a structure subjected to exceptional load conditions in order to develop a more reliable design approach taking into account global safety

considerations. Nevertheless, modelling needs to be based on a realistic behaviour to avoid misleading results. Numerical models should therefore input consistent material properties and be calibrated in order to be considered reliable for practical use.

Chapter 3

Results and discussion

3.1 Introduction

This chapter describes the contributions in Papers I, II and III. The main experimental findings are first presented for each journal publication separately. Afterwards, the obtained results and limitations of this experimental programme are discussed.

Figure 3.1 shows the connection between the three journal publications. The main goal of the project was to investigate the combined effect of fire exposure and blast load on RC slabs. As described in Chapter 2, the effect of each of these loads can be evaluated both from a material and a structural perspective. In this case, the study of the material behaviour was focused on the effect of high temperatures. The changes on the concrete behaviour are first studied in Paper I, through an extensive characterization of the material mechanical properties in residual conditions after exposure to elevated temperatures. The effect of temperature on material properties is not always linearly related to the structural response of slabs exposed to fire, which is also governed by other structural effects, e.g. temperature distribution across the thickness and stress redistribution. This can affect the structural member from a minor capacity decrease to a change of failure mode and early collapse [38]. For this reason, Paper II investigates the effect of fire on the static structural response of RC slabs. The findings in Papers I and II provide a better understanding of the slab behaviour exposed to fire, allowing to investigate the combined effect of fire and blast load on the RC slab in Paper III.

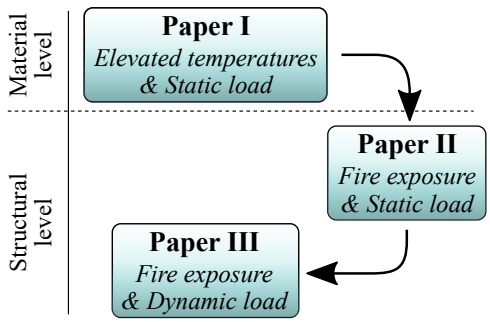

Figure 3.1: Schematic view of the connection between publications.

3.2 Summary of contributions

3.2.1 Paper I

A proper definition of the material properties is a basic precondition of a reliable numerical model. A complete overview is rarely available in the literature, where only the basic properties, such as the compressive strength and the modulus of elasticity, are typically investigated. For this reason, the effect of elevated temperatures on the mechanical behaviour of concrete was experimentally investigated on concrete cylinders in residual conditions, after a single thermal cycle at different elevated temperatures (200, 400 and 600 °C), also including some results at 800 °C.

The obtained complete compressive and tensile constitutive response of concrete allowed to calculate additional material parameters such as the fracture energy and the internal damage, and their evolution at high temperatures. In addition, a comparison with previous research studies and standards (Eurocode 2-Part 1-2 [20], Model Code 2010 [36]) confirmed the negative effect that elevated temperatures cause on the basic mechanical properties of concrete. The relationships of mechanical properties at high temperatures proposed in the new version of the Eurocode 2-Part 1-2 partially agree with the experimental findings, even though a large scatter in the results was found in the literature. The relationships of the specific tensile and compressive fracture energy, respectively presented by the Model Code 2010 [36] and Nakamura and Higai [70], are not meant to, and should not, be used at high temperature as they yield inaccurate results. In addition, the model by Nechnech et al. [72], was found to accurately predict the evolution of internal damage at elevated temperatures in tension, although it requires detailed material parameters which are seldom found in the literature.

Results from the comprehensive experimental approach presented can be instrumental to the parameter definition and calibration of common constitutive numerical models for concrete at high temperatures, increasing accuracy on the prediction of the structural behaviour. In addition, results from basic properties may contribute to the already available data from the literature, where discrepancies between research studies are reported.

This work is described in the paper "Material characterization approach for modelling high-strength concrete after cooling from elevated temperatures".

3.2.2 Paper II

The characterization of the material behaviour at high temperatures does not provide a complete description of the structural response of a member subjected to fire, since other effects, such as reinforcement or stress redistribution, need to be taken into account. In this contribution, the effect of fire exposure in the static structural response of RC slabs was investigated. A hydrocarbon fire curve was applied to the slab by means of a gas burner, studying two fire exposure times (60 and 120 min) in addition to the reference (non-exposed) case. The main objective was to evaluate the effect of fire exposure on the load-bearing response of the slab. Simplified mechanical models (including the yield-line approach) were used to discuss the obtained experimental

results. Thermocouples embedded in the specimen and a UPV equipment allowed to study the effect of high temperatures across the thickness, and evaluate the decrease of the overall stiffness of the slab.

Results of the load-deflection response showed two main peak loads, corresponding to two different structural mechanisms. A stiffer peak was first obtained through an arch mechanism, caused by the specific set-up used in the tests, which enhanced the bending capacity. The arch peak load was considerably reduced after the fire exposure, due to the negative effect on the concrete mechanical behaviour. At large deflections, the tensile membrane action (TMA) enhanced the ultimate load reached. Unlike the arch peak load, the ultimate load was not significantly influenced by the exposure to high temperatures. This was mainly due to the strong recovery of steel after cooling, thus confirming the robustness and structural reliability of this RC slab in residual conditions.

The experimental investigation conducted may contribute to develop simplified design methods for assessing the influence of fire exposure on the capacity of RC slabs. In addition, measurements of the complete load-deflection response can contribute to validate existing models to predict the enhancement of bending capacity due to the arch effect and its reduction after exposure to high temperatures, as well as the enhanced ultimate load due to the TMA. This can be useful to assess the robustness and reliability of the structural member subjected to fire exposure.

This study is presented in the paper "Failure characteristics of reinforced concrete circular slabs subjected to fire exposure and static load: an experimental study".

3.2.3 Paper III

The combined action of fire exposure and explosion load plays an important role for the investigated accidental scenario in the SFTB structure. For this reason, the structural performance of RC slabs subjected to fire exposure and subsequent blast loading was studied. In this study, specimens identical to those tested in Paper II (RC circular slabs) were used. A hydrocarbon fire curve was applied by means of a gas burner, considering the same two fire exposure times (60 and 120 min) in addition to the non-exposed case. Dynamic tests were then carried out in residual conditions using a shock tube device. Two different pressure histories with respective peak pressures of 0.35 and 1.1 MPa were evaluated. Measurements taken from a UPV equipment, thermocouples embedded in the specimen, and accelerometers attached on the specimen, allowed to study the effect of high temperatures across the thickness and the dynamic response of the thermally damaged RC slab. Simplified numerical tools (SDOF and FE) were used to discuss the obtained results.

Results showed that thermal damage from the fire exposure causes a reduction of the overall stiffness in the RC slab. As a consequence, the main frequency of the specimen is considerably reduced, by half, thus elongating the oscillation period. Such damage in the specimen leads to a plastic state with irreversible deformations. As a result, higher energy is dissipated, leading to an increase of the damping ratio. The blast load has a relatively low effect on the main frequency of the specimen, while further affects (increases) the damping ratio. In addition, similar measurements

from three accelerometers at the same distance from the centre indicate a comparable thermal damage throughout the exposed region, despite the unevenly distributed spalling region after the fire tests. Results from a linear elastic FE model agree with the experimental frequency and deformation of the first mode of vibration, therefore validating the simply supported boundary conditions from the experimental test set-up. Moreover, similar time history acceleration values at the central point are achieved using the simplified SDOF model, although slightly overestimating the stiffness of the slab and thus showing a lower oscillation period compared to the FE model and the experimental results.

The experimental investigation presented contributes to the few research studies available in the literature investigating the combined effect of fire and blast on RC structures. This can provide a reliable benchmark for the development and calibration of numerical models, considering the complexity of such load scenario involving temperature and strain rate effects on the material and structural behaviour.

This work is described in the paper "Experimental investigation on the structural response of RC slabs subjected to combined fire and blast".

3.3 Discussion and limitations

The experimental findings presented in the three journal publications are discussed in this section, addressing the common topics of the different contributions.

3.3.1 Effect of thermally damaged stiffness on the static and dynamic response of RC slabs

The stiffness of the material plays an important role on the structural behaviour both under static and dynamic loads. As presented in Paper I, exposure at elevated temperatures affects the modulus of elasticity of concrete, being strongly reduced as maximum temperature increases. Such decrease is even more pronounced than that observed for the compressive strength.

The exposure at elevated temperature also leads to a decrease of the overall stiffness of the RC slab exposed to fire. The stiffness of the specimen mainly depends on the fire exposure and the temperature levels reached across the thickness. The change in stiffness, however, may not correspond to that observed in the modulus of elasticity. There are two aspects which should be taken into consideration. Firstly, the temperature in the slab is not applied at the slow rate used for the material testing, since fire exposure is characterized by a rapid growth to high temperatures. Structural effects are therefore present in the specimen, potentially leading to induced stresses and increased microcracking, which can cause further reduction of the overall stiffness. In addition, concrete is not the only material present in the slab. Steel reinforcement greatly contributes to the overall stiffness of the specimen, especially when it is cooled to room temperature after the fire exposure. The strong recovery on the steel material properties may prevent, up to a certain level, the strong decrease of stiffness of the RC slab.

A quantitative measurement of the stiffness reduction is obtained when comparing the ultrasonic pulse velocity measurements. The UPV is obtained by measuring the travelling time of a pulse-wave through the concrete material of the slab. As concrete is exposed to elevated temperatures, microcracking in the material increases the travelling time. From the results presented in Paper I, a relationship between the UPV and temperature can be obtained, which can be related to the direct UPV measurements taken across the thickness of the slab in Papers II and III, where the UPV decreases as the fire exposure time increases.

The thermally damaged stiffness after fire exposure is clearly visible in the experimental results presented in Papers II and III. The static response of the heated RC slabs is investigated in Paper II in terms of load-displacement curve. The slope of the first branch of such curve shows the stiffness of the tested structural member. The effect of high temperatures on the stiffness can be easily recognized as there is a clear change (reduction) in the slope for the exposed specimens, which is further reduced as the exposure time increases. The effect of fire exposure on the dynamic response of the slab is investigated in Paper III. Among the dynamic properties evaluated, the natural frequency is known to be directly related to the stiffness of the member. This study shows the considerable effect of fire exposure on the stiffness, as the natural frequency is reduced by half when the RC slab is exposed to a 120-min fire.

Another important point of the thermally damaged stiffness is regarding modelling structures exposed to blast. Generally, the fluid dynamic process is considered uncoupled from the structural behaviour due to the high stiffness of structural members, allowing to apply pre-defined pressure-time histories to the structure. In this case, the reduction of structural stiffness of the slabs caused by the effect of fire exposure could arise some doubts on this. However, a comparison of measured pressure-time histories presented in Paper III showed well repeatability between the different specimens, even those exposed to fire, thus confirming that fluid-structure interaction can be disregarded for this case.

3.3.2 Fire exposure: residual and hot conditions

The objective of this project was to investigate the combined action of fire exposure and blast loading in RC slabs. The interaction between these two loads can be evaluated in hot conditions, i.e. at maximum temperature, or in residual conditions, i.e. with a cooling phase after the fire exposure. Performing tests in hot conditions could be considered more realistic when evaluating the accidental scenario in a tunnel. However, in a laboratory setup it is rather complicated to apply a shock wave (or even a static load) to a specimen exposed to a fire curve. The most convenient and feasible alternative could be, then, to perform the test in residual conditions after the specimen has cooled to room temperature.

In this experimental research study, the effect of high temperatures was investigated in residual conditions applying a cooling phase to the concrete cylinders and RC slabs. This leads to some differences in terms of structural response, compared to the real case, which need to be considered.

At a material level, elevated temperatures cause a considerable permanent damage

to concrete material, see Chapter 2. Evaluating concrete mechanical properties in residual conditions may be more conservative since additional thermal damage can occur during the cooling phase [29]. This is very dependent on the heating and cooling rates used, which should be sufficiently low to avoid any structural effects on the concrete cylinders. Steel material, on the contrary, experiences a strong recovery of its mechanical properties after cooling from elevated temperatures (up to about 600 °C) [31].

The residual mechanical properties of concrete are of great interest when considering safety aspects of a RC structure after a fire event. Knowing the behaviour of the material after fire exposure can enable the assessment of the structure reliability and robustness, and therefore determine the severity of the repairing action. In this context, a limitation of the experiments performed in Paper I may be the small sample size used, resulting from a trade-off between the temperature values evaluated (target temperatures), the properties investigated (mechanical tests performed) and the number of nominally identical tests (repeatability). Nevertheless, the increase of target temperature led to smaller scatter in the obtained results for most of the properties studied.

At a structural level, the response of the RC slab is obviously affected by the testing conditions, especially due to the behaviour of the reinforcement. The results provided in Paper II show that high temperatures were obtained all over the thickness of the RC slab. Nevertheless, reinforcement grid, especially in the tensile side, recovered full strength and ductility after the cooing phase. This is clearly seen in the load-deflection results in Paper II, as the ultimate load reached by the different specimens was not significantly influenced by the fire exposure or exposure time. If the tests were performed in hot conditions, considerable thermal damage would most probably be present in the reinforcement, thus considerably decreasing the ultimate capacity of the heated RC slab.

3.3.3 Fire exposure: scale effects

This research study involved small-scale experiments in RC slabs. Experimental testing is generally affected by scaling effects, meaning that the dimensions of the investigated structural member are often smaller than the real structure. This factor should be considered when analysing the obtained results, in order to properly use the findings in the assessment of a large-scale structure.

The investigated accidental scenario considers a fire exposure prior to the blast loading. For a tunnel structure, such as the SFTB, a hydrocarbon fire curve with an exposure time of 120 min should be used [47]. Because of the relatively small dimensions of the RC slab tested, Paper II shows that such fire exposure causes high temperatures across the whole thickness of the specimens, reaching about 370 °C on the non-exposed side. The thickness of a real-scale tunnel section is several times larger than the one here studied, therefore affecting the temperature profile across the thickness.

Figure 3.2 compares the experimental temperature distribution obtained on the tested RC slab and the numerical temperature distribution simulated in a real tunnel

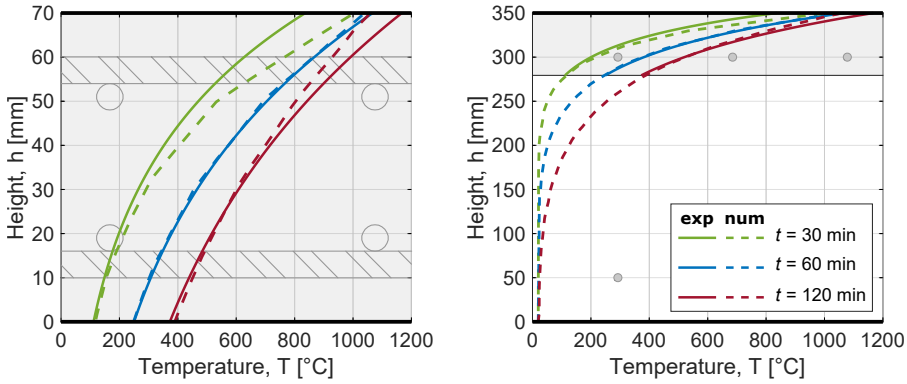

(a) (b)

Figure 3.2: Temperature distribution across the thickness of (a) RC slab (Paper II), and (b) tunnel section [26].

section [26], after exposure to a hydrocarbon fire curve. The experimental results are illustrated by a continuous line, while a dashed line denotes the numerical values. The top surface represents the exposed surface, and the green, blue, and red lines indicate the temperature profiles across the thickness after 30, 60 and 120 min, respectively.

Figure 3.2a shows agreement between the experimental and numerical temperature distribution across the slabs thickness, although the temperature on the exposed surface is slightly different. As shown in Figure 3.2b, severe thermal damage caused by high temperatures is limited to a relatively small depth of the cross-section due to the low thermal conductivity of concrete. A large part of the cross-section remains considerably less damaged or even undamaged, as for example the tensile reinforcement.

Although the two loads might be applied in a short time in a real accidental scenario, i.e. the blast load is applied while the structure is still exposed to high temperatures, the thermal damage would not be as severe as in the tested RC slab. The compressive side of the specimen would be considerably affected (concrete subjected to high temperatures), while the tensile side would experience almost no damage (steel properties not affected). Comparing the temperature distribution in Figure 3.2b with the cross-sectional analysis provided in Paper II, we can see that the small-scale specimen tested in residual conditions may be somehow similar to the real accidental scenario in hot conditions.

The temperature distribution across the thickness of a RC structure clearly determines the change in the capacity or dynamic behaviour after a fire exposure. From the comparison in Figure 3.2, the robustness of the RC slab obtained in Paper II, with a similar ultimate capacity for the exposed specimens, could be representative of the behaviour of the large-scale structure. The effect on the dynamic properties may be less severe than presented in Paper III. Nevertheless, the material characterization

of concrete at elevated temperatures in Paper I provides the information required to numerically investigate the scaling effects on the SFTB.

3.3.4 Dynamic behaviour of heated RC slabs

The dynamic behaviour of RC slabs subjected to fire exposure and blast loading is presented in Paper III. The effect of such loads can be evaluated studying the change in dynamic properties such as the natural frequency, which is linked to the oscillation period, and the damping ratio. The dynamic tests were performed using two different pressure levels, low-pressure (LP) and high-pressure (HP). The RC slabs were dimensioned, within the limits of the shock tube device, to obtain an elastic response when the LP shock wave was applied. The effect of only the fire exposure on the dynamic response of the RC slab can therefore be evaluated through the results from the LP tests, while the combined effect of fire and blast loading can be studied comparing those results to the ones obtained in the HP tests.

Results indicate that the natural frequency of the slabs is mainly influenced by the thermal effect from the fire exposure, due to the direct relation between the frequency and the stiffness previously described. The effect on the frequency due to the effect of blast loading alone can be quantified when comparing the results for the non-exposed specimens at different pressure values (LP0 and HP0). Such variation, however, becomes less significant when the specimen is exposed to fire, where similar values of natural frequency are obtained between the LP and HP tests. The two exposure times (60 and 120 min) lead to similar frequency reduction, meaning that the high temperatures reached across the thickness after 60 min induce sufficient irreversible thermal damage for which the stiffness of the specimen is considerably reduced. This slightly differs from the experimental results from the static tests observed in Paper II, where the load deflection curve shows a visible difference of initial stiffness comparing the specimens exposed to 60 and 120 min.

The central acceleration response can also be used to compare the dynamic behaviour of the slab under different load conditions. The response from the different tests show an increase of the period of oscillation, which is expected since the natural period is inversely related to the frequency of the specimen, thus increasing when the stiffness is thermally damaged. Moreover, the amplitude of the acceleration response slightly increases for the LP tests exposed to fire, further increasing with a longer fire exposure.

A different behaviour is observed for the central acceleration response of the HP tests. One could expect larger amplitudes when the high-pressure is applied, especially for the thermally damaged specimens. However, this effect was only observed for the HP120 test, while a fire exposure of 60 min led to similar amplitude than the non-exposed specimen (HP0). This effect is even clearer when comparing the derived central displacements, where only the results of the HP120 test show a significant increase (three times larger). This may be due to a non-uniform thermal damage along the exposed surface of the specimen. The crack pattern presented in Paper III shows a circular crack on the exposed surface of the HP60 test. This can be attributed to a difference of stiffness between the outer part and the inner core of the specimens

caused by a variation of the maximum temperature levels reached throughout the fire test. In Paper II, this effect is related to the radial cracks on the exposed surface of all the specimens subjected to fire exposure. When the specimen is exposed to a 60-min fire, a significant difference of stiffness between the two parts may cause the outer stiffer part slightly to constrain the inner core, therefore reaching smaller central displacements. As the specimen is subjected to 120 min, the damage caused by the fire exposure is more homogeneous throughout the whole surface, and thus the maximum displacements considerably increase.

The damping ratio can be considered a reliable indicator of damage, as it indicates an extent of energy dissipation in the specimen. As the specimen is subjected to fire exposure and/or HP blast loading, the thermal damage and cracks in the specimen enlarge the dissipation of energy, thus resulting in an increase of damping ratio. The effect of fire and blast on the damping ratio of the RC slab was investigated in Paper III, comparing the experimental damping from the different tests to the elastic value from the LP0 test. The results from the exposed specimens subjected to LP shock wave indicate that fire exposure leads to a nearly linear increase of the damping ratio. The combined effect is not significantly visible for the 60-min fire case, as a similar increase rate is observed comparing the results from LP60 and HP60 tests. This may be caused by the abovementioned stiffness variation between the inner core and the outer part in this fire exposure case. Nevertheless, the combined effect of the two loads is clearly visible after 120 min of fire exposure, leading to a considerable further increase of damping ratio of the RC slab.

Chapter 4

Conclusion

4.1 Concluding remarks

In this research study, the effect of elevated temperatures on the mechanical properties of concrete, in conjunction with the static and dynamic tests on heated RC circular slabs, was investigated in order to evaluate the combined effect of fire exposure and blast loading on RC slabs.

The obtained constitutive behaviour of concrete material, in compression and tension, at several elevated temperatures confirm the pronounced reduction of strength and modulus of elasticity reported in the literature and standards (Eurocode 2 and Model Code 2010), while both the strain at maximum stress and the ultimate strain increase. This results in flattened stress-strain relationships as temperature increases, which indicates an overall softening of the material. The observed modification of the constitutive relationships at high temperature results in a decrease of the specific fracture energy in compression, while it increases in tension. Moreover, elevated temperatures considerably affect the evolution of internal damage, for which the change in the tensile damage law is well predicted by the model by Nechnech et al. [72].

The structural mechanisms during static tests on circular RC slabs have been identified for both non-exposed and fire-exposed slabs. The enhanced bending capacity from the arch mechanism at small deflections is considerably affected by the fire exposure, as it is dominated by the adverse permanent damage on the compressive response of concrete. On the contrary, the strong recovery of steel after cooling leads to a similar enhanced ultimate load, caused by the tensile membrane action (TMA), thus confirming the robustness and structural reliability of this RC slab in residual conditions. Simplified predictions using the yield-line approach, together with a good knowledge of the material at elevated temperatures, provide satisfactory results of the reduced bending capacity of the RC slab after exposure to fire.

Dynamic tests show a considerable reduction (by half) of the fundamental frequency of the RC slab after fire exposure, also resulting in an elongation of the fundamental period in the central acceleration response. This is mainly caused by the decrease of the overall stiffness at high temperatures. The softening of the material leads to a more distributed crack pattern, also enlarging the maximum amplitude of the acceleration response. Both the thermal damage and microcracks lead to a higher dissipation of energy, resulting in a nearly linear increase of the damping ratio with fire exposure. The contribution of the blast loading does not significantly reduce

the natural frequency of the exposed specimens. Nevertheless, the additional damage and microcracks on the specimen lead to a great increase of the damping ratio. The results of SDOF and FE models agree with the experimental findings, thus proving to be useful and reliable tools to assess the dynamic response of RC slabs.

Safety considerations of concrete structures require the evaluation of accidental load scenarios involving extreme load conditions. The findings of the present study are valuable in order to define a reliable benchmark for numerical models which, upon numerical upscaling, will be instrumental for the design of the submerged floating tube bridge (SFTB) under the exceptional case of fire exposure and blast loading.

4.2 Further research

The study presented provides experimental data on the barely researched topic of fire and blast loads in RC structures. Recommendations for future research are here described to compliment the presented study.

- The mechanical properties of a HSC and their evolution after exposure at elevated temperatures were investigated. Further research could be carried out to study the effect of high temperatures on the thermal properties and also the transient creep effect (or LITS), as it plays an important role when concrete is heated under load. Moreover, the present study was limited to tests in residual conditions. Additional tests in hot conditions could be performed to quantify the difference between these two testing conditions for this type of concrete.

- The material characterization was narrowed to only temperature effects. Chapter 2 describes the strain rate effects on concrete, which also play a significant role on the material and structural behaviour. Material testing could be carried out to properly characterize the DIF both for compression and tension for this type of concrete. In addition, it was shown that very little research has been performed on the combined temperature and strain rate effects at a material level. This could be further investigated in order to define proper constitutive laws which can later be used in a numerical model to assess RC structures under such combined action.

- The use of UPV measurements has proven to be very useful to quantify the thermal damage on the stiffness both at a material (concrete cylinders) and structural level (RC slabs). Further investigation could be performed to develop an analytical relationship which relates the change in UPV to the decrease of the natural frequency of the slab. This will be convenient when assessing the dynamic behaviour of RC structures.

- The specific scenario of the combined effect of a hydrocarbon fire curve and a blast load was considered in this study. Alternative scenarios, such as the combination of loads in hot conditions or a longer fire exposure time, can be investigated using NLFEA, as described in Chapter 2. For this purpose, the material characterization provided in Paper I can be implemented in advanced

material models to predict the material behaviour at high temperatures. Moreover, the experimental results presented in Papers II and III can be used as a benchmark to calibrate the numerical model for a reliable investigation of the effect of temperature on the structural response of RC slabs, and the combination of fire exposure and blast loading.

- Scale effects are an essential issue which should be addressed using a reliable numerical model, as described in Chapter 3. In this context, the complete material characterization provides the required knowledge on the material behaviour at elevated temperatures, regardless of the size of the structure. A complete model of the SFTB can be developed to investigate the scale effects and simulate the accidental scenario with realistic boundary conditions and external loads, including the presence of water.

Bibliography

[1] M. S. Abrams. Compressive strength of concrete at temperatures to 1600 F. In *Temperature and Concrete, ACI Special Publication*, 25, pages 33–58, 1971.

[2] A. Agrawal and V. K. R. Kodur. A novel experimental approach for evaluating residual capacity of fire damaged concrete members. *Fire Technology*, 56(2):715–735, 2020.

[3] Y. Anderberg. Fire-engineering design of structures based on design guides. In *Proc. 2nd Int. Conf. on 'Performance-Based Codes and Fire Safety Design Methods'*, Maui (Hawaii, USA), 1998.

[4] Y. Anderberg and S. Thelandersson. Stress and Deformation Characteristics of Concrete: Experimental Investigation and Material Behaviour Model. Bulletin 54, University of Lund, Lund (Sweden), 1976.

[5] A. Arano, M. Colombo, P. Martinelli, J. A. Øverli, M. A. N. Hendriks, T. Kanstad, and M. di Prisco. Heated reinforced concrete slabs subjected to blast load: Experimental and numerical results. In *Proc. 17rd fib Symposium on 'Concrete Structures for Resilient Society'*, pages 820–827, 2020.

[6] A. Arano, M. Colombo, P. Martinelli, J. A. Øverli, M. A. N. Hendriks, T. Kanstad, and M. di Prisco. Material characterization approach for modeling high-strength concrete after cooling from elevated temperatures. *Journal of Materials in Civil Engineering*, 33(5):04021086, 2021.

[7] W. Baker, P. Cox, P. Westine, J. Kulesz, and R. Strehlow. *Explosion Hazards and Evaluation*. Elsevier Science, 1983.

[8] P. Bamonte, R. Felicetti, P. G. Gambarova, and A. Meda. Structural behavior and failure modes of R/C at high temperature: R/C sections and 2D members. In P. G. Gambarova, R. Felicetti, A. Meda, and P. Riva, editors, *Fire Design of Concrete Structures: What now? What next?*, pages 159–174, Brescia (Italy), 2005. Starrylink.

[9] P. Bamonte and P. G. Gambarova. Thermal and mechanical properties at high temperature of a very high-strength durable concrete. *Journal of Materials in Civil Engineering*, 22(6):545–555, 2010.

[10] P. Bamonte and P. G. Gambarova. A study on the mechanical properties of self-compacting concrete at high temperature and after cooling. *Materials and Structures*, 45(9):1375–1387, 2012.

[11] P. Bamonte and P. G. Gambarova. Properties of concrete subjected to extreme thermal. *Journal of Structural Fire Engineering*, 5(1):47–62, 2014.

[12] P. Bamonte, P. G. Gambarova, and A. Meda. Today's concretes exposed to fire—test results and sectional analysis. *Structural Concrete*, 9(1):19–29, 2008.

[13] N. P. Banthia, S. Mindess, and A. Bentur. Impact behaviour of concrete beams. *Materials and Structures*, 20(4):293–302, 1987.

[14] A. Beard and R. O. Carvel. *Handbook of Tunnel Fire Safety.* ICE Publishing, second edition, 2012.

[15] J. Biggs. *Introduction to Structural Dynamics.* McGraw-Hill, New York, 1964.

[16] P. H. Bischoff and S. H. Perry. Compressive behaviour of concrete at high strain rates. *Materials and Structures*, 24(6):425–450, 1991.

[17] A. Caverzan, E. Cadoni, and M. di Prisco. Dynamic tensile behaviour of high performance fibre reinforced cementitious composites after high temperature exposure. *Mechanics of Materials*, 59:87–109, 2013.

[18] CEN - European Committee for Standardization. EN 1992-1-2. *Eurocode 2: Design of concrete structures — Part 1-2: General rules — Structural fire design.* Brussels (Belgium), 2004.

[19] CEN - European Committee for Standardization. EN 1994-1-2. *Eurocode 4: Design of composite steel and concrete structures — Part 1-2: General rules — Structural fire design.* Brussels (Belgium), 2005.

[20] CEN - European Committee for Standardization. prEN 1992-1-2:2019-10. *Eurocode 2: Design of composite steel and concrete structures — Part 1-2: General rules — Structural fire design.* Brussels (Belgium), 2019.

[21] L. Chen, Q. Fang, X. Jiang, Z. Ruan, and J. Hong. Combined effects of high temperature and high strain rate on normal weight concrete. *International Journal of Impact Engineering*, 86:40–56, 2015.

[22] M. Colombo. *FRC Bending Behaviour: a Damage Model for High Temperatures.* PhD thesis, Politecnico di Milano, Milan (Italy), 2006.

[23] M. Colombo, M. di Prisco, and P. Martinelli. A new shock tube facility for tunnel safety. *Experimental Mechanics*, 51(7):1143–1154, 2011.

[24] M. Colombo and P. Martinelli. Pressure–impulse diagrams for RC and FRC circular plates under blast loads. *European Journal of Environmental and Civil Engineering*, 16(7):837–862, 2012.

[25] M. Colombo, P. Martinelli, A. Arano, J. A. Øverli, M. A. Hendriks, T. Kanstad, and M. di Prisco. Experimental investigation on the structural response of RC slabs subjected to combined fire and blast. *Structures*, 31:1017–1030, 2021.

[26] M. Colombo, P. Martinelli, and M. di Prisco. A design approach for tunnels exposed to blast and fire. *Structural Concrete*, 16(2):262–272, 2015.

[27] H. Fares, A. Noumowe, and S. Remond. Self-consolidating concrete subjected to high temperature: Mechanical and physicochemical properties. *Cement and Concrete Research*, 39(12):1230–1238, 2009.

[28] R. Felicetti. Assessment methods of fire damages in concrete tunnel linings. *Fire Technology*, 49(2):509–529, 2013.

[29] R. Felicetti and P. G. Gambarova. Effects of high temperature on the residual compressive strength of high-strength siliceous concretes. *ACI Materials Journal*, 95(4):395–406, 1998.

[30] R. Felicetti and P. G. Gambarova. On the residual properties of high performance siliceous concrete exposed to high temperature. In *Proc. Int. Work. on 'Mechanics of Quasi-Brittle Materials and Structures'*, pages 167–186, Prague (Czech Republic), 1999.

[31] R. Felicetti, P. G. Gambarova, and A. Meda. Residual behavior of steel rebars and R/C sections after a fire. *Construction and Building Materials*, 23(12):3546–3555, 2009.

[32] R. Felicetti, P. G. Gambarova, M. P. Natali-Sora, and G. A. Khoury. Mechanical behaviour of HPC and UHPC in direct tension at high temperature and after cooling. In *Proc. 5^{th} Symposium on 'Fibre-Reinforced Concrete' BEFIB 2000*, pages 749–758, Lyon (France), 2000.

[33] R. Felicetti, P. G. Gambarova, and M. Semiglia. Residual capacity of HSC thermally damaged deep beams. *Journal of Structural Engineering*, 125(3):319–327, 1999.

[34] *fib* - International Federation for Structural Concrete. *fib Bulletin 1: Structural Concrete – Textbook on Behaviour, Design and Performance. Updated knowledge of the CEB/FIP Model Code 1990.* Lausanne (Switzerland), 1999.

[35] *fib* - International Federation for Structural Concrete. *fib Bulletin 38: Fire design of concrete structures – materials, structures and modelling.* Lausanne (Switzerland), 2007.

[36] *fib* - International Federation for Structural Concrete. *fib model code for concrete structures 2010.* Berlin (Germany), 2013.

[37] *fib* - International Federation for Structural Concrete. *fib Bulletin 96: Guidelines for submerged floating tube bridges.* Lausanne (Switzerland), 2020.

[38] I. A. Fletcher, S. Welch, J. L. Torero, R. O. Carvel, and A. Usmani. Behaviour of concrete structures in fire. *Thermal Science*, 11(2):37–52, 2007.

[39] J. M. Franssen. *A Study of the Behavior of Composite Steel-Concrete Structures in Fire (in French)*. PhD thesis, Liège University, Liège (Belgium), 1987.

[40] N. Gebbeken, S. Greulich, and A. Pietzsch. Performance of concrete based building materials against blast and impact. In *Proc. 3rd fib Symposium 2001 on 'Concrete and Environment'*, pages –, Berlin (Germany), 2001.

[41] I. Hager and K. Mróz. Role of polypropylene fibres in concrete spalling risk mitigation in fire and test methods of fibres effectiveness evaluation. *Materials*, 12(23):3869, 2019.

[42] I. Hager and P. Pimienta. Mechanical properties of HPC at high temperatures. In P. G. Gambarova, R. Felicetti, A. Meda, and P. Riva, editors, *Fire Design of Concrete Structures: What now? What next*, pages 95–100, Brescia (Italy), 2005. Starrylink.

[43] T. Z. Harmathy. *Fire Safety Design and Concrete*. Longman Scientific and Technical, Harlow (Essex, UK), 1993.

[44] Y. He, J. Huo, and Y. Xiao. Experimental study on dynamic behavior of concrete at elevated temperatures. *Advanced Science Letters*, 4(3):1128–1131, 2011.

[45] J. S. Huo, Y. M. He, L. P. Xiao, and B. S. Chen. Experimental study on dynamic behaviours of concrete after exposure to high temperatures up to 700 °C. *Materials and Structures*, 46(1):255–265, 2013.

[46] H. Ingason, Y. Z. Li, and A. Lönnermark. *Tunnel Fire Dynamics*. Springer New York, 2015.

[47] ITA-AITES. *Guidelines for structural fire resistance for road tunnels*. 2004.

[48] A. Jain, A. Kathuria, A. Kumar, Y. Verma, and K. Murari. Combined use of non-destructive tests for assessment of strength of concrete in structure. *Procedia Engineering*, 54:241–251, 2013.

[49] I. Janotka and L. Bágel. Pore structures, permeabilities, and compressive strengths of concrete at temperatures up to 800°C. *ACI Materials Journal*, 99(2):196–200, 2002.

[50] M. Johansson. *Structural Behaviour in Concrete Frame Corners of Civil Defence Shelters—Non-linear Finite Element Analyses and Experiments*. PhD thesis, Chalmers University of Technology, Göteborg (Sweden), 2000.

[51] D. Kakogiannis, F. Pascualena, B. Reymen, L. Pyl, J. M. Ndambi, E. Segers, D. Lecompte, J. Vantomme, and T. Krauthammer. Blast performance of reinforced concrete hollow core slabs in combination with fire: Numerical and experimental assessment. *Fire Safety Journal*, 57:69–82, 2013.

[52] P. Kalifa, G. Chéné, and C. Gallé. High-temperature behaviour of HPC with polypropylene fibres: From spalling to microstructure. *Cement and Concrete Research*, 31(10):1487–1499, 2001.

[53] W. Khaliq and V. Kodur. High temperature mechanical properties of high-strength fly ash concrete with and without fibers. *ACI Materials Journal*, 109(6):665–674, 2012.

[54] G. A. Khoury. Effect of fire on concrete and concrete structures. *Progress in Structural Engineering and Materials*, 2(4):429–447, 2000.

[55] G. A. Khoury. Strain of heated concrete during two thermal cycles. Part 1: strain over two cycles, during first heating and at subsequent constant temperature. *Magazine of Concrete Research*, 58(6):367–385, 2006.

[56] G. A. Khoury and S. Algar. Mechanical behaviour of HPC and UHPC concretes at high temperatures in compression and tension. In *Proc. ACI Int. Conf. on 'State-of-the-Art in High Performance Concrete'*, Chicago (Illinois, USA), 1999.

[57] V. Kodur. Properties of concrete at elevated temperatures. *International Scholarly Research Notices*, 2014:468510, 2014.

[58] V. K. R. Kodur, M. M. S. Dwaikat, and M. B. Dwaikat. High-temperature properties of concrete for fire resistance modeling of structures. *ACI Materials Journal*, 105(5):517–527, 2008.

[59] V. K. R. Kodur and M. Z. Naser. *Structural Fire Engineering*. McGraw-Hill, 2020.

[60] T. Krauthammer. *Modern Protective Structures*. Taylor Francis Group, Boca Raton, FL, 2008.

[61] A. Lau and M. Anson. Effect of high temperatures on high performance steel fibre reinforced concrete. *Cement and Concrete Research*, 36(9):1698–1707, 2006.

[62] Z. Li, J. Xu, and E. Bai. Static and dynamic mechanical properties of concrete after high temperature exposure. *Materials Science and Engineering: A*, 544:27–32, 2012.

[63] G. Lilliu and A. Meda. Nonlinear phased analysis of reinforced concrete tunnels under fire exposure. *Journal of Structural Fire Engineering*, 4(3):131–142, 2013.

[64] Y. Liu, Z. Li, B. Jin, and J. Huo. Experimental investigation on dynamic behavior of concrete after exposure to elevated temperatures. *European Journal of Environmental and Civil Engineering*, 24(13):2151–2167, 2020.

[65] Q. Ma, R. Guo, Z. Zhao, Z. Lin, and K. He. Mechanical properties of concrete at high temperature—A review. *Construction and Building Materials*, 93:371–383, 2015.

[66] J. M. Magallanes, Y. Wu, L. J. Malvar, and J. E. Crawford. Recent improvements to release III of the KC concrete model. In *Proc. 11th Int. LS-DYNA Users Conf.*, pages 37–47, Dearborn (MI, USA), 2010.

[67] M. Malik, S. K. Bhattacharyya, and S. V. Barai. Thermal and mechanical properties of concrete and its constituents at elevated temperatures: A review. *Construction and Building Materials*, 270:121398, 2021.

[68] L. J. Malvar and J. E. Crawford. Dynamic increase factors for concrete. Technical report, Naval Facilities Engineering Service Center, Port Hueneme (CA, USA), 1998.

[69] A. Minoretti, X. Xiang, I. L. Johansen, and M. Eidem. The future of the tunnel crossing: The submerged floating tube bridge. *Structural Engineering International*, 30(4):493–497, 2020.

[70] H. Nakamura and T. Higai. *Compressive Fracture Energy and Fracture Zone Length of Concrete*. ASCE, 2001.

[71] D. J. Naus and H. L. Graves. A review of the effects of elevated temperature on concrete materials and structures. In *Proc. 14th Int. Conf. on 'Nuclear Engineering'.*, pages 615–624, Miami (Florida, USA), 2006. ASME.

[72] W. Nechnech, F. Meftah, and J. M. Reynouard. An elasto-plastic damage model for plain concrete subjected to high temperatures. *Engineering Structures*, 24(5):597–611, 2002.

[73] Norwegian Public Road Administration. The E39 Coastal Highway Route. https://www.vegvesen.no/en/roads/Roads+and+bridges/Road+projects/e39coastalhighwayroute.

[74] A. Noumowe. Mechanical properties and microstructure of high strength concrete containing polypropylene fibres exposed to temperatures up to 200 °C. *Cement and Concrete Research*, 35(11):2192–2198, 2005.

[75] J. Novák and A. Kohoutková. Fibre reinforced concrete exposed to elevated temperature. *IOP Conf. Ser.: Materials Science and Engineering*, 246:012045, 2017.

[76] J. Ožbolt, J. Bošnjak, and E. Sola. Dynamic fracture of concrete compact tension specimen: Experimental and numerical study. *International Journal of Solids and Structures*, 50(25):4270–4278, 2013.

[77] J. Ožbolt, K. K. Rah, and D. Meštrović. Influence of loading rate on concrete cone failure. *International Journal of Fracture*, 139(2):239–252, 2006.

[78] J. Ožbolt, A. Sharma, and H.-W. Reinhardt. Dynamic fracture of concrete – compact tension specimen. *International Journal of Solids and Structures*, 48(10):1534–1543, 2011.

[79] J. Ožbolt, A. Sharma, B. İrhan, and E. Sola. Tensile behavior of concrete under high loading rates. *International Journal of Impact Engineering*, 69:55–68, 2014.

[80] F. Pascualena, J. M. Ndambi, B. Reymen, B. Desmet, E. Segers, and J. Vantomme. Blast performance of concrete slabs in combination with fire. In *Proc. 8th Int. Conf. on 'Structural Dynamics'. EURODYN 2011*, pages 3310–3317, Leuven (Belgium), 2011.

[81] L. T. Phan and N. J. Carino. Review of mechanical properties of HSC at elevated temperature. *Journal of Materials in Civil Engineering*, 10(1):58–65, 1998.

[82] C. Pichler, R. Lackner, and H. A. Mang. Safety assessment of concrete tunnel linings under fire load. *Journal of Structural Engineering*, 132(6):961–969, 2006.

[83] P. Pimienta, J.-C. Mindeguia, G. Debicki, U. Diederichs, I. Hager, and S. Huismann. Mechanical properties. In P. Pimienta, R. J. McNamee, and J.-C. Mindeguia, editors, *Physical Properties and Behaviour of High-Performance Concrete at High Temperature. RILEM State-of-the-Art Report*, pages 71–218. Springer Int. Publishing, Switzerland, 2019.

[84] C. Poon, Z. Shui, and L. Lam. Compressive behavior of fiber reinforced high-performance concrete subjected to elevated temperatures. *Cement and Concrete Research*, 34(12):2215–2222, 2004.

[85] Z. Ruan, L. Chen, and Q. Fang. Numerical investigation into dynamic responses of RC columns subjected for fire and blast. *Journal of Loss Prevention in the Process Industries*, 34:10–21, 2015.

[86] K. Sakkas, N. Vagiokas, K. Tsiamouras, D. Mandalozis, A. Benardos, and P. Nomikos. In-situ fire test to assess tunnel lining fire resistance. *Tunnelling and Underground Space Technology*, 85:368–374, 2019.

[87] E. Sancak, Y. D. Sari, and O. Simsek. Effects of elevated temperature on compressive strength and weight loss of the light-weight concrete with silica fume and superplasticizer. *Cement and Concrete Composites*, 30(8):715–721, 2008.

[88] K. Savov, R. Lackner, and H. Mang. Stability assessment of shallow tunnels subjected to fire load. *Fire Safety Journal*, 40(8):745–763, 2005.

[89] U. Schneider. Behaviour of concrete at high temperatures. RILEM-Committee 44-PHT, Department of Civil Engineering, Kassel University, Kassel (Germany), 1985.

[90] B. A. Schrefler, C. E. Majorana, G. A. Khoury, and D. Gawin. Thermo-hydro-mechanical modelling of high performance concrete at high temperatures. *Engineering Computations*, 19(7):787–819, 2002.

[91] S. N. R. Shah, F. W. Akashah, and P. Shafigh. Performance of high strength concrete subjected to elevated temperatures: A review. *Fire Technology*, 55(5):1571–1597, 2019.

[92] Y. Shi, H. Hao, and Z.-X. Li. Numerical derivation of pressure–impulse diagrams for prediction of RC column damage to blast loads. *International Journal of Impact Engineering*, 35(11):1213–1227, 2008.

[93] R. Siddique and A. N. Noumowe. An overview of the properties of high-strength concrete subjected to elevated temperatures. *Indoor and Built Environment*, 19(6):612–622, 2010.

[94] K. K. Sideris. Mechanical characteristics of self-consolidating concretes exposed to elevated temperatures. *Journal of Materials in Civil Engineering*, 19(8):648–654, 2007.

[95] R. Stucchi and F. Amberg. A practical approach for tunnel fire verification. *Structural Engineering International*, 30(4):515–529, 2020.

[96] Z. Sun, Y. Zhang, Y. Yuan, and H. A. Mang. Stability analysis of a fire-loaded shallow tunnel by means of a thermo-hydro-chemo-mechanical model and discontinuity layout optimization. *International Journal for Numerical and Analytical Methods in Geomechanics*, 43(16):2551–2564, 2019.

[97] M. J. Terro. Numerical modeling of the behavior of concrete structures in fire. *ACI Structural Journal*, 95(2):183–193, 1998.

[98] F. Wang, M. Wang, and J. Huo. The effects of the passive fire protection layer on the behavior of concrete tunnel linings: A field fire testing study. *Tunnelling and Underground Space Technology*, 69:162–170, 2017.

[99] A. M. Weidner, C. P. Pantelides, W. D. Richins, T. K. Larson, and J. E. Blakeley. Dynamic properties of concrete at moderately elevated temperatures. *ACI Materials Journal*, 112(5):663–672, 2015.

[100] H. Wu, X. Lin, and A. Zhou. A review of mechanical properties of fibre reinforced concrete at elevated temperatures. *Cement and Concrete Research*, 135:106117, 2020.

[101] J. Xiao, Z. Li, Q. Xie, and L. Shen. Effect of strain rate on compressive behaviour of high-strength concrete after exposure to elevated temperatures. *Fire Safety Journal*, 83:25–37, 2016.

[102] Z.-G. Yan, H.-H. Zhu, J. Woody Ju, and W.-Q. Ding. Full-scale fire tests of RC metro shield TBM tunnel linings. *Construction and Building Materials*, 36:484–494, 2012.

[103] C. Zhai, L. Chen, Q. Fang, W. Chen, and X. Jiang. Experimental study of strain rate effects on normal weight concrete after exposure to elevated temperature. *Materials and Structures*, 2016.

[104] C. Zhai, L. Chen, H. Xiang, and Q. Fang. Experimental and numerical investigation into RC beams subjected to blast after exposure to fire. *International Journal of Impact Engineering*, 97:29–45, 2016.

[105] Q. Zhang, W.-Y. Wang, S.-S. Bai, and Y.-H. Tan. Response analysis of tunnel lining structure under impact and fire loading. *Advances in Mechanical Engineering*, 11(3):1–6, 2019.

Part II

APPENDED PAPERS

Paper I

Material characterization approach for modelling high-strength concrete after cooling from elevated temperatures

Arano, A., Colombo, M., Martinelli, P., Øverli, J. A., Hendriks, M. A. N., Kanstad, T. and di Prisco, M.

Journal of Materials in Civil Engineering, 2021, 33(5): 04021086

doi: https://doi.org/10.1061/(ASCE)MT.1943-5533.0003694

Paper II

Failure characteristics of reinforced concrete circular slabs subjected to fire exposure and static load: an experimental study

Arano, A., Colombo, M., Martinelli, P., Øverli, J. A., Hendriks, M. A. N., Kanstad, T. and di Prisco, M.

Under review in "Engineering Structures", 2021

Paper III

Experimental investigation on the structural response of RC slabs subjected to combined fire and blast

Colombo, M., Martinelli, P., Arano, A., Øverli, J. A., Hendriks, M. A. N., Kanstad, T. and di Prisco, M.

Structures, 2021, 31: 1017-1030

doi: https://doi.org/10.1016/j.istruc.2021.02.029

Structures 31 (2021) 1017–1030

Contents lists available at ScienceDirect

Structures

journal homepage: www.elsevier.com/locate/structures

Experimental investigation on the structural response of RC slabs subjected to combined fire and blast

Matteo Colombo [a], Paolo Martinelli [a,*], Assis Arano [b], Jan Arve Øverli [b], Max A.N. Hendriks [b,c], Terje Kanstad [b], Marco di Prisco [a]

[a] Politecnico di Milano, Department of Civil and Environmental Engineering, Piazza L. da Vinci 32, 20133 Milan, Italy
[b] Norwegian University of Science and Technology, Department of Structural Engineering, NO-7491 Trondheim, Norway
[c] Technical University of Delft, Faculty of Civil Engineering and Geosciences, Stevinweg 1, Delft, Netherlands

ARTICLE INFO

Keywords:
Fire exposure
Blast loading
High temperatures
Shock tube
RC slabs
Fire-blast interaction

ABSTRACT

Reinforced concrete (RC) submerged floating tunnels (SFTs) represent a possible solution for crossing wide, deep fjords, and is considered for the E39 highway route along the Norwegian west coast. With regard to SFTs, the specific accidental scenario that is under investigation is the combined action of fire and subsequent internal explosion, as this is a crucial safety design condition for this type of structure. To assess the structural performance of reinforced concrete structures under combined fire and blast actions, gas burner equipment and a shock tube device were used to generate high temperature and blast loading, respectively, on RC circular slabs. A proper set of instruments consisting of thermocouples embedded in the specimens, accelerometers and ultrasonic pulse velocity (UPV) equipment made it possible to capture the behaviour of the slabs under the combined fire and blast actions and to distinguish the specific role of fire and blast. Simplified numerical tools such as an equivalent elastic single degree of freedom (SDOF) model and a linear elastic finite element (FE) model were used to interpret the experimental results. By considering all combinations of three fire exposure times and two shock waves, the effect of damage accumulation from a combined action of fire and subsequent internal explosion was mapped. A reliable benchmark for numerical models was obtained.

1. Introduction

Tunnels represent one of the most critical infrastructures in the whole transport network of Europe. Their fragility when exposed to exceptional events like fire and/or explosion is a crucial point in the robustness of a wider transport system, from damage of the infrastructure itself to a more far-reaching domino effect, propagating consequences over a wider region due to the tunnel closure. Tunnels are bottlenecks in transport networks that can threaten the overall robustness of the system, because the breakdown of those single components can lead to the complete collapse of the transportation infrastructure. From this point of view, a capacity design approach should be adopted to minimize the failure probability of the critical points.

Disastrous events that occurred in European road tunnels, such as those of the Mont Blanc Tunnel (1999), the Gotthard Tunnel (2001), the Tauern Tunnel (2002) and the Frejus Tunnel (2005), increased attention paid to safety issues in tunnels and underlined the importance of these infrastructures from human, economic and cultural points of views.

Fire has been regarded as the main physical threat in the design of a tunnel and a wide range of research activities including experimental tests, modelling methods and design approaches have been devoted to the investigation of this problem [1–15]. However, nowadays, fire cannot be regarded as the only extreme accidental action: recent terroristic attacks have raised the doubt that tunnel infrastructures can also be regarded as critical targets, not only for significant life losses, but also for the huge overall costs to society, that critical damage to this kind of infrastructure can induce. Over the last decade, several researchers started to examine the behaviour of tunnels (particularly metro tunnels) subjected to internal explosion encompassing both simplified and refined numerical models [16–25]. At present, there are no experimental studies reported in literature on the topic of tunnels subjected to internal blast loads.

The research presented in this paper concerns the preliminary design of the submerged-floating tunnel (SFT), or “Archimede bridge”, or

* Corresponding author at: Politecnico di Milano, Department of Civil and Environmental Engineering, Piazza L. da Vinci 32, 20133 Milan, Italy.
E-mail addresses: matteo.colombo@polimi.it (M. Colombo), paolo.martinelli@polimi.it (P. Martinelli), assis.arano@ntnu.no (A. Arano), jan.overli@ntnu.no (J.A. Øverli), max.hendriks@ntnu.no (M.A.N. Hendriks), terje.kanstad@ntnu.no (T. Kanstad), marco.diprisco@polimi.it (M. di Prisco).

https://doi.org/10.1016/j.istruc.2021.02.029
Received 17 November 2020; Received in revised form 12 January 2021; Accepted 11 February 2021
Available online 5 March 2021

Submerged Floating Tube Bridge (SFTB), that is planned for crossing Norwegian fjords. The Norwegian Public Roads Administration's Ferry-free coastal route E39 project aims to establish a coastal highway route, approximately 1100 km long, between Kristiansand and Trondheim without ferry connections. The wide, deep fjords along the Norwegian coast require new large structures to be built, and SFT is a realistic alternative [26].

The tunnel will be suspended approximately 30 m under the water's surface. The structure will comprise two tubes fixed to floating pontoons with a gap of approximately 250 m. This design allows ships to sail freely over the structure, while submarines can cross underneath it. With regard to SFTs, a specific accident scenario that is under investigation is the combined action of fire and subsequent internal explosion, as this is a crucial safety design condition for this structure. The tragic collision of two trucks on the Casalecchio (close to Bologna, Italy) junction of the A14 highway that occurred on August 6th 2018 can be regarded as an example of this kind of scenario: both trucks loaded with flammable materials (GPL and chemical solvents) triggered a chain of explosions that gutted the overpass, causing two deaths and 145 injuries. A recent study conducted by Kristoffersen et al. [23] analysed the response of SFTs with circular and rectangular cross-sections, subjected to internal explosion without fire using a finite element (FE) approach.

With reference to reinforced concrete (RC) structures, limited research is available in literature on the combined effects of fire and blast loads and is mostly confined to numerical studies. Kakogiannis et al. [27] and Pascualena et al. [28] reported the analysis of the blast bearing capacity of reinforced concrete hollow core slabs when they are subjected first to fire and then to a blast load. The blast response of the hollow core slab was assessed numerically in [28] and both numerically and experimentally in [27]. A numerical investigation into dynamic responses of RC columns subjected to fire and blast was proposed by Ruan et al. [29]. Zhai et al. [30] reported an experimental and numerical investigation of RC beams subjected to a blast after exposure to fire. A prestressed concrete panel was numerically evaluated under impact-blast-fire combined loading scenarios using an FE approach. Moving the attention to tunnels, the response behaviour of the tunnel lining under the action of vehicle impact and fire load has been numerically analysed [31]. A numerical simplified procedure was proposed by Colombo et al. [32] for the response behaviour of underground tunnels subjected to combined fire and internal explosion.

The work presented here aims to define a reliable benchmark for the numerical model that will be instrumental for the design of the tunnel under exceptional load conditions, by assessing the blast load-bearing resistance of RC slabs subjected to high temperatures. For this purpose, a comprehensive experimental program was carried out at Politecnico di Milano in conjunction with the Norwegian University of Science and Technology (NTNU), adopting a shock tube and gas burner equipment, able to apply a fire and blast sequence [33]. The work presented in this study is part of a larger research programme in which static slab tests and material tests, have been performed for further understanding of the slab's behaviour [34].

The structural response of RC circular slabs subjected to shock wave load conditions was investigated in residual conditions, after being exposed to a fire curve. According to [35], a hydrocarbon fire curve, typical of tunnel designing, was first applied to five specimens. Two fire exposure times were considered (t = 60 and 120 min) in addition to the reference case (t = 0 min). The same guideline [35] indicates t = 120 min as the fire exposure time in the case of a tunnel that is a primary structure, with truck/tanker type traffic.

Two different shock wave loading conditions were taken into account: a "low pressure" condition (LP) characterized by an incident shock wave travelling at a velocity about 1.5 Mach and a maximum reflected pressure of about 400 kPa, and a "High Pressure" condition (HP) characterized by an incident shock wave travelling at a velocity of about 2 Mach and a maximum reflected pressure of 1100 kPa.

Thermocouples embedded in the specimens made it possible to measure the temperature distribution through the thickness of the specimens during the fire application, whilst accelerometers, applied to the back of the slab during the shock tube tests, made it possible to measure the acceleration at several points of the specimens. Moreover, ultrasonic pulse velocity (UPV) measurements were acquired, before and after the fire tests and also after the shock tube tests, in order to quantify the decrease of the cross-section stiffness caused by both the fire exposure and the shock wave application.

Table 1
Summary of the experimental programme.

Specimen ID	UPV test	fire exposure			blast test	
		0 min	60 min	120 min	low pressure	high pressure
LP0	Y	Y	–	–	Y	–
LP60	Y	–	Y	–	Y	–
LP120	Y	–	–	Y	Y	–
HP0	Y	Y	–	–	–	Y
HP60	Y	–	Y	–	–	Y
HP120-1	Y	–	–	Y	–	Y
HP120-2	Y	–	–	Y	–	Y

2. Experimental programme

In this work, RC circular slabs were subjected to combined fire and shock wave loads. An overview of the whole experimental programme is presented in Section 2.1. A description of the materials composing the specimens (i.e. concrete and steel) is given in Section 2.2. The specimen's geometry and the instrumentation are presented in Section 2.3.

2.1. Test programme

In total seven specimens were tested in this study, of which five were tested under combined fire and shock wave loads. Two specimens were tested under blast conditions only. Table 1 summarizes the whole set of tests performed. In all the tests, exposure to fire (if applied) always preceded the blast load.

The experimental tests differ in terms of the reflected pressure history applied to the specimens and the time exposure at the fire curve eventually applied before the blast. Three tests, hereafter indicated as the low pressure tests, are characterised by an average peak pressure of 370 kPa and an average specific impulse of 3386 kPa × ms. The other four tests, hereafter indicated as the high pressure experiments, are characterised by an average peak pressure of 1111 kPa and an average specific impulse of 6241 kPa × ms. This study considers two different fire exposure times (t = 60 min and t = 120 min), in addition to the non-heated condition (t = 0 min). An abbreviation is used to indicate different tests that correspond to different specimens (for example HP120-1): LP or HP at the beginning of the abbreviation stand for low and high pressure tests, 0, 60 and 120 stand for the exposure time in minutes where 0 means that specimen was not exposed to fire, while the eventual ascending number at the end of the abbreviation identifies nominally identical specimens.

In all the tests, direct UPV measurements were performed before and after the fire tests and before and after the blast tests in order to quantify the internal damage produced by the combined effect of thermal exposure and blast load through the thickness of the specimen.

2.2. Materials

2.2.1. Concrete

A detailed and comprehensive discussion of the mechanical properties of the concrete used for the RC slabs is given in [34]. Mechanical properties of concrete were evaluated at ambient and high temperatures. Only the main points of interest are summarized in the following description.

Table 2
Concrete mix design.

Component	Content (kg/m^3)
CEM II/B-M 42.5R	223.40
CEM II/A-V 42.5 N	193.33
Silica fume	12.89
Water	174.13
Aggregate 8–16	754.95
Aggregate 0–8	1026.48
Acrylic superplasticizer	3.06
Set-retarding admixture	0.64
Polypropylene fibres	1.00

The concrete mix design ordered as a C45/55 grade is listed in Table 2. The concrete compressive strength (f_c) measured on cylinders (D = 100 mm and H = 200 mm) was equal to 73 MPa. The concrete cylinders were demoulded 24 h after casting, cured in water for 28 days, and rested for five/six months at 20 °C in a lab environment. The density (ρ) at 28 days was equal to 2370 kg/m^3. The concrete has a water-cement ratio (w/c) of 0.42, and a maximum aggregate size (d_{max}) of 16 mm. The siliceous aggregates were composed of granite, gneiss, sandstone and siltstone. Polypropylene microfibres were also added into the mix (1 kg/m^3) to prevent explosive spalling.

A set of quasi-static concrete tests, namely uniaxial compression test (UCT) and uniaxial direct tensile test (UTT) was carried out to assess the mechanical material properties of concrete at four different temperatures. Twelve standard cylinders (100 × 200 mm) were tested in uniaxial compression, measuring the modulus of elasticity as indicated in [36] and the compressive strength. Three nominally identical specimens were tested at different temperature levels (20, 200, 400, and 600 °C), in residual conditions. Eight cylinders (100 × 100 mm) were tested in uniaxial tension with hinged end-platens by controlling the crack opening displacement (COD). Two nominally identical specimens were tested in residual conditions at different temperature levels (20, 200, 400, and 600 °C). Further details on the material test set-up, specimen sizes and instrumentation can be found in [34].

The average modulus of elasticity from the three tests at 20 °C, and its standard deviation were equal to $E_{c,20}$ = 27609 ± 829 MPa. A significant decrease in the modulus of elasticity in concrete subjected to high temperature was observed. On average, from 20 to 200 °C, the modulus slightly reduces until 0.90$E_{c,20}$. Between 200–400 °C and 400–600 °C, the material suffers a faster reduction, reaching 0.50$E_{c,20}$ and 0.20$E_{c,20}$, respectively.

The average compressive peak strength from the three tests at 20 °C, and its standard deviation were equal to $f_{c,20}$ = 73.00 ± 2.44 MPa. The compressive strength of concrete was significantly reduced due to the exposure to elevated temperatures, with a trend similar to that observed for the modulus of elasticity. After exposure to elevated temperatures, the residual peak strength decreases to approximately 0.90$f_{c,20}$ after 200 °C, 0.50$f_{c,20}$ after 400 °C, and 0.30$f_{c,20}$ after 600 °C.

The average peak tensile strength from the two tests at 20 °C, and its standard deviation were equal to $f_{ct,20}$ = 3.62 ± 0.56 MPa. The maximum stress reached at 200 °C is about 20% higher than the maximum stress at 20 °C. Above 200 °C, the residual peak tensile strength significantly decreases to approximately 0.70$f_{ct,20}$ for 400 °C and 0.30$f_{ct,20}$ for 600 °C. Complete stress–strain and stress-COD curves were measured during the UCTs and UTTs, in addition to peak compressive strength and peak tensile strength, but are omitted here for the sake of brevity. A detailed and comprehensive discussion of the mechanical properties of concrete exposed to high temperatures is given in [34].

2.2.2. Steel

Traditional B450 steel with Ø6 mm rebars were used to prepare the RC circular slabs. Eight steel reinforcing bars were tested in uniaxial tension according to [37], using an INSTRON machine with a maximum capacity of 200 kN. The tests were carried out under displacement control by means of a high-accuracy transducer, with a gauge length of 50 mm, placed at the central part measuring the elongation of the rebar until it reached 2%. An internal transducer of the machine was then used to follow the test until complete failure of the specimen. Two nominally identical specimens were tested, in residual conditions at different temperature levels (20, 200, 400, and 600 °C). By controlling the displacement, complete stress–strain curves were measured during the tests, in addition to yielding and ultimate strengths. After the tests, the elongation at failure was measured according to [37]. The average yielding strength for the steel rebar at room temperature is $f_{y,20}$ = 500.85 MPa. The average ultimate strength and strain at room temperature are $f_{t,20}$ = 648.77 MPa and $\varepsilon_{su,20}$ = 0.328, respectively. The mechanical properties at high temperatures experienced a strong recovery during the cooling phase. The yielding and ultimate strength after exposure to 600 °C were very similar to those for the non-heated specimens.

2.3. Specimen geometry and instrumentation

The slab specimens consist of reinforced concrete circular slabs, 70 mm thick, with a diameter of 690 mm. Two layers of bi-directional reinforcement (Ø6/60 mm both in x and y direction) were positioned as shown in Fig. 1. A net concrete cover of 10 mm was used. The specimen sizes are detailed in Fig. 1.

The specimen's geometry was mainly dictated by the dimensions of the shock tube equipment. In addition, the thickness and reinforcement ratio were determined in order to ensure a linear elastic behaviour of the slab under the reference load conditions (test LP0). An elastic analytical computation of the slab [38], considering not thermally damaged

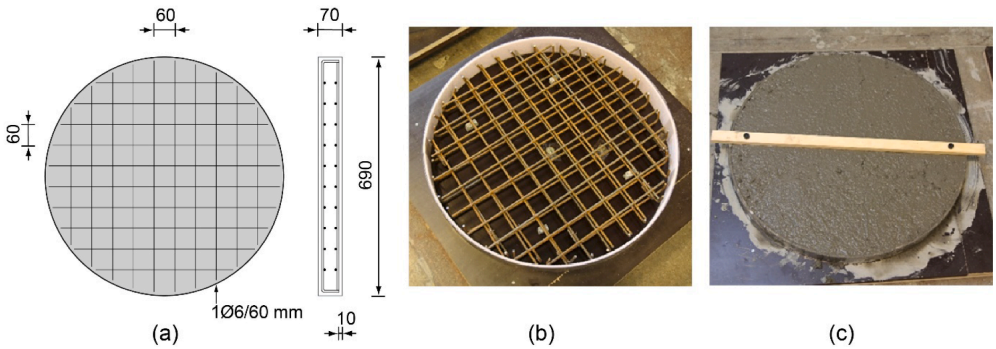

Fig. 1. Reinforced concrete slab specimen: (a) specimen size, (b) mould used to cast the slab and (c) view of the cast slab (units: mm).

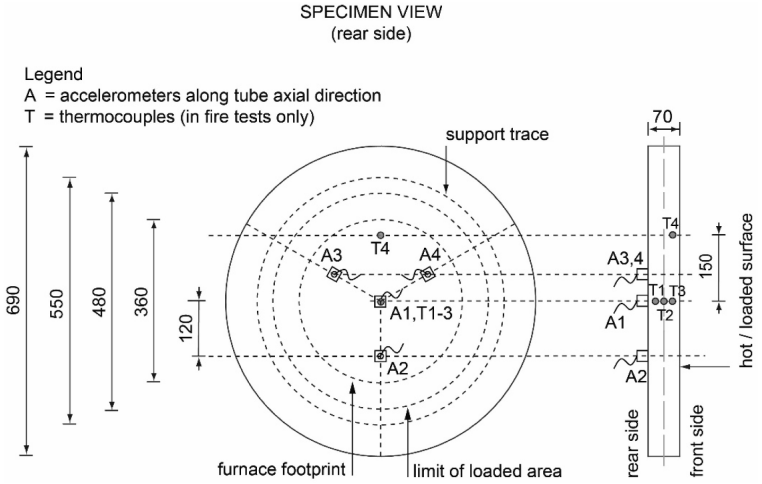

Fig. 2. Instrumentation installed on the specimen (units: mm).

material, provides a pressure corresponding to the first cracking (p_{cr}) in static condition equal to 400 kPa, while the ultimate pressure (p_u) computed according to a yield line approach [39] for static condition is equal to 1100 kPa.

The specimen's acceleration along the shock tube axis (out-of-plane slab acceleration) was measured by means of four ICP (Integrate Circuit Piezoelectric) accelerometers: one (A1) placed at the specimen's centre and the other three (A2–A4) placed at relative angular positions of 120° at 120 mm from the specimen's centre (Fig. 2). A fifth accelerometer (A5) was mounted on the shock tube at the end of the driven chamber to record the axial accelerations of the device (Fig. 6 and Fig. 7b). The accelerometer characteristics are: a quartz sensing element with a measuring range of ±500 g pk (peak acceleration), a band width larger than 10 kHz, a broadband resolution of 0.005 g rms (root mean square) and a resonant frequency higher than 70 kHz.

A set of three ICP dynamic pressure sensors was positioned along the tube's axis as indicated in Fig. 6. The pressure sensors (PT1-PT3) have a quartz sensing element with a full-scale pressure of 6.9 MPa, a sensitivity of 0.7 mV/kPa, a rise time lower than 1 μs and a resonant frequency higher than 500 kHz. The signal conditioning for both accelerometers and pressure sensors mounted on the shock tube (see Section 3.3 for its description) is performed with an ICP signal conditioner with gain equal to one, a bandwidth equal to 10 kHz and a broadband electrical noise equal to 3.5 μV rms. All channels are acquired by means of the same data acquisition system with 56 parallel channels with the maximum sampling rate of 3 MS/s per channel and a 14-bit resolution. The data acquisition for all the channels is triggered by the signal of the pressure sensor PT1 placed at a distance of 2250 mm from the driven end flange: when the shock wave goes through its position, the system starts acquiring data with a sampling rate of 1 MS/s.

Specimens exposed to high temperatures were instrumented with four thermocouples each. Type-K chromel/alumel thermocouples (0.91 mm thick) were installed during fabrication at three different depths in the specimen. Thermocouples T1-T3 were located at the centre of the specimen at 54, 35 and 16 mm from the "hot surface", respectively, for measuring the concrete temperature through the thickness. Thermocouple T4 was located at 150 mm from the centre along the radial direction at a depth of 16 mm from the "hot surface" (see Fig. 2).

3. Description of slab tests

The tests were conducted according to the following sequence: (a) application of UPV tests on virgin specimen, (b) application of the fire curve with exposure time equal to t = 60 min or t = 120 min, (c) UPV measurements for evaluation of fire damage, (d) application of low or high pressure blast tests and (e) UPV measurements for the assessment of combined fire and blast damage. Tests where high-temperature exposure was not applied (t = 0 min) served as reference tests; in these cases phases (b) and (c) were not applied. The description of UPV measurements, fire tests and blast tests is given in Sections 3.1–3.3.

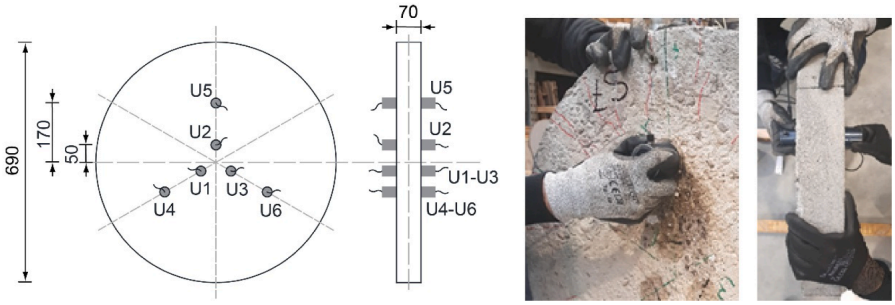

Fig. 3. Direct UPV measurements on RC slab specimen (units: mm).

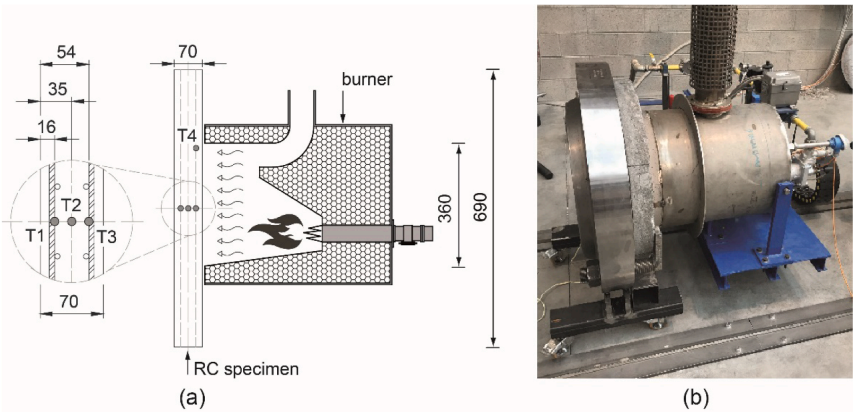

Fig. 4. Fire curve application: (a) schematic view of the burner equipment and (b) picture of the burner and of the specimen ready for the fire test (units: mm).

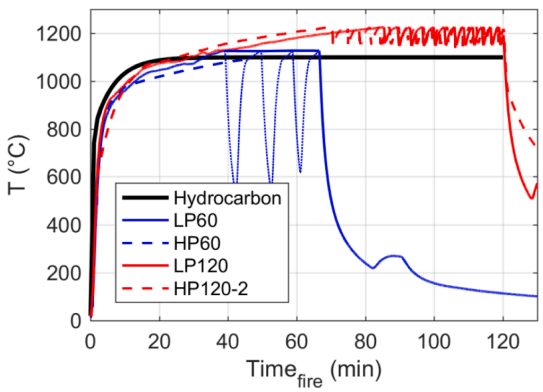

Fig. 5. Recorded and target fire curves.

3.1. UPV measurements

Direct UPV measurements [40] were carried out on the specimens before and after the fire and blast tests. The aim of these measurements was to quantify the internal damage produced by the thermal exposure and by the blast load through the thickness of each specimen. The emitting and receiving probes were placed on opposite specimen faces since a direct UPV method was adopted. Six points were monitored: points U1-U3 were located at a distance of 50 mm from the specimen's centre, whereas points U4-U6 were located at a distance of 170 mm (see Fig. 3). Gel was used to avoid air between the transducer and the specimen's surface.

3.2. Fire exposure

The fire curve was applied to the specimens by means of a gas burner. The burner equipment comprises a nozzle mix burner in which gas and air are mixed at the point of discharge. The burner is mounted by means of a proper flange to a chamber in which the burning process takes place. The chamber is designed to allow proper smoke evacuation and it is closed on one side by the specimen itself in order to heat the specimen's surface. A hydrocarbon curve [14], typical of accidents in tunnels, was applied on one face of the specimen (the free surface during casting) on a circular area with a diameter equal to 360 mm (Fig. 4). A thermal sensor installed inside the burner makes it possible to automatically regulate the intensity of the flame to achieve the desired temperature vs time curve (i.e. fire curve). Two different high temperature exposure times, t = 60 min and t = 120 min, were considered. The fire curves recorded during the fire tests are shown in Fig. 5 and compared with the target hydrocarbon fire curve. The specimens were allowed to expand freely due to increase of temperature during the test. Once the desired exposure time was reached, the burner was turned off and the specimens cooled naturally in the free laboratory environment. During the LP60 test there was a problem in following the target temperature. The problem was solved during the other tests and did not have any impact on the results that are presented in Section 4.

All specimens subjected to the fire curve were instrumented with four thermocouples for measuring the concrete temperature through the thickness (see Section 2.3 for the description of the instrumentation). Despite the addition of polypropylene microfibers in the concrete matrix, minor explosive spalling occurred during the first minutes of all the tests subjected to fire exposure. Nevertheless, this phenomenon was limited to a small region of the specimen and with a maximum depth close to the concrete cover (c = 10 mm). The region characterized by the spalling phenomenon is highlighted as a grey region in Fig. 13.

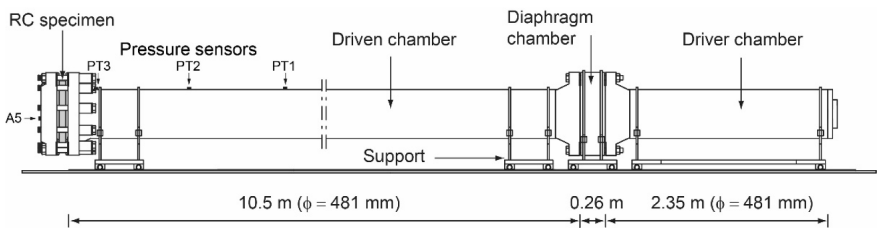

Fig. 6. Schematic view of the shock tube.

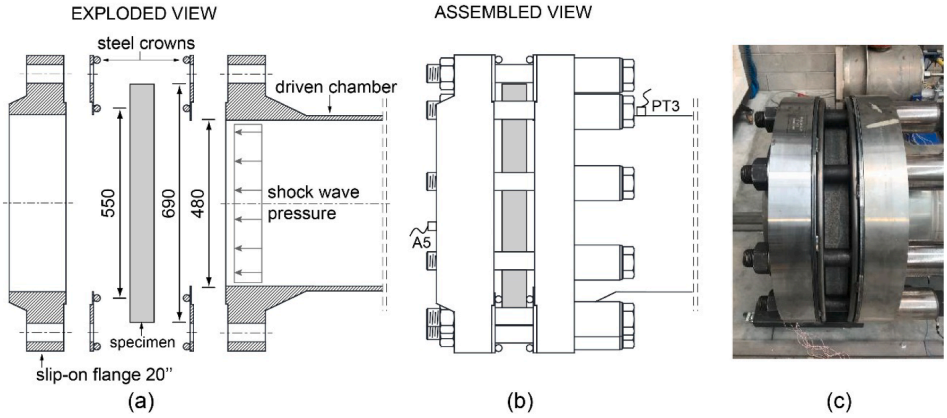

Fig. 7. Details of the test set-up area: (a) exploded view, (b) assembled view and (c) picture in the assembled configuration.

3.3. Blast tests

The blast tests were carried out at Politecnico di Milano by adopting a double diaphragm shock tube facility. The shock tube was used as blast simulator; the idea to use shock tubes to simulate blast loading on structures is not new and this technique was developed to reproduce blast waves nearly identical to those obtained in live explosive tests [41,42]. Examples of the use of shock tubes to analyse the dynamic behaviour of concrete slabs and RC slabs according to several boundary conditions, like simply supported/clamped or resting on the ground can be found in [43–45].

The shock tube was originally adopted to investigate the behaviour of underground tunnel linings under blast conditions [45,46] through the use of an ad-hoc chamber designed to investigate soil-structure interaction. The shock tube was easily adapted to study plates under blast loads with different boundary conditions by changing the end chamber. The shock tube is able to produce a high pressure loading range, with a maximum reflected target pressure of about 3000 kPa. A detailed description of all the shock tube's components can be found in [33], while a comprehensive discussion on the shock tube's performance is given in [47]; only the main points of interest are summarized below.

Fig. 6 shows a schematic layout of the shock tube device in the assembled configuration. It consists of three chambers that can move on a linear guide system: the driver chamber, the diaphragm chamber (i.e. firing section or buffer chamber) and the driven chamber. The test area in which the specimen is fixed is placed at the end of the driven chamber. The tests were carried out using pressurized helium inside the driver and buffer chambers, and air at ambient condition in the driven chamber.

Driver, buffer and driven chambers have a length of 2.35, 0.26 and 10.5 m, respectively, thus resulting in a total shock tube length, excluding the test area, of 13.11 m. The driver and driven chambers have a 13.5 mm thick wall, while the buffer chamber has an external diameter of 857 mm that corresponds to the maximum diameter of the flange welded on the driver and driven ends; for all three chambers the internal diameter is equal to 481 mm.

The firing mechanism is activated when the two scored steel diaphragms that separate the buffer chamber from the driver and driven chambers fail. The diaphragms' failure is obtained by a differential pressure created between the driver/buffer and buffer/driven chambers. During the failure of diaphragms four petals form and the rapid propagation of the pressurized gas into the driven chamber occurs leading to the creation of a shock wave.

A picture of the test set-up area is shown in Fig. 7. The equipment used to fix the specimen consists of two steel crowns and a steel reaction flange (see Fig. 7a). The specimens were placed between two steel crowns specifically designed to guarantee a bilateral simply supported condition. The reaction end flange, consisting of a slip-on flange of 20″, was connected to the driven end flange using ten M52 bolts. An exploded view of the test set-up area highlighting all the components is shown in Fig. 7a, while an assembled view of the test set-up area is shown in Fig. 7b-c.

Mounting pressure sensors on a test sample to measure the load is not an easily practicable solution. Nevertheless, if deformations in the concrete slabs are small, the data from the sensor closest to the specimen face (sensor PT3) will provide a good approximation of the load that the concrete slabs experience.

Table 3
Shock wave characteristics.

Specimen ID	P_{peak} (kPa)	i_e^+ (kPa × ms)	t^+ (ms)	v_s (m/s)
LP0	339.1	3430	33.2	502
LP60	393.6	3451	39.7	500
LP120	376.3	3278	29.2	502
HP0	1090	6255	17.5	652
HP60	–	–	–	–
HP120-1	1118	6288	17.7	674
HP120-2	1126	6181	16.9	714

Table 3 summarizes the main properties that characterize the shock wave for each test: the peak pressure (P_{peak}), the positive specific impulse (i_e^+) the duration of the positive specific impulse (t^+), and the shock wave velocity (v_s). The latter was calculated using the data from sensors PT1-PT3. The pressure time histories for all the blast tests recorded by the transducer closest to the specimen (sensor PT3 in Fig. 6) are shown in Fig. 8. It is important to point out that the reflected pressure histories applied to the specimens are very repeatable. This means that the change in stiffness of the specimens due to fire application does not lead to any significant contribution to the fluid–structure interaction phenomenon and therefore the mechanical problem can be considered uncoupled by shock wave propagation.

A problem occurred during test HP60 that prevented the correct recording of transducers PT1-PT3. Nevertheless, the high repeatability of these tests, clearly visible in Fig. 8, allows the HP60 test results to be used as well.

4. Test results

This section describes the main results obtained in the experimental investigation. Fig. 9 shows the evolution of temperatures, recorded by

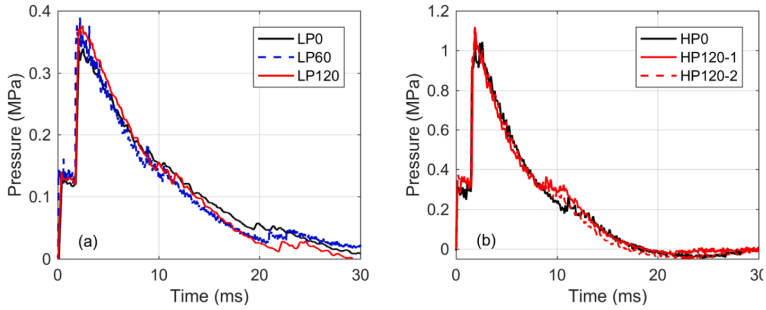

Fig. 8. Pressure–time histories for sensor PT3 in shock tube tests.

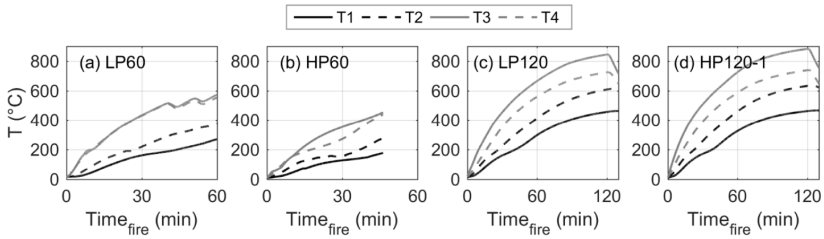

Fig. 9. Evolution of temperatures vs fire exposure time: (a) test LP60, (b) test HP 60, (c) test LP120 and (d) HP120-1.

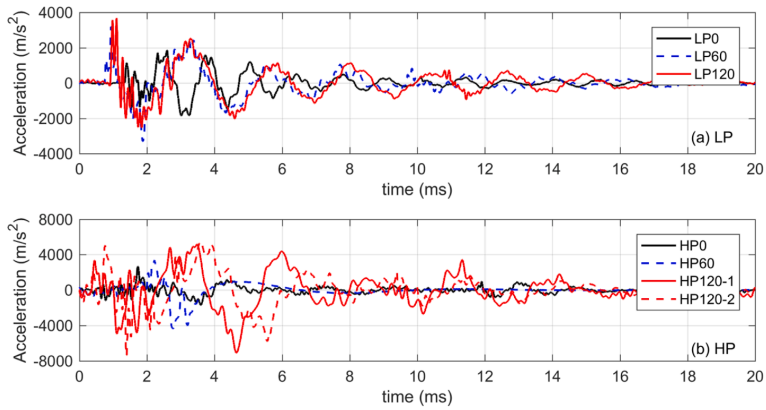

Fig. 10. Axial central specimen accelerations A1: (a) tests LP0, LP60, LP120 and (b) tests HP0, HP60, HP120-1, HP120-2.

thermocouples T1-T4, as the fire exposure time varies. Clearly, the highest temperature is read by thermocouple T3 that is closest to the burner (see Fig. 4). In specimens LP60 and HP60 (Fig. 9a-b), exposed to high temperature for a time of 60 min, the maximum temperature reached is about 600 °C, while the temperature on the specimen side not exposed to the fire is about 250 °C. Looking at specimens LP120 and HP120-1 (Fig. 9c-d) both characterized by a fire exposure time of 120 min, the maximum temperature reached is about 900 °C, while the temperature on the specimen side not exposed to the fire is about 450 °C. Although the fire curve was correctly applied to the HP60 specimen, a problem in data acquisition occurred in this test after approximately 45 min of fire exposure (Fig. 9b) and therefore the final data was lost.

The central accelerations of the specimens are compared in Fig. 10 for all the experimental tests. Fig. 10a and Fig. 10b compare low pressure (LP) and high pressure (HP) tests respectively, exposed to different fire exposure times (0, 60, 120 min). The influence of fire exposure time on the acceleration response of the specimens is illustrated and the elongation of the fundamental period of the specimens exposed to fire is clearly visible compared to the specimens not subjected to fire exposure. While for LP tests the exposure to fire modifies the frequency content of the response without significantly altering the maximum accelerations, in the HP tests the exposure to fire involves both a modification of the frequency content and an increase in the amplitude of the accelerations, thus indicating that the interaction between fire and blast is more pronounced.

When examining the frequency content of the recorded signals, it is important to remember that the shock tube is deformable and not fixed to the ground but can be moved on a linear guide system. For this reason, the axial acceleration of the tube was recorded during the tests using accelerometer A5 in order to distinguish the frequency content of the

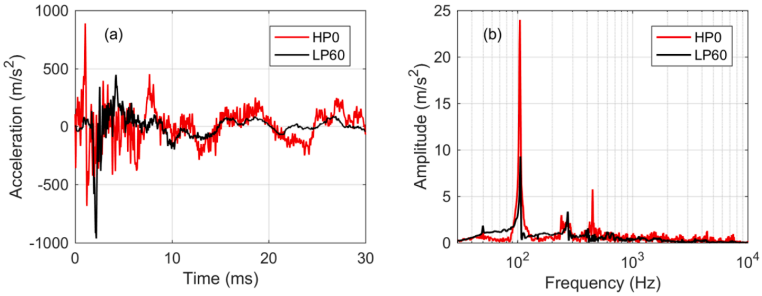

Fig. 11. (a) Shock tube axial acceleration A5 for tests HP0 and LP60 and (b) corresponding frequency spectrum.

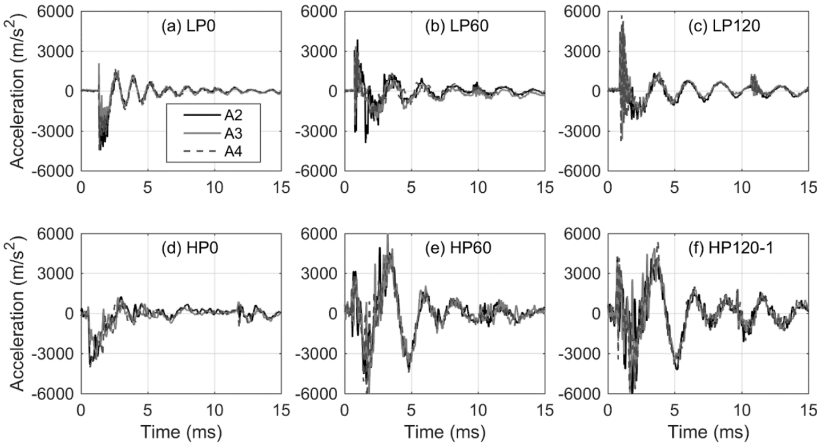

Fig. 12. Axial specimen accelerations A2-A4: (a) test LP0, (b) test LP60, (c) test LP120, (d) test HP0, (e) test HP60 and (f) HP120-1.

shock tube from the frequency content associated with the response of the specimens. The shock tube axial accelerations (A5) for tests HP0 and LP60, taken as an example, are shown in Fig. 11 together with the corresponding frequency spectrum. The main frequency associated with the axial movement of the tube is clearly visible in Fig. 11b and is equal to about 100 Hz.

Fig. 12 reports the results of the three accelerometers (A2–A4) placed at 120° in relation to each other on the specimens. The specimens' responses are characterised by an elevated symmetry. While this result was to be expected since the specimens are circular symmetric in terms of geometry and load, on the other hand the planarity of the shock wave impacting the specimens is confirmed. It is also interesting to note that the symmetry in the response is also preserved in the specimens exposed to the fire and which have therefore suffered damage (Fig. 12b-c-e-f). In fact, the presence of spalling is limited to small regions and even where it affects the symmetry of the specimen's geometry, it does not play a significant role on the symmetry of the specimens' response.

Fig. 13 shows front and rear crack patterns for all the tests with the exception of the LP0 test where no cracks were detected at the end of blast test. Cracks that formed after the fire exposure are depicted in red, whilst cracks that formed after the blast test are depicted in black. The LP0 test in which the blast load was applied without a high temperature exposure was characterized by the absence of cracks indicating as planned a linear elastic behaviour of the specimen. Looking at the HP0 specimen, characterized by a higher peak pressure and a higher impulse than specimen LP0 without fire exposure, a slight crack pattern both on the rear and front faces can be noted. Fire exposure induces quite severe damage in the specimens, revealed by the crack patterns shown in Fig. 13a-b-d-e-f. On the front face, the area in contact with the flame is clearly identifiable having a different colour and slight concrete spalling is visible in all the specimens exposed to fire (see grey regions in Fig. 13a-b-d-e-f). Fig. 14 shows the exposed surface of LP60 and HP120-2 specimens after the fire tests, as an example of each exposure time. In the pictures, both the area in contact with the flame and the region of concrete spalling can be easily recognized.

Radial cracks are always visible in all specimens exposed to fire. The radial cracks on the outer ring region of the slabs are mainly caused by the heating process that is directly applied to the central core of the slab. The thermal gradient between the central core and the external ring, because of the compatibility of the two regions, causes a circumferential tensile state of stress in the outer ring leading to the radial crack formation. In the specimens tested in HP conditions after fire exposure it is also possible to observe some circumferential cracks on the loaded surface (especially visible for HP60, Fig. 13d). This is due to the fact that, because the fire is applied only to the central region, the initial damage of the structure is not uniform along the radius but is more concentrated in the central heated region thus also creating a variation of the local sectional stiffness along the radius. The presence of an outer stiffer region affects the boundary condition thus also leading to the formation of radial tensile stresses on the loaded surface. In the case of a fire exposure time of 120 min, these cracks are less pronounced because the longer fire exposure leads to a more uniform distribution of the temperature and subsequently more uniform damage even along the radius.

The application of a blast load after the fire exposure has limited

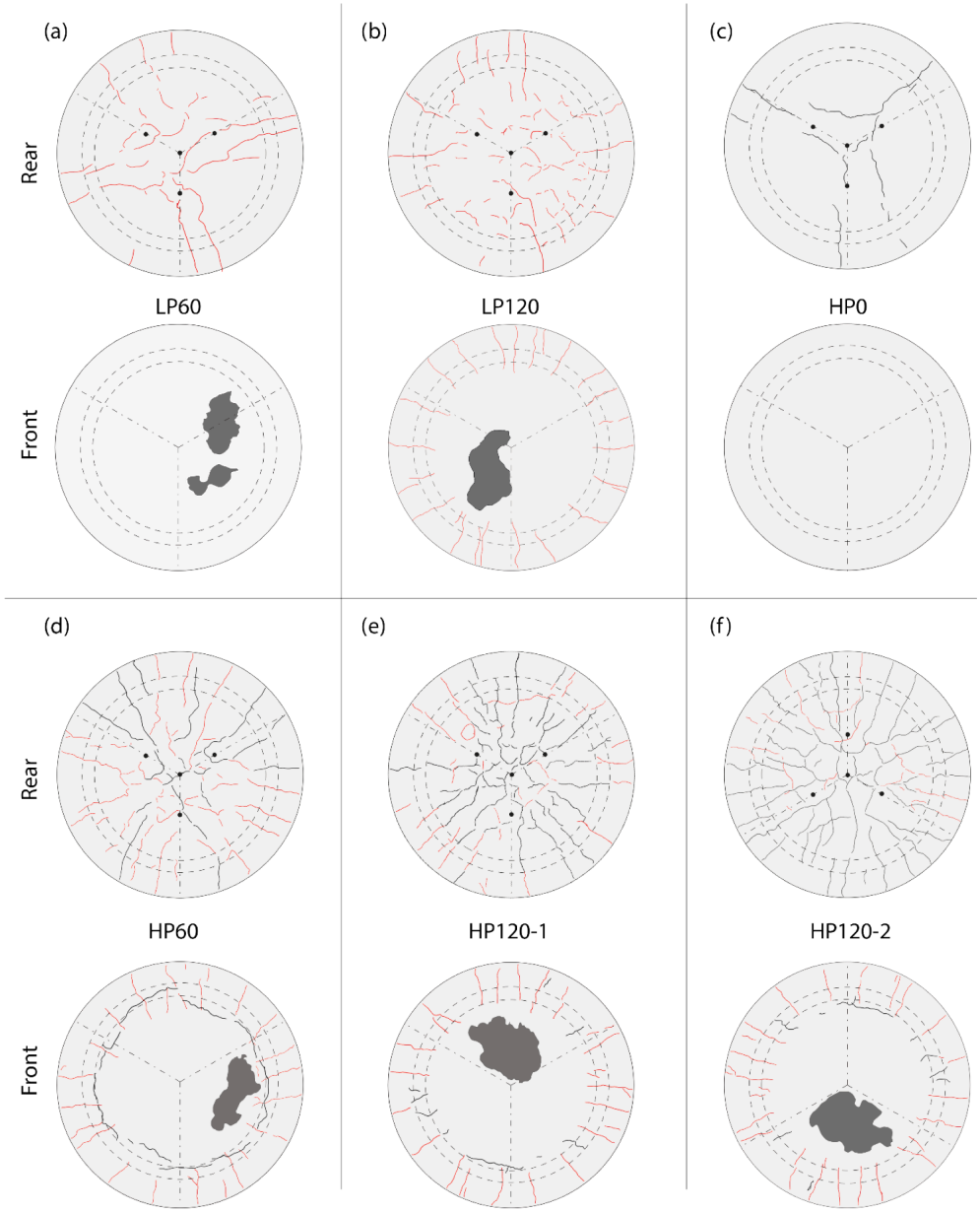

Fig. 13. Front and rear crack patterns for tests (a) LP60, (b) LP120, (c) HP0, (d) HP60, (e) HP120-1 and (f) HP120-2. Thermal and pressure cracks are indicated in red and in black respectively. (For interpretation of the references to colour in this figure legend, the reader is referred to the web version of this article.)

effects for specimens LP60 and LP120 since no new cracks were detected after the exposure to fire (Fig. 13a-b). A different trend can be observed in Fig. 13d-e-f for HP tests where the application of a blast load after the fire exposure produces further cracks in the specimens. It can be concluded that in LP tests, the main source of damage is the fire, while in HP tests both fire and blast contribute to the damage of the specimens, and the effect of blast is more amplified when a more severe fire exposure is applied.

Direct UPV measurements were carried out on the specimens before and after fire and blast loads. The aim of these measurements was to establish if, in case of fire and blast, the wave velocity decreases compared to the velocity in the pristine specimen, thus indicating that internal damage occurred in the specimen. Six points were monitored (Fig. 3) and average wave velocities are considered in the following discussion. Fig. 15 reports the average percentage reduction of wave velocity induced by fire and blast compared to the initial undamaged situation. In Fig. 15a, LP tests are examined first: effects of fire exposure are clearly visible leading to a wave velocity reduction of about 40% and

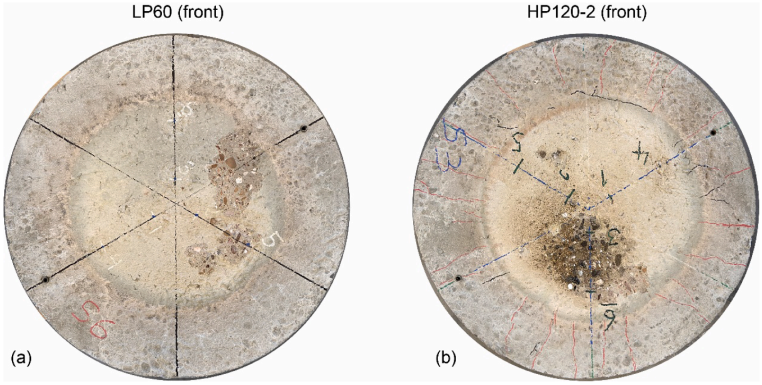

Fig. 14. Furnace flame footprint and spalling area for tests (a) LP60 and (b) HP120-2.

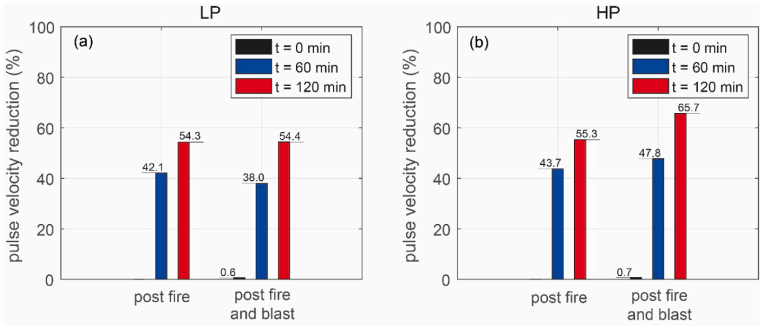

Fig. 15. Percentage reduction of direct ultrasonic pulse velocity results induced by fire and blast: (a) LP tests and (b) HP tests.

55% for fire exposure of 60 min and 120 min, respectively. In LP tests, the application of the blast load after the fire exposure does not significantly change the wave velocity, in line with the observed crack patterns discussed above. Looking at the HP tests, the wave velocity reduction due to fire exposure only is similar to that of LP tests. The application of a blast load in specimens already damaged by fire leads to a further reduction of the wave's velocity highlighting an increase in damage especially in specimens subjected to a fire exposure of 120 min. It should be emphasized that the cracks through the thickness of the specimen are not fully visible with direct UPV measurements. This justifies crack patterns on the specimens that are more severe than suggested by measurements with direct UPV.

5. Discussion

The experimental results presented in Section 4 are further analysed in this section using simplified tools, specifically: (i) an equivalent elastic single degree of freedom (SDOF) model and (ii) a linear elastic finite element (FE) model. Despite their simplicity, methods (i) and (ii) can be a useful tool to provide a deeper insight into the experimental results.

With reference to the equivalent SDOF model, the mass, the stiffness and the applied load of the RC slabs are replaced in the equation of motion with the equivalent values of a lumped mass–spring system. The principle of virtual displacement makes it possible to find the transformation coefficients that relate the equivalent mass, stiffness and load

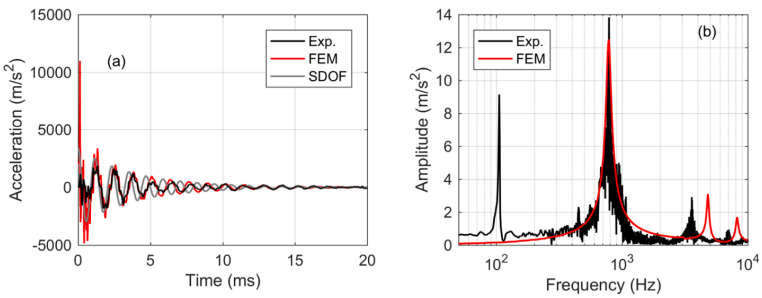

Fig. 16. Test LP0: a) time history acceleration A1 and b) frequency spectrum of signal A1.

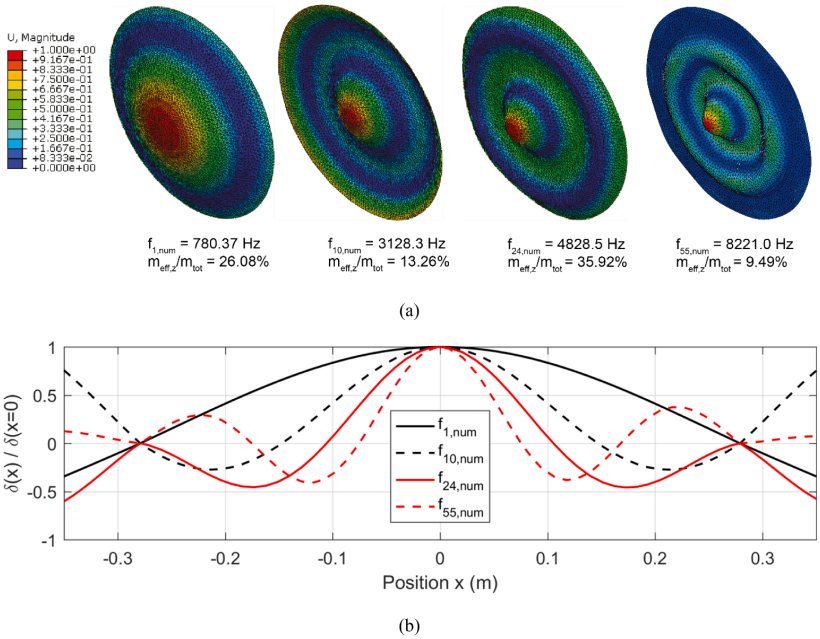

Fig. 17. First, tenth, twenty-fourth and fifty-fifth numerical modal shapes: (a) 3D views and (b) normalized displacement profiles along one diameter (U: normalized displacement amplitude).

in the SDOF system to their respective quantities in the actual slabs. The equivalent system has kinetic energy, strain energy and external work equal to the distributed system [48]. In calculating the transformation factors necessary to develop the equivalent SDOF model, a simplification was adopted: the loading area is extended up to the radius $r_1 = 275$ mm equal to the position of the support (see Fig. 7a). The equivalent system has a total diameter equal to the real specimen slab ($r_2 = 345$ mm). The elastic transformation factors used in this study are similar to those given in [49] for a simply supported plate; the exception is represented by the slab radius r_2 that does not coincide with the support radius r_1. The material parameters necessary to describe the SDOF model are the average values reported in Section 2.1.

With reference to the linear elastic FE model, this was built and processed in the Abaqus 6.14-5 environment [50], and consists of 7987 3-node triangular shell elements (element S3, average edge size 10 mm) connected through 4103 nodes. Boundary conditions and the blast load are applied according to the experimental set-up shown in Fig. 7. The elastic modulus of the concrete measured experimentally ($E \cong$ 28000 MPa) was corrected by a factor of 1.15 to take into account the stiffening effect of the reinforcement following an homogenized approach for RC sections. The Young's modulus E, the Poisson's ratio ν and the density ρ adopted in the FE model are then assumed to be equal to $E = 32000$ MPa, $\nu = 0.2$ and $\rho = 2500$ kg/m^3. The finite element model, due to its simplicity, was used mainly for eigenfrequency analysis and for studying the dynamic response of the specimen that under blast loads did not show any damage (i.e. LP0). In this regard, specimen LP0 is an important reference to better understand the structural behaviour of all the other specimens.

Fig. 16a compares the central slab acceleration A1 recorded during the reference test LP0 with those obtained with the equivalent elastic SDOF model and with the FE model. The experimental acceleration is well reproduced by both simplified models. The frequency spectrum of the experimental signal A1 is compared with the numerical one (i.e. FE) in figure Fig. 16b. The first numerical frequency ($f_{1,num} = 780$ Hz) is

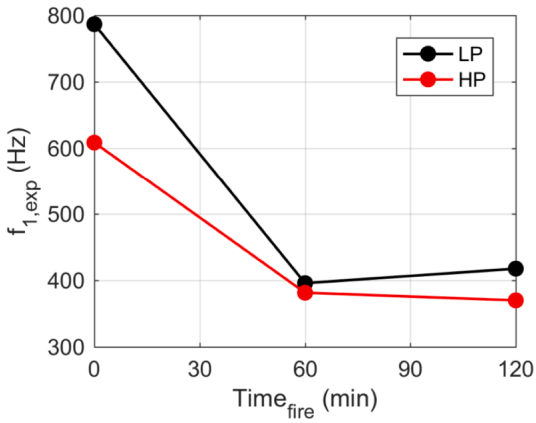

Fig. 18. Variation of the first experimental frequency $f_{1,exp}$ with the variation of the fire exposure time for the LP and HP tests.

almost identical to the experimental one ($f_{1,exp} = 787$ Hz); the second and third experimental peaks visible in Fig. 16b are overestimated by the FE model that results to be stiffer than the real slab. The SDOF model provides a first natural frequency equal to $f_{1,SDOF} = 812$ Hz that is slightly higher than the experimental one, but it can be considered a satisfactory prediction.

The experimental peak visible at the lowest frequency of about 100 Hz is not related to the slab response, but it depends on the shock tube's axial movement and should not be considered in the following discussion (see Section 4).

Fig. 17 illustrates the first four significant mode shapes of the FE model (Modes 1, 10, 24 and 55). These four mode shapes involve an out-

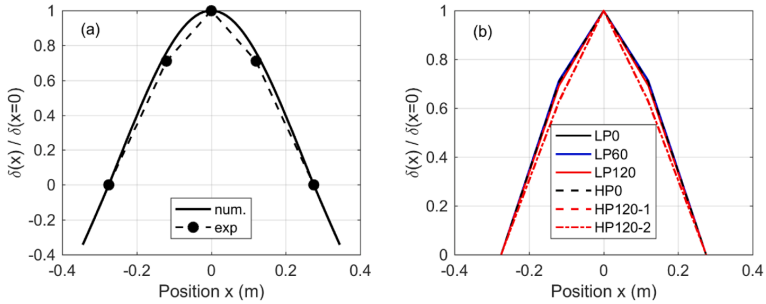

Fig. 19. (a) Comparison between experimental (LP0) and numerical first modal shape; (b) first modal shape derived from experimental data for all the specimens.

of-plane translation (the z direction) with an activation of the effective mass involved in z direction normalized with respect to the total mass of the model of 26%, 13%, 36% and 9% respectively. Mode shapes not shown in Fig. 17 involve negligible effective mass.

Given the good prediction of the slab's central acceleration provided by the SDOF system, it could be stated that the first mode of vibration mainly governs the slab's response. For this reason, a detailed analysis of this mode is discussed in the following.

By examining the frequency content of the signal A1 of all the specimens recorded during the blast tests it is also possible to establish the variation of the fundamental frequency $f_{1,exp}$ as the fire exposure time varies (Fig. 18). The variation of the fundamental frequency is directly correlated to the variation (reduction) of the stiffness of the specimen and is ultimately a measure of the accumulated damage. Looking at the LP tests and keeping in mind that test LP0 corresponds to an undamaged state, the fire exposure reduced the fundamental frequency by 50% providing a first frequency equal to about 400 Hz for a fire exposure time of both 60 and 120 min. Observing the HP tests, there is a reduction of the first frequency of 25% compared to the non-damaged situation for the blast effect only (test HP0). The exposure to fire further reduces the first frequency to values below 400 Hz for the HP120 tests, that corresponds to a first frequency reduction higher than 50% compared to the pristine specimen.

A Frequency Domain Decomposition (FDD) approach [51] was adopted to define the experimental modes of vibration of the slabs starting from the measurements of the accelerations during the tests. Fig. 19a compares the mode shape of the first mode of vibration provided by the eigenfrequency analysis with the mode shape obtained by the application of an FDD procedure to the experimental accelerations measured for test LP0. The figure represents the deformed shape of a diameter of the specimen considering a reference system placed in the centre of the slab (x = 0). Due to the small amount of accelerometers placed on the specimens, just the dotted points at x = 0 and x = ±0.12 m can be experimentally obtained, while the zero displacement condition is imposed at the support (x = ± 0.275 m). The figure shows good agreement between the experimental deformed shape and the numerical prediction; this comparison proves that the boundary conditions applied in the tests represent a simply supported condition well.

Fig. 19b presents the mode shape of the first mode of vibration for the different tests performed. The deformed shape of the first mode is almost identical for all the LP tests and for the HP0 test, while a slight difference can be observed for the two HP120 tests. The damage induced both by fire and by blast seems to have a limited effect on the first mode shape despite the change in mode frequency.

Damping is generally considered as a reliable indicator of damage in structures [52] and several studies have pointed out the effect of damage on damping [53–57]. Other investigations have even shown how cracks in RC structures could induce an increase of damping ratio [58] and that the change in damping is well correlated even to the crack depth [59].

The analysis of the decay of the acceleration peaks for all the experimental tests makes it possible to estimate the damping ratio ζ_{exp} and its variation compared to the undamaged situation (Fig. 20). Using the acceleration record ($\ddot{u}$) of the free vibration phase, the damping ratio was determined from:

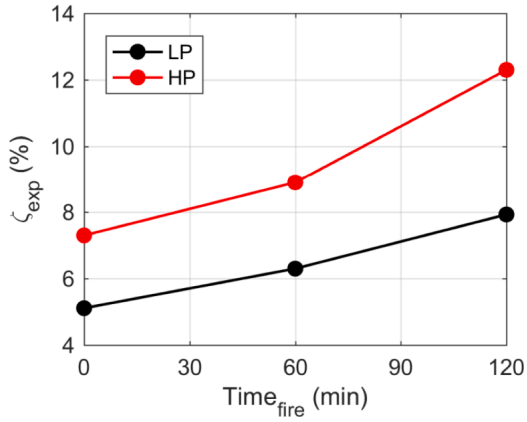

Fig. 20. Variation of damping ratio ζ_{exp} with the variation of the fire exposure time for the LP and HP tests.

$$\zeta_{exp} = \frac{1}{2\pi j} \ln \frac{\ddot{u}_i}{\ddot{u}_{i+j}} \tag{1}$$

where $\ddot{u}_i$ is the acceleration at the peak i and $\ddot{u}_{i+j}$ the acceleration at the peak $i+j$. Eq. (1) is valid for a lightly damped system. The damping ratio defined in Eq. (1) is a linear feature of damping and represents the extent of energy dissipation in the samples [52]. The presence of fire damage and/or cracks leads to larger energy dissipation and therefore to a larger damping ratio.

While the damping was approximately 5% for the LP0 specimen, the 60 min fire exposure (test LP60) increases the damping to 6%, and the 120 min fire exposure (LP120) further increases it to 7%. Looking at the HP tests, applying a higher peak pressure and impulse than the LP tests results in an increase of damping ratio equal to 7%. The combined effect of blast and fire leads to an increase in damping ratios of 9% and 12% for fire exposure times of 60 and 120 min, respectively. While the black curve in Fig. 20 can be seen as the exclusive contribution of the fire, the red curve represents the combined effect of blast and fire.

An ad-hoc subroutine was developed in a LabVIEW environment to derive reliable displacement measurements from the central acceleration signals A1 (Fig. 21). This subroutine consists of a double time integration of the acceleration applying a low pass filter at a frequency of 80 kHz before each time integration step.

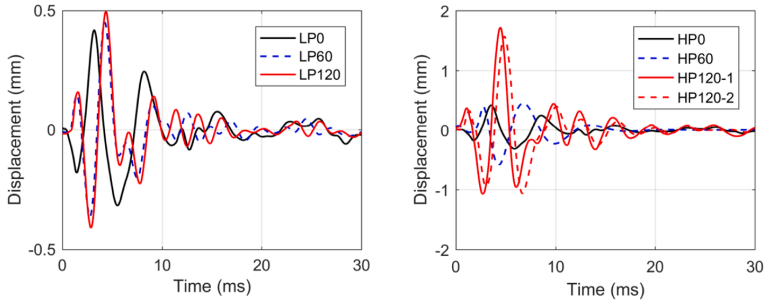

Fig. 21. Displacement-time history responses derived using a LabVIEW subroutine for (a) LP tests and (b) HP tests.

The effect of damage due to exposure to fire compared to the pristine specimen is clearly visible for both the LP (Fig. 21a) and HP (Fig. 21b) tests. In both figures the period elongation due to the combined effects of blast and fire is visible. For HP tests, the period elongation is also combined with an amplification of the maximum displacements with peaks that can be 3 times higher for specimens subjected to a fire exposure of 120 min compared to specimens without fire exposure.

6. Concluding remarks

In this study, the structural performance of reinforced concrete (RC) slabs subjected to combined fire and blast actions were investigated experimentally. The sequence of fire and blast was obtained using proper gas burner equipment and a shock tube device. Simplified numerical tools, namely (i) an equivalent elastic single degree of freedom (SDOF) model and (ii) a linear elastic finite element (FE) model were also used to provide a deeper insight into the experimental results. Based on this research, the following conclusions can be drawn:

- The shock tube used in the blast tests produced consistent and blast-like loading conditions characterized by high repeatability. Accelerometer recordings placed at 120° on the specimens confirm the planarity of the shock wave impacting the specimens.
- Test results pointed out the negligible role of the fluid–structure interaction in the cases investigated even when the samples were previously exposed to fire curves.
- Temperature evolutions, monitored using thermocouples embedded through the thickness of the slabs, show that the slabs reach temperatures between 250–600 °C and between 450–900 °C for fire exposure times of 60 and 120 min, respectively.
- Fire exposure causes cracks on both faces of the specimen; some of these cracks pass through the thickness. Limited concrete spalling was observed when the fire exposure was equal to 120 min. In LP tests, the subsequent application of blast loads after fire exposure does not significantly change the crack pattern. On the contrary, in HP tests the higher peak pressure and the higher impulse compared to LP tests induce new cracks in the specimens. This effect is maximized when the fire exposure time is higher (120 min).
- Fire exposure induces a pronounced decrease of strength and stiffness in the specimens, as pointed out by the analysis of (i) the crack patterns, (ii) the first frequency shift and (iii) the reduction of the wave velocity recorded using UPV measurements.
- The analysis of the frequency spectrum of the accelerometer signals shows a significant reduction of the slab's first frequency that was higher than 50% for HP120 tests compared to the pristine specimen.
- Experimental data makes it possible to estimate the evolution of the damping ratio as the fire exposure time varies and for different blast pressure levels. The damping ratios range from 5% for pristine specimen to 12% for HP120 tests, thus providing an indication of the damage accumulated by the slab specimens.
- The eigenvalue analysis on a simplified FE shell model provides a first numerical frequency that is in good agreement with the experimental one. This confirms the correctness of the set-up used during the shock tube tests that can be schematized as a simply supported condition. The simplified SDOF model also provides a fundamental frequency in good agreement with the experimental data.
- An ad-hoc subroutine developed in a LabVIEW environment made it possible to derive displacement estimations from the acceleration signals. The analysis of the specimens' central displacement shows that a greater exposure time to fire corresponds to greater displacement peaks in response to the blast loads. The maximum displacement values were 3 times higher for specimens subjected to a fire exposure of 120 min compared to specimens without fire exposure.
- The experimental data presented in this work is valuable in order to define a reliable benchmark for numerical models which, upon numerical upscaling, will be instrumental for the design of tunnels under exceptional load conditions, such as the combined action of fire and subsequent internal explosion.

Declaration of Competing Interest

The authors declare that they have no known competing financial interests or personal relationships that could have appeared to influence the work reported in this paper.

Acknowledgements

The work presented in this paper is part of an ongoing PhD study funded by the Norwegian Public Roads Administration as part of the Coastal Highway Route E39 project.

References

[1] Beard A, Carvel R. Handbook of tunnel fire safety. Second ed. ICE Publishing 2012.
[2] Kodur V, Naser M. Structural fire engineering. McGraw-Hill; 2020.
[3] Savov K, Lackner R, Mang HA. Stability assessment of shallow tunnels subjected to fire load. Fire Saf J 2005;40:745–63. https://doi.org/10.1016/j.firesaf.2005.07.004.
[4] Pichler C, Lackner R, Mang HA. Safety assessment of concrete tunnel linings under fire load. J Struct Eng 2006;132:961–9. https://doi.org/10.1061/(asce)0733-9445(2006)132:6(961).
[5] Yan ZG, Zhu HH, Woody JJ, Ding WQ. Full-scale fire tests of RC metro shield TBM tunnel linings. Constr Build Mater 2012;36:484–94. https://doi.org/10.1016/j.conbuildmat.2012.06.006.
[6] Lilliu G, Meda A. Nonlinear phased analysis of reinforced concrete tunnels under fire exposure. J Struct Fire Eng 2013;4:131–42. https://doi.org/10.1260/2040-2317.4.3.131.
[7] Felicetti R. Assessment methods of fire damages in concrete tunnel linings. Fire Technol 2013;49:509–29. https://doi.org/10.1007/s10694-011-0229-6.
[8] Wang F, Wang M, Huo J. The effects of the passive fire protection layer on the behavior of concrete tunnel linings: a field fire testing study. Tunn Undergr Sp Technol 2017;69:162–70. https://doi.org/10.1016/j.tust.2017.06.021.
[9] Sakkas K, Vagiokas N, Tsiamouras K, Mandalozis D, Benardos A, Nomikos P. In-situ fire test to assess tunnel lining fire resistance. Tunn Undergr Sp Technol 2019;85:368–74. https://doi.org/10.1016/j.tust.2019.01.002.

[10] Sun Z, Zhang Y, Yuan Y, Mang HA. Stability analysis of a fire-loaded shallow tunnel by means of a thermo-hydro-chemo-mechanical model and discontinuity layout optimization. Int J Numer Anal Methods Geomech 2019;43:2551–64. https://doi.org/10.1002/nag.2991.
[11] Lo Monte F, Felicetti R, Meda A, Bortolussi A. Explosive spalling in reinforced concrete tunnels exposed to fire: Experimental assessment and numerical modelling. In: Peila D, Viggiani G, Viggiani G, Celestino T, editors. Tunnels Undergr. Cities Eng. Innov. meet Archaeol. Archit. Art- Proc. WTC 2019 ITA-AITES World Tunn. Congr., CRC Press/Balkema 2019, 2519–26.
[12] Agrawal A, Kodur VKR. A novel experimental approach for evaluating residual capacity of fire damaged concrete members. Fire Technol 2020;56:715–35. https://doi.org/10.1007/s10694-019-00900-1.
[13] Stucchi R, Amberg F. A practical approach for tunnel fire verification. Struct Eng Int 2020;30:515–29. https://doi.org/10.1080/10168664.2020.1772697.
[14] EN 1991-1-2. Eurocode 1: Actions on structures—Part 1–2: General actions—Actions on structures exposed to fire. Brussels: 2004.
[15] EN 1992-1-2. Eurocode 2: Design of concrete structures— Part 1–2: General rules—Structural fire design. Brussel: 2004.
[16] Feldgun VR, Kochetkov AV, Karinski YS, Yankelevsky DZ. Internal blast loading in a buried lined tunnel. Int J Impact Eng 2008;35:172–83. https://doi.org/10.1016/j.ijimpeng.2007.01.001.
[17] Liu H. Dynamic analysis of subway structures under blast loading. Geotech Geol Eng 2009;27:699–711. https://doi.org/10.1007/s10706-009-9269-9.
[18] Liu H. Soil-structure interaction and failure of cast-iron subway tunnels subjected to medium internal blast loading. J Perform Constr Facil 2012;26:691–701. https://doi.org/10.1061/(asce)cf.1943-5509.0000292.
[19] Colombo M, Martinelli P, di Prisco M. Underground tunnels exposed to internal blast: Effect of the explosive source position. 711. 2016. doi:10.4028/www.scientific.net/KEM.711.852.
[20] Gao M, Zhang JY, Chen QS, Gao GY, Yang J, Li DY. An exact solution for three-dimensional (3D) dynamic response of a cylindrical lined tunnel in saturated soil to an internal blast load. Soil Dyn Earthq Eng 2016;90:32–7. https://doi.org/10.1016/j.soildyn.2016.08.031.
[21] Yu H, Wang Z, Yuan Y, Li W. Numerical analysis of internal blast effects on underground tunnel in soils. Struct Infrastruct Eng 2016;12:1090–105. https://doi.org/10.1080/15732479.2015.1077260.
[22] Zhao Y, Chu C, Vafeidis A, Li J. Vibration of a cylindrical tunnel under a centric point-source explosion. Shock Vib 2017;2017. https://doi.org/10.1155/2017/9152632.
[23] Kristoffersen M, Minoretti A, Børvik T. On the internal blast loading of submerged floating tunnels in concrete with circular and rectangular cross-sections. Eng Fail Anal 2019;103:462–80. https://doi.org/10.1016/j.engfailanal.2019.04.074.
[24] Prasanna R, Boominathan A. Finite-element studies on factors influencing the response of underground tunnels subjected to internal explosion. Int J Geomech 2020;20:04020089. https://doi.org/10.1061/(asce)gm.1943-5622.0001678.
[25] Goel MD, Verma S, Panchal S. Effect of internal blast on tunnel lining and surrounding soil. Indian Geotech J 2020. https://doi.org/10.1007/s40098-020-00451-1.
[26] Minoretti A, Xiang X, Johansen IL, Eidem M. The future of the tunnel crossing: the submerged floating tube bridge. Struct Eng Int 2020;30:493–7. https://doi.org/10.1080/10168664.2020.1775165.
[27] Kakogiannis D, Pascualena F, Reymen B, Pyl L, Ndambi JM, Segers E, et al. Blast performance of reinforced concrete hollow core slabs in combination with fire: Numerical and experimental assessment. Fire Saf J 2013;57:69–82. https://doi.org/10.1016/j.firesaf.2012.10.027.
[28] Pascualena F, Ndambi J, Reymen B, Desmet B, Segers E, Vantomme J. Blast performance of concrete slabs in combination with fire. Proc. 8th Int. Conf. Struct. Dyn. EURODYN 2011, Leuven Belgium: 2011, 3310–7.
[29] Ruan Z, Chen L, Fang Q. Numerical investigation into dynamic responses of RC columns subjected for fire and blast. J Loss Prev Process Ind 2015;34:10–21. https://doi.org/10.1016/j.jlp.2015.01.009.
[30] Zhai C, Chen L, Xiang H, Fang Q. Experimental and numerical investigation into RC beams subjected to blast after exposure to fire. Int J Impact Eng 2016;97:29–45. https://doi.org/10.1016/j.ijimpeng.2016.06.004.
[31] Zhang Q, Wang WY, Bai SS, Tan YH. Response analysis of tunnel lining structure under impact and fire loading. Adv Mech Eng 2019;11:1–6. https://doi.org/10.1177/1687814019834473.
[32] Colombo M, Martinelli P, di Prisco M. A design approach for tunnels exposed to blast and fire. Struct Concr 2015;16:262–72. https://doi.org/10.1002/suco.201400052.
[33] Colombo M, di Prisco M, Martinelli P. A new shock tube facility for tunnel safety. Exp Mech 2011;51:1143–54. https://doi.org/10.1007/s11340-010-9430-7.
[34] Arano A, Colombo M, Martinelli P, Øverli JA, Hendriks MA, Kanstad T, et al. Material characterization approach for modelling high-strength concrete after cooling from elevated temperatures. J Mater Civ Eng 2021;33:04021086. https://doi.org/10.1061/(ASCE)MT.1943-5533.0003694.
[35] ITA-AITES. Guidelines for structural fire resistance for road tunnels. 2004.
[36] ISO 1920-10:2010. Testing of concrete - Part 10: Determination of static modulus of elasticity in compression. 2010.
[37] ISO 15630-1:2019. Steel for the reinforcement and prestressing of concrete - Test methods - Part 1: Reinforcing bars, rods and wire. 2019.
[38] Timoshenko S, Woinowsky-Krieger S. Theory of plates and shells. New York: McGraw-Hill; 1959.
[39] Johansen K. Yield-line theory. London: Cement and Concrete Association; 1962.
[40] Bungey J, Millard S, Grantham M. Testing of concrete in structures. 4th ed. London: Taylor and Francis; 2006. https://doi.org/10.1201/9781482264685.
[41] Ritzel D, Thibault P. Development of an efficient low-cost blast tube facility. Tenth Int. Symp. Mil. Appl. Blast Simul. (MABS 10), Freiburg, Germany: 1987.
[42] NATO-AEP-25. Nuclear Blast and Thermal Test Methods and Procedures. NATO Allied Engineering Publication; 1995.
[43] Toutlemonde F, Rossi P, Boulay C, Gourraud C, Guedon D. Dynamic behaviour of concrete: tests of slabs with a shock tube. Mater Struct 1995;28:293–8. https://doi.org/10.1007/BF02473264.
[44] Kristoffersen M, Pettersen JE, Aune V, Børvik T. Experimental and numerical studies on the structural response of normal strength concrete slabs subjected to blast loading. Eng Struct 2018;174:242–55. https://doi.org/10.1016/j.engstruct.2018.07.022.
[45] Colombo M, Martinelli P, di Prisco M. Layered high-performance concrete plates interacting with granular soil under blast loads: An experimental investigation. Eur J Environ Civ Eng 2013;17:1002–25. https://doi.org/10.1080/19648189.2013.841595.
[46] Colombo M, Martinelli P, di Prisco M. On the blast resistance of high performance tunnel segments. Mater Struct Constr 2016;49:117–31. https://doi.org/10.1617/s11527-014-0480-7.
[47] Andreotti R, Colombo M, Guardone A, Martinelli P, Riganti G, di Prisco M. Performance of a shock tube facility for impact response of structures. Int J Non Linear Mech 2015;72:262–72. https://doi.org/10.1016/j.ijnonlinmec.2015.02.010.
[48] Biggs J. Introduction to structural dynamics. New York: McGraw-Hill; 1964.
[49] Colombo M, Martinelli P. Pressure-impulse diagrams for RC and FRC circular plates under blast loads. Eur J Environ Civ Eng 2012;16:837–62. https://doi.org/10.1080/19648189.2012.675149.
[50] Dassault Systèmes. Abaqus analysis user's manual - version 6.14 2016.
[51] Brincker R, Zhang L, Andersen P. Modal identification from ambient responses using frequency domain decomposition. Proc. Int. Modal Anal. Conf. - IMAC 2000: 625–30.
[52] Cao MS, Sha GG, Gao YF, Ostachowicz W. Structural damage identification using damping: A compendium of uses and features. Smart Mater Struct 2017;26:043001. https://doi.org/10.1088/1361-665X/aa550a.
[53] Kennedy J, Grace N. Prestressed continuous composite bridges under dynamic load. J Struct Eng (United States) 1990;116:1660–78.
[54] Rezaee M, Hassannejad R. Free vibration analysis of simply supported beam with breathing crack using perturbation method. Acta Mech Solida Sin 2010;23:459–70. https://doi.org/10.1016/S0894-9166(10)60048-1.
[55] Chandra R, Singh SP, Gupta K. A study of damping in fiber-reinforced composites. J Sound Vib 2003;262:475–96. https://doi.org/10.1016/S0022-460X(03)00107-X.
[56] Kyriazoglou C, Guild FJ. Quantifying the effect of homogeneous and localized damage mechanisms on the damping properties of damaged GFRP and CFRP continuous and woven composite laminates-an FEA approach. Compos Part A Appl Sci Manuf 2005;36:367–79. https://doi.org/10.1016/j.compositesa.2004.06.037.
[57] Birman V, Byrd LW. Effect of matrix cracks on damping in unidirectional and cross-ply ceramic matrix composites. J Compos Mater 2002;36:1859–77. https://doi.org/10.1177/0021998302036015247.
[58] Daneshjoo F, Gharighoran A. Experimental and theoretical dynamic system identification of damaged RC beams. Electron J Struct Eng 2008;8:29–39.
[59] Panteliou SD, Chondros TG, Argyrakis VC, Dimarogonas AD. Damping factor as an indicator of crack severity. J Sound Vib 2001;241:235–45. https://doi.org/10.1006/jsvi.2000.3299.

DEPARTMENT OF STRUCTURAL ENGINEERING
NORWEGIAN UNIVERSITY OF SCIENCE AND TECHNOLOGY

N–7491 TRONDHEIM, NORWAY
Telephone: +47 73 59 47 00

DOCTORAL THESES

"Reliability Analysis of Structural Systems using Nonlinear Finite Element Methods",
C. A. Holm, 1990:23, ISBN 82-7119-178-0.

"Uniform Stratified Flow Interaction with a Submerged Horizontal Cylinder",
Ø. Arntsen, 1990:32, ISBN 82-7119-188-8.

"Large Displacement Analysis of Flexible and Rigid Systems Considering Displacement-Dependent Loads and Nonlinear Constraints",
K. M. Mathisen, 1990:33, ISBN 82-7119-189-6.

"Solid Mechanics and Material Models including Large Deformations",
E. Levold, 1990:56, ISBN 82-7119-214-0, ISSN 0802-3271.

"Inelastic Deformation Capacity of Flexurally-Loaded Aluminium Alloy Structures",
T. Welo, 1990:62, ISBN 82-7119-220-5, ISSN 0802-3271.

"Visualization of Results from Mechanical Engineering Analysis",
K. Aamnes, 1990:63, ISBN 82-7119-221-3, ISSN 0802-3271.

"Object-Oriented Product Modeling for Structural Design",
S. I. Dale, 1991:6, ISBN 82-7119-258-2, ISSN 0802-3271.

"Parallel Techniques for Solving Finite Element Problems on Transputer Networks",
T. H. Hansen, 1991:19, ISBN 82-7119-273-6, ISSN 0802-3271.

"Statistical Description and Estimation of Ocean Drift Ice Environments",
R. Korsnes, 1991:24, ISBN 82-7119-278-7, ISSN 0802-3271.

"Properties of concrete related to fatigue damage: with emphasis on high strength concrete",
G. Petkovic, 1991:35, ISBN 82-7119-290-6, ISSN 0802-3271.

"Turbidity Current Modelling",
B. Brørs, 1991:38, ISBN 82-7119-293-0, ISSN 0802-3271.

"Zero-Slump Concrete: Rheology, Degree of Compaction and Strength. Effects of Fillers as Part Cement-Replacement",
C. Sørensen, 1992:8, ISBN 82-7119-357-0, ISSN 0802-3271.

"Nonlinear Analysis of Reinforced Concrete Structures Exposed to Transient Loading",
K. V. Høiseth, 1992:15, ISBN 82-7119-364-3, ISSN 0802-3271.

“Finite Element Formulations and Solution Algorithms for Buckling and Collapse Analysis of Thin Shells”,
R. O. Bjærum, 1992:30, ISBN 82-7119-380-5, ISSN 0802-3271.

“Response Statistics of Nonlinear Dynamic Systems”,
J. M. Johnsen, 1992:42, ISBN 82-7119-393-7, ISSN 0802-3271.

“Digital Models in Engineering. A Study on why and how engineers build and operate digital models for decision support”,
J. Høyte, 1992:75, ISBN 82-7119-429-1, ISSN 0802-3271.

“Sparse Solution of Finite Element Equations”,
A. C. Damhaug, 1992:76, ISBN 82-7119-430-5, ISSN 0802-3271.

“Some Aspects of Floating Ice Related to Sea Surface Operations in the Barents Sea”,
S. Løset, 1992:95, ISBN 82-7119-452-6, ISSN 0802-3271.

“Modelling of Cyclic Plasticity with Application to Steel and Aluminium Structures”,
O. S. Hopperstad, 1993:7, ISBN 82-7119-461-5, ISSN 0802-3271.

“The Free Formulation: Linear Theory and Extensions with Applications to Tetrahedral Elements with Rotational Freedoms”,
G. Skeie, 1993:17, ISBN 82-7119-472-0, ISSN 0802-3271.

“Høyfast betongs motstand mot piggdekkslitasje. Analyse av resultater fra prøving i Veisliter'n”,
T. Tveter, 1993:62, ISBN 82-7119-522-0, ISSN 0802-3271.

“A Nonlinear Finite Element Based on Free Formulation Theory for Analysis of Sandwich Structures”,
O. Aamlid, 1993:72, ISBN 82-7119-534-4, ISSN 0802-3271.

“The Effect of Curing Temperature and Silica Fume on Chloride Migration and Pore Structure of High Strength Concrete”,
C. J. Hauck, 1993:90, ISBN 82-7119-553-0, ISSN 0802-3271.

“Failure of Concrete under Compressive Strain Gradients”,
G. Markeset, 1993:110, ISBN 82-7119-575-1, ISSN 0802-3271.

“An experimental study of internal tidal amphidromes in Vestfjorden”,
J. H. Nilsen, 1994:39, ISBN 82-7119-640-5, ISSN 0802-3271.

“Structural analysis of oil wells with emphasis on conductor design”,
H. Larsen, 1994:46, ISBN 82-7119-648-0, ISSN 0802-3271.

“Adaptive methods for non-linear finite element analysis of shell structures”,
K. M. Okstad, 1994:66, ISBN 82-7119-670-7, ISSN 0802-3271.

“On constitutive modelling in nonlinear analysis of concrete structures”,
O. Fyrileiv, 1994:115, ISBN 82-7119-725-8, ISSN 0802-3271.

“Fluctuating wind load and response of a line-like engineering structure with emphasis on motion-induced wind forces”,
J. Bogunovic Jakobsen, 1995:62, ISBN 82-7119-809-2, ISSN 0802-3271.

“An experimental study of beam-columns subjected to combined torsion, bending and axial actions”,
A. Aalberg, 1995:66, ISBN 82-7119-813-0, ISSN 0802-3271.

“Scaling and cracking in unsealed freeze/thaw testing of Portland cement and silica fume concretes”,
S. Jacobsen, 1995:101, ISBN 82-7119-851-3, ISSN 0802-3271.

“Damping of water waves by submerged vegetation. A case study of laminaria hyperborea”,
A. M. Dubi, 1995:108, ISBN 82-7119-859-9, ISSN 0802-3271.

“The dynamics of a slope current in the Barents Sea”,
Sheng Li, 1995:109, ISBN 82-7119-860-2, ISSN 0802-3271.

“Modellering av delmaterialenes betydning for betongens konsistens”,
Ernst Mørtsell, 1996:12, ISBN 82-7119-894-7, ISSN 0802-3271.

“Bending of thin-walled aluminium extrusions”,
Birgit Søvik Opheim, 1996:60, ISBN 82-7119-947-1, ISSN 0802-3271.

“Material modelling of aluminium for crashworthiness analysis”,
Torodd Berstad, 1996:89, ISBN 82-7119-980-3, ISSN 0802-3271.

“Estimation of structural parameters from response measurements on submerged floating tunnels”,
Rolf Magne Larssen, 1996:119, ISBN 82-471-0014-2, ISSN 0802-3271.

“Numerical modelling of plain and reinforced concrete by damage mechanics”,
Mario A. Polanco-Loria, 1997:20, ISBN 82-471-0049-5, ISSN 0802-3271.

“Nonlinear random vibrations - numerical analysis by path integration methods”,
Vibeke Moe, 1997:26, ISBN 82-471-0056-8, ISSN 0802-3271.

“Numerical prediction of vortex-induced vibration by the finite element method”,
Joar Martin Dalheim, 1997:63, ISBN 82-471-0096-7, ISSN 0802-3271.

“Time domain calculations of buffeting response for wind sensitive structures”,
Ketil Aas-Jakobsen, 1997:148, ISBN 82-471-0189-0, ISSN 0802-3271.

“A numerical study of flow about fixed and flexibly mounted circular cylinders”,
Trond Stokka Meling, 1998:48, ISBN 82-471-0244-7, ISSN 0802-3271.

“Estimation of chloride penetration into concrete bridges in coastal areas”,
Per Egil Steen, 1998:89, ISBN 82-471-0290-0, ISSN 0802-3271.

“Stress-resultant material models for reinforced concrete plates and shells”,
Jan Arve Øverli, 1998:95, ISBN 82-471-0297-8, ISSN 0802-3271.

“Chloride binding in concrete. Effect of surrounding environment and concrete composition”,
Claus Kenneth Larsen, 1998:101, ISBN 82-471-0337-0, ISSN 0802-3271.

“Rotational capacity of aluminium alloy beams”,
Lars A. Moen, 1999:1, ISBN 82-471-0365-6, ISSN 0802-3271.

“Stretch Bending of Aluminium Extrusions”,
Arild H. Clausen, 1999:29, ISBN 82-471-0396-6, ISSN 0802-3271.

“Aluminium and Steel Beams under Concentrated Loading”,
Tore Tryland, 1999:30, ISBN 82-471-0397-4, ISSN 0802-3271.

“Engineering Models of Elastoplasticity and Fracture for Aluminium Alloys”,
Odd-Geir Lademo, 1999:39, ISBN 82-471-0406-7, ISSN 0802-3271.

“Kapasitet og duktilitet av dybelforbindelser i trekonstruksjoner”,
Jan Siem, 1999:46, ISBN 82-471-0414-8, ISSN 0802-3271.

“Etablering av distribuert ingeniørarbeid; Teknologiske og organisatoriske erfaringer fra en norsk ingeniørbedrift”,
Lars Line, 1999:52, ISBN 82-471-0420-2, ISSN 0802-3271.

“Estimation of Earthquake-Induced Response”,
Símon Ólafsson, 1999:73, ISBN 82-471-0443-1, ISSN 0802-3271.

“Coastal Concrete Bridges: Moisture State, Chloride Permeability and Aging Effects”,
Ragnhild Holen Relling, 1999:74, ISBN 82-471-0445-8, ISSN 0802-3271.

“Capacity Assessment of Titanium Pipes Subjected to Bending and External Pressure”,
Arve Bjørset, 1999:100, ISBN 82-471-0473-3, ISSN 0802-3271.

“Validation of Numerical Collapse Behaviour of Thin-Walled Corrugated Panels”,
Håvar Ilstad, 1999:101, ISBN 82-471-0474-1, ISSN 0802-3271.

“Strength and Ductility of Welded Structures in Aluminium Alloys”,
Miroslaw Matusiak, 1999:113, ISBN 82-471-0487-3, ISSN 0802-3271.

“Thermal Dilation and Autogenous Deformation as Driving Forces to Self-Induced Stresses in High Performance Concrete”,
Øyvind Bjøntegaard, 1999:121, ISBN 82-7984-002-8, ISSN 0802-3271.

“Some Aspects of Ski Base Sliding Friction and Ski Base Structure”,
Dag Anders Moldestad, 1999:137, ISBN 82-7984-019-2, ISSN 0802-3271.

“Electrode reactions and corrosion resistance for steel in mortar and concrete”,
Roy Antonsen, 2000:10, ISBN 82-7984-030-3, ISSN 0802-3271.

"Hydro-Physical Conditions in Kelp Forests and the Effect on Wave Damping and Dune Erosion. A case study on Laminaria Hyperborea",
Stig Magnar Løvås, 2000:28, ISBN 82-7984-050-8, ISSN 0802-3271.

"Random Vibration and the Path Integral Method",
Christian Skaug, 2000:39, ISBN 82-7984-061-3, ISSN 0802-3271.

"Buckling and geometrical nonlinear beam-type analyses of timber structures",
Trond Even Eggen, 2000:56, ISBN 82-7984-081-8, ISSN 0802-3271.

"Structural Crashworthiness of Aluminium Foam-Based Components",
Arve Grønsund Hanssen, 2000:76, ISBN 82-7984-102-4, ISSN 0809-103X.

"Kinematics in Regular and Irregular Waves based on a Lagrangian Formulation",
Svein Helge Gjøsund, 2000:86, ISBN 82-7984-112-1, ISSN 0809-103X.

"Measurements and simulations of the consolidation in first-year sea ice ridges, and some aspects of mechanical behaviour",
Knut V. Høyland, 2000:94, ISBN 82-7984-121-0, ISSN 0809-103X.

"Self-Induced Cracking Problems in Hardening Concrete Structures",
Daniela Bosnjak, 2000:121, ISBN 82-7984-151-2, ISSN 0809-103X.

"Ballistic Penetration and Perforation of Steel Plates",
Tore Børvik, 2000:124, ISBN 82-7984-154-7, ISSN 0809-103X.

"Freeze-Thaw resistance of Concrete. Effect of: Curing Conditions, Moisture Exchange and Materials",
Terje Finnerup Rønning, 2001:14, ISBN 82-7984-165-2, ISSN 0809-103X.

"Structural behaviour of post tensioned concrete structures. Flat slab. Slabs on ground",
Steinar Trygstad, 2001:52, ISBN 82-471-5314-9, ISSN 0809-103X.

"Slipforming of Vertical Concrete Structures. Friction between concrete and slipform panel",
Kjell Tore Fosså, 2001:61, ISBN 82-471-5325-4, ISSN 0809-103X.

"Some numerical methods for the simulation of laminar and turbulent incompressible flows",
Jens Holmen, 2002:6, ISBN 82-471-5396-3, ISSN 0809-103X.

"Improved Fatigue Performance of Threaded Drillstring Connections by Cold Rolling",
Steinar Kristoffersen, 2002:11, ISBN 82-421-5402-1, ISSN 0809-103X.

"Deformations in Concrete Cantilever Bridges: Observations and Theoretical Modelling",
Peter F. Takâcs, 2002:23, ISBN 82-471-5415-3, ISSN 0809-103X.

"Stiffened aluminium plates subjected to impact loading",
Hilde Giæver Hildrum, 2002:69, ISBN 82-471-5467-6, ISSN 0809-103X.

"Full- and model scale study of wind effects on a medium-rise building in a built up area",
Jónas Thór Snæbjørnsson, 2002:95, ISBN 82-471-5495-1, ISSN 0809-103X.

"Evaluation of Concepts for Loading of Hydrocarbons in Ice-infested water",
Arnor Jensen, 2002:114, ISBN 82-417-5506-0, ISSN 0809-103X.

"Numerical and Physical Modelling of Oil Spreading in Broken Ice",
Janne K. Økland Gjøsteen, 2002:130, ISBN 82-471-5523-0, ISSN 0809-103X.

"Diagnosis and protection of corroding steel in concrete",
Franz Pruckner, 2002:140, ISBN 82-471-5555-4, ISSN 0809-103X.

"Oblique Loading of Aluminium Crash Components",
Aase Reyes, 2003:15, ISBN 82-471-5562-1, ISSN 0809-103X.

"Tensile and Compressive Creep of Young Concrete: Testing and Modelling",
Dawood Atrushi, 2003:17, ISBN 82-471-5565-6, ISSN 0809-103X.

"Rheology of Particle Suspensions. Fresh Concrete, Mortar and Cement Paste with Various Types of Lignosulfonates",
Jon Elvar Wallevik, 2003:18, ISBN 82-471-5566-4, ISSN 0809-103X.

"Utilization of Ethiopian Natural Pozzolans",
Surafel Ketema Desta, 2003:26, ISBN 82-471-5574-5, ISSN 0809-103X.

"Behaviour and strength prediction of reinforced concrete structures with discontinuity regions",
Helge Brå, 2004:11, ISBN 82-471-6222-9, ISSN 1503-8181.

"High-strength steel plates subjected to projectile impact. An experimental and numerical study",
Sumita Dey, 2004:38, ISBN 82-471-6282-2 (printed ver.), ISBN 82-471-6281-4 (electronic ver.), ISSN 1503-8181.

"Alkali-reactive and inert fillers in concrete. Rheology of fresh mixtures and expansive reactions",
Bård M. Pedersen, 2004:92, ISBN 82-471-6401-9 (printed ver.), ISBN 82-471-6400-0 (electronic ver.), ISSN 1503-8181.

"Thermal Aspects of corrosion of Steel in Concrete",
Jan-Magnus Østvik, 2005:5, ISBN 82-471-6869-3 (printed ver.), ISBN 82-471-6868 (electronic ver.), ISSN 1503-8181.

"Behaviour of aluminium extrusions subjected to axial loading",
Østen Jensen, 2005:7, ISBN 82-471-6873-1 (printed ver.), ISBN 82-471-6872-3 (electronic ver.), ISSN 1503-8181.

"On the Shear Capacity of Steel Girders with Large Web Openings",
Nils Christian Hagen, 2005:9, ISBN 82-471-6878-2 (printed ver.), ISBN 82-471-6877-4 (electronic ver.), ISSN 1503-8181.

“Mechanical and adaptive behaviour of bone in relation to hip replacement. A study of bone remodelling and bone grafting”,
Sébastien Muller, 2005:34, ISBN 82-471-6933-9 (printed ver.), ISBN 82-471-6932-0 (electronic ver.), ISSN 1503-8181.

“Analysis of geometrical nonlinearities with applications to timber structures”,
Lars Wollebæk, 2005:74, ISBN 82-471-7050-5 (printed ver.), ISBN 82-471-7019-1 (electronic ver.), ISSN 1503-8181.

“Pedestrian induced lateral vibrations of slender footbridges”,
Anders Rönnquist, 2005:102, ISBN 82-471-7082-5 (printed ver.), ISBN 82-471-7081-7 (electronic ver.), ISSN 1503-8181.

“Initial Strength Development of Fly Ash and Limestone Blended Cements at Various Temperatures Predicted by Ultrasonic Pulse Velocity”,
Tom Ivar Fredvik, 2005:112, ISBN 82-471-7105-8 (printed ver.), ISBN 82-471-7103-1 (electronic ver.), ISSN 1503-8181.

“Behaviour and modelling of thin-walled cast components”,
Cato Dørum, 2005:128, ISBN 82-471-7140-6 (printed ver.), ISBN 82-471-7139-2 (electronic ver.), ISSN 1503-8181.

“Behaviour and Modelling of Aluminium Plates subjected to Compressive Load”,
Lars Rønning, 2005:154, ISBN 82-471-7169-1 (printed ver.), ISBN 82-471-7195-3 (electronic ver.), ISSN 1503-8181.

“Behaviour and modelling of selfpiercing riveted connections”,
Raffaele Porcaro, 2005:165, ISBN 82-471-7219-4 (printed ver.), ISBN 82-471-7218-6 (electronic ver.), ISSN 1503-8181.

“Bumper beam-longitudinal system subjected to offset impact loading”,
Satyanarayana Kokkula, 2005:193, ISBN 82-471-7280-1 (printed ver.), ISBN 82-471-7279-8 (electronic ver.), ISSN 1503-8181.

“Fatigue life prediction of an aluminium alloy automotive component using finite element analysis of surface topography”,
Sigmund Kyrre Ås, 2006:25, ISBN 82-471-7791-9 (printed ver.), ISBN 82-471-7791-9 (electronic ver.), ISSN 1503-8181.

“Control of Chloride Penetration into Concrete Structures at Early Age”,
Guofei Liu, 2006:46, ISBN 82-471-7838-9 (printed ver.), ISBN 82-471-7837-0 (electronic ver.), ISSN 1503-8181.

“Constitutive models of elastoplasticity and fracture for aluminium alloys under strain path change”,
Dasharatha Achani, 2006:76, ISBN 82-471-7903-2 (printed ver.), ISBN 82-471-7902-4 (electronic ver.), ISSN 1503-8181.

“Modelling of Welded Thin-Walled Aluminium Structures”,
Ting Wang, 2006:78, ISBN 82-471-7907-5 (printed ver.), ISBN 82-471-7906-7 (electronic ver.), ISSN 1503-8181.

“Simulations of 2D dynamic brittle fracture by the Element-free Galerkin method and linear fracture mechanics”,
Tommy Karlsson, 2006:125, ISBN 82-471-8011-1 (printed ver.), ISBN 82-471-8010-3 (electronic ver.), ISSN 1503-8181.

“Time-variant reliability of dynamic systems by importance sampling and probabilistic analysis of ice loads”,
Anna Ivanova Olsen, 2006:139, ISBN 82-471-8041-3 (printed ver.), ISBN 82-471-8040-5 (electronic ver.), ISSN 1503-8181.

“Penetration and Perforation of Granite Targets by Hard Projectiles”,
Chong Chiang Seah, 2006:188, ISBN 82-471-8150-9 (printed ver.), ISBN 82-471-8149-5 (electronic ver.), ISSN 1503-8181.

“Crashworthiness of dual-phase high-strength steel: Material and Component behaviour”,
Venkatapathi Tarigopula, 2007:230, ISBN 82-471-5076-4 (printed ver.), ISBN 82-471-5093-1 (electronic ver.), ISSN 1503-8181.

“Deformations, strain capacity and cracking of concrete in plastic and early hardening phases”,
Tor Arne Hammer, 2007:234, ISBN 978-82-471-5191-4 (printed ver.), ISBN 978-82-471-5207-2 (electronic ver.), ISSN 1503-8181.

“Robustness studies of structures subjected to large deformations”,
Ørjan Fyllingen, 2008:24, ISBN 978-82-471-6339-9 (printed ver.), ISBN 978-82-471-6342-9 (electronic ver.), ISSN 1503-8181.

“Low-velocity penetration of aluminium plates”,
Frode Grytten, 2008:46, ISBN 978-82-471-6826-4 (printed ver.), ISBN 978-82-471-6843-1 (electronic ver.), ISSN 1503-8181.

“Fibre reinforcement in load carrying concrete structures”,
Åse Lyslo Døssland, 2008:50, ISBN 978-82-471-6910-0 (printed ver.), ISBN 978-82-471-6924-7 (electronic ver.), ISSN 1503-8181.

“Constitutive modelling of morsellised bone”,
Knut Birger Lunde, 2008:92, ISBN 978-82-471-7829-4 (printed ver.), ISBN 978-82-471-7832-4 (electronic ver.), ISSN 1503-8181.

“Experimental Investigations of Wind Loading on a Suspension Bridge Girder”,
Bjørn Isaksen, 2008:131, ISBN 978-82-471-8656-5 (printed ver.), ISBN 978-82-471-8673-2 (electronic ver.), ISSN 1503-8181.

“Cracking Risk of Concrete Structures in The Hardening Phase”,
Guomin Ji, 2008:198, ISBN 978-82-471-1079-9 (printed ver.), ISBN 978-82-471-1080-5 (electronic ver.), ISSN 1503-8181.

“Modelling and numerical analysis of the porcine and human mitral apparatus”,
Victorien Emile Prot, 2008:249, ISBN 978-82-471-1192-5 (printed ver.), ISBN 978-82-471-1193-2 (electronic ver.), ISSN 1503-8181.

“Strength analysis of net structures”,
Heidi Moe, 2009:48, ISBN 978-82-471-1468-1 (printed ver.), ISBN 978-82-471-1469-8 (electronic ver.), ISSN 1503-8181.

“Modelling of Dynamic Material Behaviour and Fracture of Aluminium Alloys for Structural Applications”,
Yan Chen, 2009:69, ISBN 978-82-471-1515-2 (printed ver.), ISBN 978-82 471-1516-9 (electronic ver.), ISSN 1503-8181.

“Numerical analysis of ductile fracture in surface cracked shells”,
Espen Berg, 2009:80, ISBN 978-82-471-1537-4 (printed ver.), ISBN 978-82-471-1538-1 (electronic ver.), ISSN 1503-8181.

“Subject specific finite element analysis of bone – for evaluation of the healing of a leg lengthening and evaluation of femoral stem design”,
Sune Hansborg Pettersen, 2009:99, ISBN 978-82-471-1579-4 (printed ver.), ISBN 978-82-471-1580-0 (electronic ver.), ISSN 1503-8181.

“Evaluation of fracture parameters for notched multi-layered structures”,
Lingyun Shang, 2009:137, ISBN 978-82-471-1662-3 (printed ver.), ISBN 978-82-471-1663-0 (electronic ver.), ISSN 1503-8181.

“Nanomechanics of polymer and composite particles”,
Jianying He, 2009:213, ISBN 978-82-471-1828-3 (printed ver.), ISBN 978-82-471-1829-0 (electronic ver.), ISSN 1503-8181.

“Mechanical properties of clear wood from Norway spruce”,
Kristian Berbom Dahl, 2009:250, ISBN 978-82-471-1911-2 (printed ver.), ISBN 978-82-471-1912-9 (electronic ver.), ISSN 1503-8181.

“Modeling of the degradation of TiB_2 mechanical properties by residual stresses and liquid Al penetration along grain boundaries”,
Micol Pezzotta, 2009:254, ISBN 978-82-471-1923-5 (printed ver.), ISBN 978-82-471-1924-2 (electronic ver.), ISSN 1503-8181.

“Effect of welding residual stress on fracture”,
Xiabo Ren, 2010:77, ISBN 978-82-471-2115-3 (printed ver.), ISBN 978-82-471-2116-0 (electronic ver.), ISSN 1503-8181.

“Pan-based carbon fiber as anode material in cathodic protection system for concrete structures”,
Mahdi Chini, 2010:122, ISBN 978-82-471-2210-5 (printed ver.), ISBN 978-82-471-2213-6 (electronic ver.), ISSN 1503-8181.

"Structural Behaviour of deteriorated and retrofitted concrete structures",
Irina Vasililjeva Sæther, 2010:171, ISBN 978-82-471-2315-7 (printed ver.), ISBN 978-82-471-2316-4 (electronic ver.), ISSN 1503-8181.

"Prediction of local snow loads on roofs",
Vivian Meløysund, 2010:247, ISBN 978-82-471-2490-1 (printed ver.), ISBN 978-82-471-2491-8 (electronic ver.), ISSN 1503-8181.

"Behaviour and modelling of polymers for crash applications",
Virgile Delhaye, 2010:251, ISBN 978-82-471-2501-4 (printed ver.), ISBN 978-82-471-2502-1 (electronic ver.), ISSN 1503-8181.

"Blended cement with reducted CO_2 emission – Utilizing the Fly Ash-Limestone Synergy",
Klaartje De Weerdt, 2011:32, ISBN 978-82-471-2584-7 (printed ver.), ISBN 978-82-471-2584-4 (electronic ver.), ISSN 1503-8181.

"Chloride induced reinforcement corrosion in concrete. Concept of critical chloride content – methods and mechanisms",
Ueli Angst, 2011:113, ISBN 978-82-471-2769-9 (printed ver.), ISBN 978-82-471-2763-6 (electronic ver.), ISSN 1503-8181.

"A thermo-electric-Mechanical study of the carbon anode and contact interface for Energy savings in the production of aluminium",
Dag Herman Andersen, 2011:157, ISBN 978-82-471-2859-6 (printed ver.), ISBN 978-82-471-2860-2 (electronic ver.), ISSN 1503-8181.

"Structural Capacity of Anchorage Ties in Masonry Veneer Walls Subjected to Earthquake. The implications of Eurocode 8 and Eurocode 6 on a typical Norwegian veneer wall",
Ahmed Mohamed Yousry Hamed, 2011:181, ISBN 978-82-471-2911-1 (printed ver.), ISBN 978-82-471-2912-8 (electronic ver.), ISSN 1503-8181.

"Work-hardening behaviour in age-hardenable Al-Zn-Mg(-Cu) alloys",
Ida Westermann, 2011:247, ISBN 978-82-471-3056-8 (printed ver.), ISBN 978-82-471-3057-5 (electronic ver.), ISSN 1503-8181.

"Behaviour and modelling of selfpiercing riveted connections using aluminium rivets",
Nguyen-Hieu Hoang, 2011:266, ISBN 978-82-471-3097-1 (printed ver.), ISBN 978-82-471-3099-5 (electronic ver.), ISSN 1503-8181.

"Fibre reinforced concrete: Evaluation of test methods and material development",
Sindre Sandbakk, 2011:297, ISBN 978-82-471-3167-1 (printed ver.), ISBN 978-82-471-3168-8 (electronic ver.), ISSN 1503-8181.

"Constitutive modeling of solargrade silicon materials",
Julien Cochard, 2011:307, ISBN 978-82-471-3189-3 (printed ver.), ISBN 978-82-471-3190-9 (electronic ver.), ISSN 1503-8181.

"Dynamic behaviour of cable-supported bridges subjected to strong natural wind",
Ole Andre Øiseth, 2011:315, ISBN 978-82-471-3209-8 (printed ver.), ISBN 978-82-471-3210-4 (electronic ver.), ISSN 1503-8181.

“Constitutive behavior and fracture of shape memory alloys”,
Jim Stian Olsen, 2012:57, ISBN 978-82-471-3382-8 (printed ver.), ISBN 978-82-471-3383-5 (electronic ver.), ISSN 1503-8181.

“Field measurements in mechanical testing using close-range photogrammetry and digital image analysis”,
Egil Fagerholt, 2012:95, ISBN 978-82-471-3466-5 (printed ver.), ISBN 978-82-471-3467-2 (electronic ver.), ISSN 1503-8181.

“Towards a better understanding of the ultimate behaviour of lightweight aggregate concrete in compression and bending”,
Håvard Nedrelid, 2012:123, ISBN 978-82-471-3527-3 (printed ver.), ISBN 978-82-471-3528-0 (electronic ver.), ISSN 1503-8181.

“Numerical simulations of blood flow in the left side of the heart”,
Sigrid Kaarstad Dahl, 2012:135, ISBN 978-82-471-3553-2 (printed ver.), ISBN 978-82-471-3555-6 (electronic ver.), ISSN 1503-8181.

“Moisture induced stresses in glulam”,
Vanessa Angst-Nicollier, 2012:139, ISBN 978-82-471-3562-4 (printed ver.), ISBN 978-82-471-3563-1 (electronic ver.), ISSN 1503-8181.

“Biomechanical aspects of distraction osteogensis”,
Valentina La Russa, 2012:250, ISBN 978-82-471-3807-6 (printed ver.), ISBN 978-82-471-3808-3 (electronic ver.), ISSN 1503-8181.

“Ductile fracture in dual-phase steel. Theoretical, experimental and numerical study”,
Gaute Gruben, 2012:257, ISBN 978-82-471-3822-9 (printed ver.), ISBN 978-82-471-3823-6 (electronic ver.), ISSN 1503-8181.

“Damping in Timber Structures”,
Nathalie Labonnote, 2012:263, ISBN 978-82-471-3836-6 (printed ver.), ISBN 978-82-471-3837-3 (electronic ver.), ISSN 1503-8181.

“Large-Deformation behaviour of thermoplastics at various stress states”,
Anne Serine Ognedal, 2012:298, ISBN 978-82-471-3913-4 (printed ver.), ISBN 978-82-471-3914-1 (electronic ver.), ISSN 1503-8181.

“Biomechanical modeling of fetal veins: The umbilical vein and ductus venosus bifurcation”,
Paul Roger Leinan, 2012:299, ISBN 978-82-471-3915-8 (printed ver.), ISBN 978-82-471-3916-5 (electronic ver.), ISSN 1503-8181.

“Hardening accelerator for fly ash blended cement”,
Kien Dinh Hoang, 2012:366, ISBN 978-82-471-4063-5 (printed ver.), ISBN 978-82-471-4064-2 (electronic ver.), ISSN 1503-8181.

“From molecular structure to mechanical properties”,
Jianyang Wu, 2013:186, ISBN 978-82-471-4485-5 (printed ver.), ISBN 978-82-471-4486-2 (electronic ver.), ISSN 1503-8181.

“Mechanics of ultra-thin multi crystalline silicon wafers”,
Saber Saffar, 2013:199, ISBN 978-82-471-4511-1 (printed ver.), ISBN 978-82-471-4513-5 (electronic ver.), ISSN 1503-8181.

“Experimental and numerical study of hybrid concrete structures”,
Linn Grepstad Nes, 2013:259, ISBN 978-82-471-4644-6 (printed ver.), ISBN 978-82-471-4645-3 (electronic ver.), ISSN 1503-8181.

“Through process modelling of welded aluminium structures”,
Anizahyati Alisibramulisi, 2013:325, ISBN 978-82-471-4788-7 (printed ver.), ISBN 978-82-471-4789-4 (electronic ver.), ISSN 1503-8181.

“Combined blast and fragment loading on steel plates”,
Knut Gaarder Rakvåg, 2013:361, ISBN 978-82-471-4872-3 (printed ver.), ISBN 978-82-4873-0 (electronic ver.), ISSN 1503-8181.

“Characterization and modelling of the anisotropic behaviour of high-strength aluminium alloy”,
Marion Fourmeau, 2014:37, ISBN 978-82-326-0008-3 (printed ver.), ISBN 978-82-326-0009-0 (electronic ver.), ISSN 1503-8181.

“Behaviour of threated steel fasteners at elevated deformation rates”,
Henning Fransplass, 2014:65, ISBN 978-82-326-0054-0 (printed ver.), ISBN 978-82-326-0055-7 (electronic ver.), ISSN 1503-8181.

“Sedimentation and Bleeding”,
Ya Peng, 2014:89, ISBN 978-82-326-0102-8 (printed ver.), ISBN 978-82-326-0103-5 (electronic ver.), ISSN 1503-8181.

“Impact against X65 offshore pipelines”,
Martin Kristoffersen, 2014:362, ISBN 978-82-326-0636-8 (printed ver.), ISBN 978-82-326-0637-5 (electronic ver.), ISSN 1503-8181.

“Formability of aluminium alloy subjected to prestrain by rolling”,
Dmitry Vysochinskiy, 2014:363, ISBN 978-82-326-0638-2 (printed ver.), ISBN 978-82-326-0639-9 (electronic ver.), ISSN 1503-8181.

“Experimental and numerical study of Yielding, Work-Hardening and anisotropy in textured AA6xxx alloys using crystal plasticity models”,
Mikhail Khadyko, 2015:28, ISBN 978-82-326-0724-2 (printed ver.), ISBN 978-82-326-0725-9 (electronic ver.), ISSN 1503-8181.

“Behaviour and Modelling of AA6xxx Aluminium Alloys Under a Wide Range of Temperatures and Strain Rates”,
Vincent Vilamosa, 2015:63, ISBN 978-82-326-0786-0 (printed ver.), ISBN 978-82-326-0787-7 (electronic ver.), ISSN 1503-8181.

“A Probabilistic Approach in Failure Modelling of Aluminium High Pressure Die-Castings”,
Octavian Knoll, 2015:137, ISBN 978-82-326-0930-7 (printed ver.), ISBN 978-82-326-0931-4 (electronic ver.), ISSN 1503-8181.

“Ice Abrasion on Marine Concrete Structures”,
Egil Møen, 2015:189, ISBN 978-82-326-1034-1 (printed ver.), ISBN 978-82-326-1035-8 (electronic ver.), ISSN 1503-8181.

“Fibre Orientation in Steel-Fibre-Reinforced Concrete”,
Giedrius Zirgulis, 2015:229, ISBN 978-82-326-1114-0 (printed ver.), ISBN 978-82-326-1115-7 (electronic ver.), ISSN 1503-8181.

“Effect of spatial variation and possible interference of localised corrosion on the residual capacity of a reinforced concrete beam”,
Mohammad Mahdi Kioumarsi, 2015:282, ISBN 978-82-326-1220-8 (printed ver.), ISBN 978-82-1221-5 (electronic ver.), ISSN 1503-8181.

“The role of concrete resistivity in chloride-induced macro-cell corrosion”,
Karla Horbostel, 2015:324, ISBN 978-82-326-1304-5 (printed ver.), ISBN 978-82-326-1305-2 (electronic ver.), ISSN 1503-8181.

“Flowable fibre-reinforced concrete for structural applications”,
Elena Vidal Sarmiento, 2015:335, ISBN 978-82-326-1324-3 (printed ver.), ISBN 978-82-326-1325-0 (electronic ver.), ISSN 1503-8181.

“Development of crushed sand for concrete production with microproportioning”, Rolands Cepuritis, 2016:19, ISBN 978-82-326-1382-3 (printed ver.), ISBN 978-82-326-1383-0 (electronic ver.), ISSN 1503-8181.

“Withdrawal properties of threaded rods embedded in glued-laminated timer elements”,
Haris Stamatopoulos, 2016:48, ISBN 978-82-326-1436-3 (printed ver.), ISBN 978-82-326-1437-0 (electronic ver.), ISSN 1503-8181.

“An Experimental and numerical study of thermoplastics at large deformation”,
Marius Andersen, 2016:191, ISBN 978-82-326-1720-3 (printed ver.), ISBN 978-82-326-1721-0 (electronic ver.), ISSN 1503-8181.

“Uncertainty quantification and sensitivity analysis for cardiovascular models”,
Vinzenz Gregor Eck, 2016:234, ISBN 978-82-326-1806-4 (printed ver.), ISBN 978-82-326-1807-1 (electronic ver.), ISSN 1503-8181.

“Modeling and Simulation of Ballistic Impact”,
Jens Kristian Holmen, 2016:240, ISBN 978-82-326-1818-7 (printed ver.), ISBN 978-82-326-1819-4 (electronic ver.), ISSN 1503-8181.

“Early age crack assessment of concrete structures”,
Anja B. Estensen Klausen, 2016:256, ISBN 978-82-326-1850-7 (printed ver.), ISBN 978-82-326-1851-4 (electronic ver.), ISSN 1503-8181.

“Mechanical behaviour of particle-filled elastomers at various temperatures”,
Arne Ilseng, 2016:295, ISBN 978-82-326-1928-3 (printed ver.), ISBN 978-82-326-1929-0 (electronic ver.), ISSN 1503-8181.

“Dynamic behaviour of existing and new railway catenary systems under Norwegian conditions”,
Petter Røe Nåvik, 2016:298, ISBN 978-82-326-1935-1 (printed ver.), ISBN 978-82-326-1934-4 (electronic ver.), ISSN 1503-8181.

“Nanotechnology for Anti-Icing Application”,
Zhiwei He, 2016:348, ISBN 978-82-326-2038-8 (printed ver.), ISBN 978-82-326-2019-5 (electronic ver.), ISSN 1503-8181.

“Conduction Mechanisms in Conductive Adhesives with Metal-Coated Polyer Spheres”,
Sigurd Rolland Pettersen, 2016:349, ISBN 978-326-2040-1 (printed ver.), ISBN 978-82-326-2041-8 (electronic ver.), ISSN 1503-8181.

“The interaction between calcium lignosulfonate and cement”,
Alessia Colombo, 2017:20, ISBN 978-82-326-2122-4 (printed ver.), ISBN 978-82-326-2123-1 (electronic ver.), ISSN 1503-8181.

“Behaviour and Modelling of Flexible Structures Subjected to Blast Loading”,
Vegard Aune, 2017:101, ISBN 978-82-326-2274-0 (printed ver.), ISBN 978-82-326-2275-7 (electronic ver.), ISSN 1503-8181.

“Optoelectrical Properties of a Novel Organic Semiconductor: 6,13-Dichloropentacene”,
Mao Wang, 2017:130, ISBN 978-82-326-2332-7 (printed ver.), ISBN 978-82-326-2333-4 (electronic ver.), ISSN 1503-8181.

“Aspects of design of reinforced concrete structures using nonlinear finite element analyses”,
Morten Engen, 2017:149, ISBN 978-82-326-2370-9 (printed ver.), ISBN 978-82-326-2371-6 (electronic ver.), ISSN 1503-8181.

“Behaviour of steel connections under quasi-static and impact loading”,
Erik Løhre Grimsmo, 2017:159, ISBN 978-82-326-2390-7 (printed ver.), ISBN 978-82-326-2391-4 (electronic ver.), ISSN 1503-8181.

“Core-shell structured microgels and their behavior at oil and water interface”,
Yi Gong, 2017:182, ISBN 978-82-326-2436-2 (printed ver.), ISBN 978-82-326-2437-9 (electronic ver.), ISSN 1503-8181.

“An experimental and numerical study of cortical bone at the macro and Nano-scale”,
Masoud Ramenzanzadehkoldeh, 2017:208, ISBN 978-82-326-2488-1 (printed ver.), ISBN 978-82-326-2489-8 (electronic ver.), ISSN 1503-8181.

“Modelling and Assessment of Hydrogen Embrittlement in Steels and Nickel Alloys”,
Haiyang Yu, 2017:278, ISBN 978-82-326-2624-3 (printed ver.), ISBN 978-82-326-2625-0 (electronic ver.), ISSN 1503-8181.

“Numerical studies on ductile failure of aluminium alloys”,
Lars Edvard Dæhli, 2017:284, ISBN 978-82-326-2636-6 (printed ver.), ISBN 978-82-326-2637-3 (electronic ver.), ISSN 1503-8181.

“Thermomechanical behaviour of semi-crystalline polymers: experiments, modelling and simulation”,
Joakim Johnsen, 2017:317, ISBN 978-82-326-2702-8 (printed ver.), ISBN 978-82-326-2703-5 (electronic ver.), ISSN 1503-8181.

“Network arch timber bridges with light timber deck on transverse crossbeams”,
Anna Weronika Ostrycharczyk, 2017:318, ISBN 978-82-326-2704-2 (printed ver.), ISBN 978-82-326-2705-9 (electronic ver.), ISSN 1503-8181.

“Splicing of Large Glued Laminated Timber Elements by Use of Long Threated Rods”,
Martin Cepelka, 2017:320, ISBN 978-82-326-2708-0 (printed ver.), ISBN 978-82-326-2709-7 (electronic ver.), ISSN 1503-8181.

“Risk and Reliability Based Calibration of Structural Design Codes”,
Michele Baravalle, 2017:342, ISBN 978-82-326-2752-3 (printed ver.), ISBN 978-82-326-2753-0 (electronic ver.), ISSN 1503-8181.

“Small-Scale Plasticity under Hydrogen Environment”,
Kai Zhao, 2017:356, ISBN 978-82-326-2782-0 (printed ver.), ISBN 978-82-326-2783-7 (electronic ver.), ISSN 1503-8181.

“Dynamic behaviour of floating bridges exposed to wave excitation”,
Knut Andreas Kvåle, 2017:365, ISBN 978-82-326-2800-1 (printed ver.), ISBN 978-82-326-2801-8 (electronic ver.), ISSN 1503-8181.

“Dolomite calcined clay composite cement – hydration and durability”,
Alisa Lydia Machner, 2018:39, ISBN 978-82-326-2872-8 (printed ver.), ISBN 978-82-326-2873-5 (electronic ver.), ISSN 1503-8181.

“Modelling of the self-excited forces for bridge decks subjected to random motions: an experimental study”,
Bartosz Siedziako, 2018:52, ISBN 978-82-326-2896-4 (printed ver.), ISBN 978-82-326-2897-1 (electronic ver.), ISSN 1503-8181.

“A probabilistic-based methodology for evaluation of timber facade constructions”,
Klodian Gradeci, 2018:69, ISBN 978-82-326-2928-2 (printed ver.), ISBN 978-82-326-2929-9 (electronic ver.), ISSN 1503-8181.

“Behaviour and modelling of flow-drill screw connections”,
Johan Kolstø Sønstabø, 2018:73, ISBN 978-82-326-2936-7 (printed ver.), ISBN 978-82-326-2937-4 (electronic ver.), ISSN 1503-8181.

“Full-scale investigation of the effects of wind turbulence characteristics on dynamic behavior of long-span cable-supported bridges in complex terrain”,
Aksel Fenerci, 2018:100, ISBN 9978-82-326-2990-9 (printed ver.), ISBN 978-82-326-2991-6 (electronic ver.), ISSN 1503-8181.

“Modeling and simulation of the soft palate for improved understanding of the obstructive sleep apnea syndrome”,
Hongliang Liu, 2018:101, ISBN 978-82-326-2992-3 (printed ver.), ISBN 978-82-326-2993-0 (electronic ver.), ISSN 1503-8181.

“Long-term extreme response analysis of cable-supported bridges with floating pylons subjected to wind and wave loads”,
Yuwang Xu, 2018:229, ISBN 978-82-326-3248-0 (printed ver.), ISBN 978-82-326-3249-7 (electronic ver.), ISSN 1503-8181.

“Reinforcement corrosion in carbonated fly ash concrete”,
Andres Belda Revert, 2018:230, ISBN 978-82-326-3250-3 (printed ver.), ISBN 978-82-326-3251-0 (electronic ver.), ISSN 1503-8181.

“Direct finite element method for nonlinear earthquake analysis of concrete dams including dam-water-foundation rock interaction”,
Arnkjell Løkke, 2018:252, ISBN 978-82-326-3294-7 (printed ver.), ISBN 978-82-326-3295-4 (electronic ver.), ISSN 1503-8181.

“Determining the tensile properties of Artic materials and modelling their effects on fracture”,
Shengwen Tu, 2018:269, ISBN 978-82-326-3328-9 (printed ver.), ISBN 978-82-326-3329-6 (electronic ver.), ISSN 1503-8181.

“Electromechanical characterization of metal-coated polymer spheres for conductive adhesives”,
Molly Strimbeck Bazilchuk, 2018:295, ISBN 978-82-326-3380-7 (printed ver.), ISBN 978-82-326-3381-4 (electronic ver.), ISSN 1503-8181.

“Atomistic Insight into Transportation of Nanofluid in Ultra-confined Channel”,
Xiao Wang, 2018:334, ISBN 978-82-326-3456-9 (printed ver.), ISBN 978-82-326-3457-6 (electronic ver.), ISSN 1503-8181.

“Load model of historic traffic for fatigue life estimation of Norwegian railway bridges”,
Gunnstein T. Frøseth, 2019:73, ISBN 978-82-326-3748-5 (printed ver.), ISBN 978-82-326-3749-2 (electronic ver.), ISSN 1503-8181.

“An experimental and numerical study of the mechanical behaviour of short glass-fibre reinforced thermoplastics”,
Jens Petter Henrik Holmstrøm, 2019:79, ISBN 978-82-326-3760-7 (printed ver.), ISBN 978-82-326-3761-4 (electronic ver.), ISSN 1503-8181.

“Force identification and response estimation in floating and suspension bridges using measured dynamic response”,
Øyvind Wiig Petersen, 2019:88, ISBN 978-82-326-3778-2 (printed ver.), ISBN 978-82-326-377-9 (electronic ver.), ISSN 1503-8181.

“Uncertainty quantification and sensitivity analysis informed modeling of physical systems”,
Jacob Sturdy, 2019:115, ISBN 978-82-326-3828-4 (printed ver.), ISBN 978-82-326-3829-1 (electronic ver.), ISSN 1503-8181.

“Consistent crack width calculation methods for reinforced concrete elements subjected to 1D and 2D stress states”,
Reignard Tan, 2019:147, ISBN 978-82-326-3892-5 (printed ver.), ISBN 978-82-326-3893-2 (electronic ver.), ISSN 1503-8181.

“Wind forces on bridge decks using state-of-the art FSI methods”,
Tore Andreas Helgedagsrud, 2019:180, ISBN 978-82-326-3956-4 (printed ver.), ISBN 978-82-326-3957-1 (electronic ver.), ISSN 1503-8181.

“Nonlinear static and dynamic isogeometric analysis of slender spatial and beam type structures”,
Siv Bente Raknes, 2019:181, ISBN 978-82-326-3958-8 (printed ver.), ISBN 978-82-326-3959-5 (electronic ver.), ISSN 1503-8181.

“Experimental study of concrete-ice abrasion and concrete surface topography modification”,
Guzel Shamsutdinova, 2019:182, ISBN 978-82-326-3960-1 (printed ver.), ISBN 978-82-326-3961-8 (electronic ver.), ISSN 1503-8181.

“Numerical Study on Ductile-to-Brittle Transition of Steel and its Behavior under Residual Stresses”,
Yang Li, 2019:227, ISBN 978-82-326-4050-8 (printed ver.), ISBN 978-82-326-4015-5 (electronic ver.), ISSN 1503-8181.

“Micromechanical modelling of ductile fracture in aluminium alloys”,
Bjørn Håkon Frodal, 2019:253, ISBN 978-82-326-4102-4 (printed ver.), ISBN 978-82-326-4103-1 (electronic ver.), ISSN 1503-8181.

“Monolithic and laminated glass under extreme loading: Experiments, modelling and simulations”,
Karoline Osnes, 2019:304, ISBN 978-82-326-4204-5 (printed ver.), ISBN 978-82-326-4205-2 (electronic ver.), ISSN 1503-8181.

“Plastic flow and fracture of isotropic and anisotropic 6000-series aluminium alloys: Experiments and numerical simulations”,
Susanne Thomesen, 2019:312, ISBN 978-82-326-4220-5 (printed ver.), ISBN 978-82-326-4221-2 (electronic ver.), ISSN 1503-8181.

“Connections between steel and aluminium using adhesive bonding combined with self-piercing riveting: Testing, modelling and analysis”,
Matthias Reil, 2019:319, ISBN 978-82-326-4234-2 (printed ver.), ISBN 978-82-326-4235-9 (electronic ver.), ISSN 1503-8181.

“Designing Polymeric Icephobic Materials”,
Yizhi Zhuo, 2019:345, ISBN 978-82-326-4286-1 (printed ver.), ISBN 978-82-326-4287-8 (electronic ver.), ISSN 1503-8181.

“Stress-laminated timber decks in bridges”,
Francesco Mirko Massaro, 2019:346, ISBN 978-82-326-4288-5 (printed ver.), ISBN 978-82-326-4289-2 (electronic ver.), ISSN 1503-8181.

“Fundamental Mechanisms of Ice Adhesion”,
Sigrid Rønneberg, 2020:87, ISBN 978-82-326-4527-8 (printed ver.), ISBN 978-82-326-4524-5 (electronic ver.), ISSN 1503-8181.

“Impact on porous polymer coated pipelines”,
Ole Vestrum, 2020:105, ISBN 978-82-326-4562-6 (printed ver.), ISBN 978-82-4563-3 (electronic ver.), ISSN 1503-8181.

“Conceptual form-finding in structural engineering”,
Marcin Luczkowski, 2020:232, ISBN 978-82-326-4813-9, ISSN 1503-8181.

“Self-assembled superstructures of magnetic nanoparticles: advanced nanofabrication and enhanced mechanical properties”,
Verner Håkonsen, 2020:271, ISBN 978-82-326-4890-0 (printed ver.), ISBN 978-82- 326-4891-7 (electronic ver.), ISSN 1503-8181.

“Micromechanical modelling of fracture in ductile alloys with applications to high-strength steel”,
Sondre Bergo, 2020:313, ISBN 978-82-326-4974-7 (printed ver.), ISBN 978-82-326-4975-4 (electronic ver.), ISSN 1503-8181.

“Fracture in wood of Norway spruce - Experimental and numerical study”,
Katarzyna Ostapska, 2020:314, ISBN 978-82-326-4976-1 (printed ver.), ISBN 978- 82-326-4977-8 (electronic ver.), ISSN 1503-8181.

“Dynamic anti-icing surfaces (DAIS)”,
Feng Wang, 2020:330, ISBN 978-82-326-5006-4 (printed ver.), ISBN 978-82-326-5007-1 (electronic ver.), ISSN 1503-8181.

“Multiaxial Fatigue analysis of offshore mooring chains, considering the effects of residual stresses and corrosion pits”
Ershad P. Zarandi, 2020:337, ISBN 978-82-326-5020-0 (printed ver.), ISBN 978-82-326-5021-7 (electronic ver.), ISSN 1503-8181.

“Physics-based and data-driven reduced-order blood flow models: Applications to coronary artery disease diagnostics”,
Fredrik Eikeland Fossan, 2020:362, ISBN 978-82-326-5070-5 (printed ver.), ISBN 978-82-326-5071-2 (electronic ver.), ISSN 1503-8181.

“Production and documentation of frost durable high-volume fly ash concrete: air entrainment, cracking and scaling in performance testing”,
Andrei Shpak, 2020:366, ISBN 978-82-326-5078-1 (printed ver.), ISBN 978-82-326-5079-8 (electronic ver.), ISSN 1503-8181.

“Testing and modelling of multi-material joints”,
Jon Fredrick Berntsen, 2020:368, ISBN 978-82-326-5082-8 (printed ver.), ISBN 978-82-326-5083-5 (electronic ver.), ISSN 1503-8181.

“Multi-scale modelling and simulation of ductile failure in aluminium structures”, Henrik Granum, 2020:374, ISBN 978-82-326-5094-1 (printed ver.), ISBN 978-82-326-5095-8 (electronic ver.), ISSN 1503-8181.

“Heuristic models for wear prediction and dynamic-based condition monitoring techniques in pantograph-catenary interaction”,
Stefano Derosa, 2020:381, ISBN 978-82-326-5108-5 (printed ver.), ISBN 978-82-326-5109-2 (electronic ver.), ISSN 1503-8181.

“Experimental and numerical study of dilation in mineral filled PVC”,
Sindre Nordmark Olufsen, 2020:388, ISBN 978-82-326-5122-1 (printed ver.), ISBN 978-82-326-5123-8 (electronic ver.), ISSN 1503-8181.

“Residual stresses and dimensional deviation in metal additive manufacturing: prediction and mitigation methods”,
Li Sun, 2020:411, ISBN 978-82-471-9600-7 (printed ver.), ISBN 978-82-471-9581-9 (electronic ver.), ISSN 1503-8181 (printed ver.), ISSN 2703-8084 (online ver.).

“Ductility and brittleness of lightweight aggregate concrete structures”,
Jelena Živković, 2021:16, ISBN 978-82-471-9919-0 (printed ver.), ISBN 978-82-471-9709-7 (electronic ver.), ISSN 1503-8181 (printed ver.), ISSN 2703-8084 (online ver.).

“Thermal transport in metal-polymer systems”,
Susanne Sandell, 2021:63, ISBN 978-82-326-5304-1 (printed ver.), ISBN 978-82-326-6278-4 (electronic ver.), ISSN 1503-8181 (printed ver.), ISSN 2703-8084 (online ver.).

“Moment-resisting timber frames with semi-rigid connections”,
Aivars Vilguts, 2021:88, ISBN 978-82-326-6987 (printed ver.), ISBN 978-82-326-5737-7 (electronic ver.), ISSN 1503-8181 (printed ver.), ISSN 2703-8084 (online ver.).

“Competitive timber floors”,
Sveinung Ørjan Nesheim, 2021:134, ISBN 978-82-326-6481-8 (printed ver.), ISBN 978-82-326-5399-7 (electronic ver.), ISSN 1503-8181 (printed ver.), ISSN 2703-8084 (online ver.).

“Thermodynamics of Nanoscale Films and Fluid Volumes”,
Bjørn Andre Strøm, 2021:166, ISBN 978-82-326-6778-9 (printed ver.), ISBN 978-82-326-5900-5 (electronic ver.), ISSN 1503-8181 (printed ver.), ISSN 2703-8084 (online ver.).

ISBN 978-82-326-5289-1 (printed ver.)
ISBN 978-82-326-5876-3 (electronic ver.)
ISSN 1503-8181 (printed ver.)
ISSN 2703-8084 (online ver.)

NTNU
Norwegian University of
Science and Technology